

## **Copyright Warning & Restrictions**

The copyright law of the United States (Title 17, United States Code) governs the making of photocopies or other reproductions of copyrighted material.

Under certain conditions specified in the law, libraries and archives are authorized to furnish a photocopy or other reproduction. One of these specified conditions is that the photocopy or reproduction is not to be “used for any purpose other than private study, scholarship, or research.” If a user makes a request for, or later uses, a photocopy or reproduction for purposes in excess of “fair use” that user may be liable for copyright infringement,

This institution reserves the right to refuse to accept a copying order if, in its judgment, fulfillment of the order would involve violation of copyright law.

**Please Note: The author retains the copyright while the New Jersey Institute of Technology reserves the right to distribute this thesis or dissertation**

Printing note: If you do not wish to print this page, then select “Pages from: first page # to: last page #” on the print dialog screen

The Van Houten library has removed some of the personal information and all signatures from the approval page and biographical sketches of theses and dissertations in order to protect the identity of NJIT graduates and faculty.

## **INFORMATION TO USERS**

The most advanced technology has been used to photograph and reproduce this manuscript from the microfilm master. UMI films the text directly from the original or copy submitted. Thus, some thesis and dissertation copies are in typewriter face, while others may be from any type of computer printer.

**The quality of this reproduction is dependent upon the quality of the copy submitted.** Broken or indistinct print, colored or poor quality illustrations and photographs, print bleedthrough, substandard margins, and improper alignment can adversely affect reproduction.

In the unlikely event that the author did not send UMI a complete manuscript and there are missing pages, these will be noted. Also, if unauthorized copyright material had to be removed, a note will indicate the deletion.

Oversize materials (e.g., maps, drawings, charts) are reproduced by sectioning the original, beginning at the upper left-hand corner and continuing from left to right in equal sections with small overlaps. Each original is also photographed in one exposure and is included in reduced form at the back of the book.

Photographs included in the original manuscript have been reproduced xerographically in this copy. Higher quality 6" x 9" black and white photographic prints are available for any photographs or illustrations appearing in this copy for an additional charge. Contact UMI directly to order.

# **U·M·I**

University Microfilms International  
A Bell & Howell Information Company  
300 North Zeeb Road, Ann Arbor, MI 48106-1346 USA  
313/761-4700 800/521-0600

Order Number 9108044

**On the performance of Minimum Redundancy Array for  
multisource direction finding**

Lee, Byung-Seub, D.Eng.Sc.

New Jersey Institute of Technology, 1990

**U·M·I**  
300 N. Zeeb Rd.  
Ann Arbor, MI 48106

**NOTE TO USERS**

**THE ORIGINAL DOCUMENT RECEIVED BY U.M.I. CONTAINED PAGES  
WITH SLANTED PRINT. PAGES WERE FILMED AS RECEIVED.**

**THIS REPRODUCTION IS THE BEST AVAILABLE COPY.**

**ON THE PERFORMANCE OF MINIMUM REDUNDANCY ARRAY  
FOR MULTI-SOURCE DIRECTION FINDING**

**BY**

**BYUNG SEUB LEE**

**Dissertation submitted to the FACULTY of the Graduate School  
of the New Jersey Institute of Technology in partial  
fulfillment of the requirement for the degree of Doctoral of  
Engineering Science**

**1990**

---

Approval of Dissertation

Title of Dissertation: On the Performance of Minimum Redundancy  
array for Multi-source Direction Finding.

Name of Candidate: Byung-Seub Lee  
Doctor of Engineering Science, 1990

Dissertation and Abstract Approved:

_____	_____
Dr. Y. Bar-Ness	Date
_____	_____
Dr. A. Haimovich	Date
_____	_____
Dr. C. Lu	Date
_____	_____
Dr. J. Tavantzis	Date

**VITA**

**Name: Byung Seub Lee**

**Degree and Date to be conferred: D.Eng.Sc.,1990**

<b>Collegiate institutions attended</b>	<b>Dates</b>	<b>Degree</b>	<b>Date of Degree</b>
<b>New Jersey Institute of Technology</b>	<b>1/86-5/90</b>	<b>D.Eng.Sc.</b>	<b>1990</b>
<b>Seoul National University</b>	<b>3/79-1/81</b>	<b>M.S</b>	<b>1981</b>
<b>Civil Aviation College</b>	<b>3/75-1/79</b>	<b>B.S</b>	<b>1979</b>

**Major: Electrical Engineering**



## ABSTRACT

**Title of Dissertation: On the Performance of Minimum Redundancy  
array for Multi-source direction finding.**

**Byung Seub Lee, D. Eng. Sc. E.E., 1990**

**Dissertation directed by Dr. Bar-Ness**

**Director of Center for Communication and  
Signal Processing Research.**

As an application of power spectrum estimation, the multi-source direction finding has been evolved from conventional FFT method to Superresolution methods such as Multiple Signal Classification(MUSIC) algorithm. Uniform Regular Array(URA) was mainly used in all these approaches.

The Minimum Redundancy array(MRA); a non-uniform thinned array which results in an input signals covariance matrix with minimum redundancy has been shown to have certain interesting properties for spectrum estimation. Only recently it was suggested to use the MRA for spatial estimation. The purpose of this research was to study the performance of this array in multi-source direction finding estimation and compare it to the

result obtained with URA. Although the emphasis in this research is on using the popular MUSIC algorithm, other algorithms are also considered.

Among the topics related to the MRA performance studied in the course of this research are

1. Effect of random displacement of the array element location on the performance of multi-source direction finding.

2. Performance of the MRA versus the URA using MUSIC and Minimum-Norm algorithms.

3. Performance of the MUSIC based direction finding using different covariance matrix estimates for URA and MRA.

4. The error probability of estimating the number (two in particular) of closely located sources with MRA versus URA.

## **Acknowledgement**

**The author wishes to acknowledge the helpful discussion and encouragement offered by Dr. Y. Bar-Ness.**

## TABLE OF CONTENTS

	Page
<b>1. INTRODUCTION</b>	<b>1</b>
<b>2. POWER SPATIAL SPECTRUM ESTIMATION</b>	
1) Basic Principle of Estimation Theory	11
2) Conventional Methods of Spectral Estimation	15
3) Maximum Likelihood Spectral Estimation	20
4) Spatial Spectrum Relation	23
5) The Bartlett Spatial Estimation	27
6) High Resolution Array Processing Using Eigensystem	29
7) MUSIC (Multiple Signal Classification)	37
Appendix	41
References	42
<b>3. MULTIPLE SOURCE DIRECTION FINDING WITH     MINIMUM REDUNDANCY ARRAY</b>	
1) Introduction	44

2) Array Geometry	45
3) The Augmented Matrix of MRA	52
4) Multi-Source Direction Finding using the Augmented Matrix	54
5) Simulation Results	55
References	56

#### 4. EFFECTS OF RANDOM DISPLACEMENT OF THE ARRAY ELEMENTS ON THE PERFORMANCE OF DIRECTION FINDING. URA. vs. MRA

1) Introduction	58
2) Random Perturbation in One Dimension, Uniform Probability Distribution	60
3) Random Perturbation in Two Dimensions, Uniform Probability Distribution	66
4) Random Perturbation with Gaussian Probability Distribution	68
5) Variation of Covariance Matrix due to Perturbation in element location	70
6) Statistical Randomly Perturbed Covariance Matrix	74
7) Simulation Results	75

<b>8) Conclusion</b>	<b>78</b>
<b>Appendix</b>	<b>80</b>
<b>References</b>	<b>84</b>

## **5. PERFORMANCE OF THE UNIFORM REGULAR ARRAY AND THE MINIMUM REDUNDANCY ARRAY USING MUSIC AND MINIMUM-NORM ALGORITHM**

<b>1) Introduction</b>	<b>99</b>
<b>2) MRA Array Geometries and their Covariance Matrix</b>	<b>101</b>
<b>3) Formulation of Direction Finding Algorithms</b>	<b>111</b>
<b>a) MUSIC</b>	<b>111</b>
<b>b) Minimum-Norm Algorithm</b>	<b>115</b>
<b>4) Simulation Results</b>	<b>119</b>
<b>5) Conclusion</b>	<b>122</b>
<b>References</b>	<b>123</b>

## **6. PERFORMANCE OF THE MUSIC BASED DIRECTION FINDING USING DIFFERENT COVARIANCE MATRIX ESTIMATES FOR THE UNIFORM REGULAR ARRAY(URA) AND THE MINIMUM REDUNDANCY ARRAY(MRA)**

1) Introduction	135
2) Estimates of Covariance Matrix for the URA	137
a) The Random Sampled covariance Matrix	137
b) Doubly Symmetric Covariance Matrix	138
c) The averaged Toeplitz Covariance Matrix	140
d) Optimized Toeplitz Covariance Matrix	141
3) Covariance Matrix for Minimum Redundancy Array	149
4) Simulation Results	155
5) Conclusion	156
Appendix	157
References	159

## 7. THE ERROR PROBABILITY OF ESTIMATING THE NUMBER OF TWO CLOSELY LOCATED SOURCES.

1) Introduction	165
2) Detection Performance	170
3) Probability of Error for the case of two close sources	174
4) Adequacy of the approximation for $\log Q_u(x)$	179

<b>5) Simulation Results</b>	<b>182</b>
<b>6) Conclusion</b>	<b>183</b>
<b>Appendix</b>	<b>185</b>
<b>References</b>	<b>190</b>

---



## 1. INTRODUCTION.

In direction finding, one is interested in obtaining an estimate of the spatial structure of a random spatial field. If one samples in space a random field using a linear array of  $M$  sensors then a vector time series  $\{ x(t,0), x(t,\Delta x), \dots, x(t,(M-1)\Delta x) \}$ , is obtained, where  $x(t,i\Delta x)$  is the continuous waveform at the  $i$ 'th sensor;  $i = 0, \dots, M-1$ . The field can be expressed as [1]

$$x(t,i\Delta x) = \iint \psi(f, k_x) \exp[j2\pi(ft - k_x i\Delta x)] df dk_x \quad (1)$$

which represents the field as the sum of an impinging plane waves with random amplitudes  $\psi(f, k_x)$ . The temporal frequency is denoted by  $f$ , while the spatial frequency along the  $x$  direction is denoted by  $k_x$ . The wave number component  $k_x$  is the reciprocal of the wavelength of a monochromatic plane wave along the  $x$  direction. Since  $k_x = (f/c) \sin\theta$ , where  $\theta$  is the angle from the broadside, then  $E [ |\psi(f, k_x)|^2 ]$  is the power at frequency  $f$  arriving from the  $\theta$  direction. The inverse fourier transform of (1) is

$$\begin{aligned} \psi(f, k_x) &= \sum_{i=0}^{M-1} \left[ \int x(t, i\Delta x) \exp(-j2\pi ft) dt \right] \exp(j2\pi k_x i\Delta x) \\ &= \sum_{i=0}^{M-1} X_f(i\Delta x) \exp(j2\pi k_x i\Delta x) \end{aligned} \quad (2)$$

Expression (2) is fourier the transform relationship between a spatial time series  $X_f(i\Delta x)$ , where  $\Delta x$  is the distance between the sensors, and its spectrum  $\psi(f, k_x)$ . If the spatial field is assumed homogeneous ie.

$$E [ x(t, i\Delta x) x(t, j\Delta x) ] = f(t, [i-j]\Delta x) \quad (3)$$

then the spatial time series is a wide sense stationary and the estimation of  $E(|\psi(f, k_x)|^2)$  for all  $k_x$  at a given temporal frequency  $f$  is analogous to the one-dimensional temporal power spectral estimation. Finally we can get the estimation of the spatial autocovariance

$$\hat{R}_x(k\Delta x) = \frac{1}{N(M-k)} \sum_{n=0}^{N-1} \sum_{i=0}^{M-k-1} x^*(n\Delta t, i\Delta x) x(n\Delta t, (i+k)\Delta x)$$

$$k \geq 0$$

where  $x(n\Delta t, i\Delta x)$  is assumed to be stationary over the interval  $0 \leq n\Delta t \leq (N-1)\Delta t$ . In conclusion there is a direct analogy between power spectrum estimation and source direction finding.

Conventional estimation of the power spectral density of discretely sampled deterministic and stochastic process is usually based on procedure employing the fast fourier transform. This approach to spectral analysis is computationally efficient and produces reasonable results for a large class of signal processes. In spite of these advantages, there are several inherent performance limitation of the FFT approach. The most prominent limitation is that of frequency(or direction) resolution, ie, the ability to distinguish between the spectral responses of two or more signals. A second limitation is due to the implicit windowing of the data that occurs when processing with FFT. Windowing manifest itself as "leakage" in the spectral domain, ie, energy in the main lobe of a spectral response leaks into the sidelobes, obscuring and distorting other spectral responses.

These two performance limitation of FFT approach[2]-[5] are particularly troublesome when analyzing short data records. Short data records occur frequently in practice because many measured process are brief in duration.

In an attempt to alleviate the inherent limitation of the FFT approach, many alternative modern spectral estimation procedures have been proposed. These methods are classified as 1) Parametric estimation and 2) Non-parametric estimation( Eigensystem estimation)

1) The parametric Power Spectral Estimation.

This class includes the autoregressive method(AR)[6]-[9], and the autoregressive-moving average method(ARMA) [10]-[12]. The output of this class of estimation is totally described in terms of the model parameters and the variance of the white noise process. The motivation for parametric estimation is the ability to achieve better power spectral (or spatial) density estimation based upon the model than that produced by classical FFT spectral estimations.

The parametric approach to spectral(or spatial) estimation involves three steps. In step one, an appropriate parametric time-series model is selected to represent the measured data. In step two, an estimate of the parameters of the model is made. In step three, the estimated parameters are inserted into the theoretical power spectral density expression appropriate for that model.

## b) Non-parametric Power Spectral Estimation

### (Eigensystem based Method)

A class of spectral technique based on an eigensystem of an autocovariance matrix have been promoted in the research literatures as having better resolution and better frequency(or spatial) estimation characteristics than spectral technique, such as auto-regressive method or Prony's method, especially at lower SNR, where these parametric methods often fail to resolve close frequency or direction. [13], [14]

The basis for the improved performance of the eigensystem technique is the division of the covariance matrix  $\hat{R}$  into two vector subspace, one a signal subspace and the other a noise subspace. Function of the vectors in either the signal or noise subspace can be used to create frequency(spatial) estimation that show sharp peak at the frequency or direction of measure data. These are not the true power spectral density estimator because they do not preserve the measured process power nor can the autocorrelation sequence be recovered by Fourier Transforming the frequency estimation. Included in this class of Eigensystem based frequency estimations are the Pisarenco Harmonic Decomposition [15] and multiple signal classification(MUSIC). [16], [17]

Most of the aforementioned algorithms were applied to uniform regular array(URA) which has its antenna element located at a distance  $\lambda/2$  between the adjacent element. The other type of array, called Minimum Redundancy Array(MRA), has the advantage of having a large aperture length by deploying the same number of array elements further away to remove redundancy in its distance between the array elements[18].As such, if the covariance matrix of the MRA is augmented to a Toeplitz matrix of a much larger dimension than its number of elements(shown to be possible) then this array can resolve a much larger number of sources than URA. In the next chapter we review the material on power spectral-spatial estimation which is relevant to the research at this work. In chapter 3 we discuss the principle of the minimum redundancy array and its usage for multiple source direction finding. In the last four chapters we suggest different problems related to the performance of the MRA in comparison to the URA. In chapter 4 we discuss the effect of random displacements of the array elements on the performance of MRA and compare it to that of the URA. Different density functions are assumed for these displacements. Both one and two dimensional displacements are considered. In chapter 5 a comparison of the MRA to the URA

performance is made based on using two different spatial estimation algorithm; the Multiple Signal Classification(MUSIC) and the Minimum-Norm algorithms. In chapter 6 the effect of using different estimators for the covariance matrix on the performance of the direction finders implementing URA and MRA is evaluated and compared. The knowledge of the actual number of signal impinging on the array used for direction finding is a crucial parameter for any multi-source direction finding algorithm. The error probability of estimating this number of sources is considered in chapter 7 Particularly the case of estimating the number of (actually two) closely located sources with URA and MRA is discussed and compared.

The material in this report is arranged in such a way that each chapter has its own background and references. This look rather unusual for a thesis, was thought to be the best for such a kind of work which deals with several topics, although related to the same question of "the performance of MRA versus URA", it is somewhat distinct.

## References

- [1] J. Capon, "High-resolution frequency-wave number spectrum analysis," Proc. IEEE, Vol 57, pp 1408-1418, Aug 1969
- [2] M.S. Bartlett, "Periodogram analysis and continuous spectrum," Biometrika, Vol 37, pp 1-16 June 1950
- [3] C. Bingham, M.D. Godfrey, J.W. Turkey, "Modern technique of power spectrum estimation," IEEE Trans. Audio Electroacoustic, Vol Au-15, pp 56-66, June 1967
- [4] R.B. Blackman and J.W. Turkey, "The measurement of power spectrum from the point of view of communication Engineering," New York Dover 1959
- [5] S. Betram, "Frequency analysis using the discrete fourier Transform," IEEE trans. Audio Electroacoustic, Vol AU-18 pp 495-500 Dec. 1970
- [6] E. Paezan, "Mathematical consideration in the estimation of spectra," Technometrics, Vol. 3, pp 167-190 May, 1961
- [7] J.P. Burg, "Maximum Entropy Spectral analysis," Proc. 37'th meeting society of Exploitation and Geophysicist, Oct 31, 1967



[8] A. VanDenBos, "Alternative interpretation of maximum entropy spectral analysis," IEEE trans. Inform.theory, Vol IT-28 pp 949 Nov. 1980

[9] H. Tong, "Autoregressive Model fitting with noise data by Akaike's information criterion," IEEE Trans Inf. Theory, Vol. IT-21, pp 471-480, July 1975

[10] Bruzzone, S.P. and M. Kaveh, "On Suboptimum ARMA spectral estimation," IEEE Trans acoustic, Speech Signal Processing, Vol ASSP-28 pp 753-755 Dec. 1980

[11] Cadzow, "Autoregressive Moving average spectral estimation: A model equation error procedure, IEEE Trans. Geosci. Remote sensing GE-19 pp 24-28 Jan 1981

[12] J.C. Chow, "On estimating the orders of the autoregressive moving average process with uncertain observations, IEEE Trans Auto. Control, vol AC-17, pp 707-709 Oct. 1972

[13] D.H. Johson, S.R. Degraff, "Improving the resolution of bearing in passive sonar array by eigenvalue analysis," IEEE Trans. Acostics Speech Signal Processing vol ASSP-30 pp 638-647 Aug. 1982

[14] D. Spelman, A. Paulraj, and T. Kailath, "Performance analysis of the MUSIC algorithm," Proceeding of the 1986 IEEE International conference on acoustic, Speech Signal Processing, Tokyo Japan, pp 1909-1912 Apr. 1986

[15] V.F. Pisarenco, "The retrieval of Harmonics from a covariance Function," geophysics J.R. Astro. vol 33 pp 347-366 1973

[16] R.O. schmitt, " A signal subspace approach to multiple emitter location and spectral estimation," Ph D. Dissertation Dept. E.E. Stanford, Univ. Nov 1983

[17] R.O. schmidt, "Multiple Emitter location and signal parameter estimation," IEEE Trans. Antenna Prop. Vol AP-34 pp 276-280 Mar 1986

[18] S.U. Pillai, Y. Barness, F. Haber, "A new approach to array geometry for improved spatial spectrum estimation," Proceeding of the IEEE Vol 73, No 10, Oct 1985

## 2. POWER SPATIAL-SPECTRAL ESTIMATION.

### 1. Basic Principles of Estimation Theory.[1]

Consider a stationary random sequence  $x_n$ . Its *ensemble* mean value,  $m_x$ , is defined by equation (1) below. The time average mean of this random process,  $x_n$ , is defined in equation (2) below. Also assume that the random sequence  $x_n$  is the "ergodic process", i.e., a random sequence whose *ensemble* average is equal to time average, with probability one (W.P.1). That is the *ensemble* average,

$$m_x = E [x_n] = \int_{-\infty}^{+\infty} x p_x(x) dx \quad (1)$$

and the time average,

$$m_x = \langle x_n \rangle = \lim_{N \rightarrow \infty} \frac{1}{2N} \sum_{n=-N}^N x_n \quad (2)$$

are equal WP1. Similarly variance and autocovariance are

$$\sigma_x^2 = E [ (x_n - m_x)^2 ] = \langle (x_n - m_x)^2 \rangle \quad (3)$$

$$\gamma_{xx}(m) = E [ (x_n - m_x)(x_{n+m}^* - m_x^*) ] = \langle (x_n - m_x)(x_{n+m}^* - m_x^*) \rangle \quad (4)$$

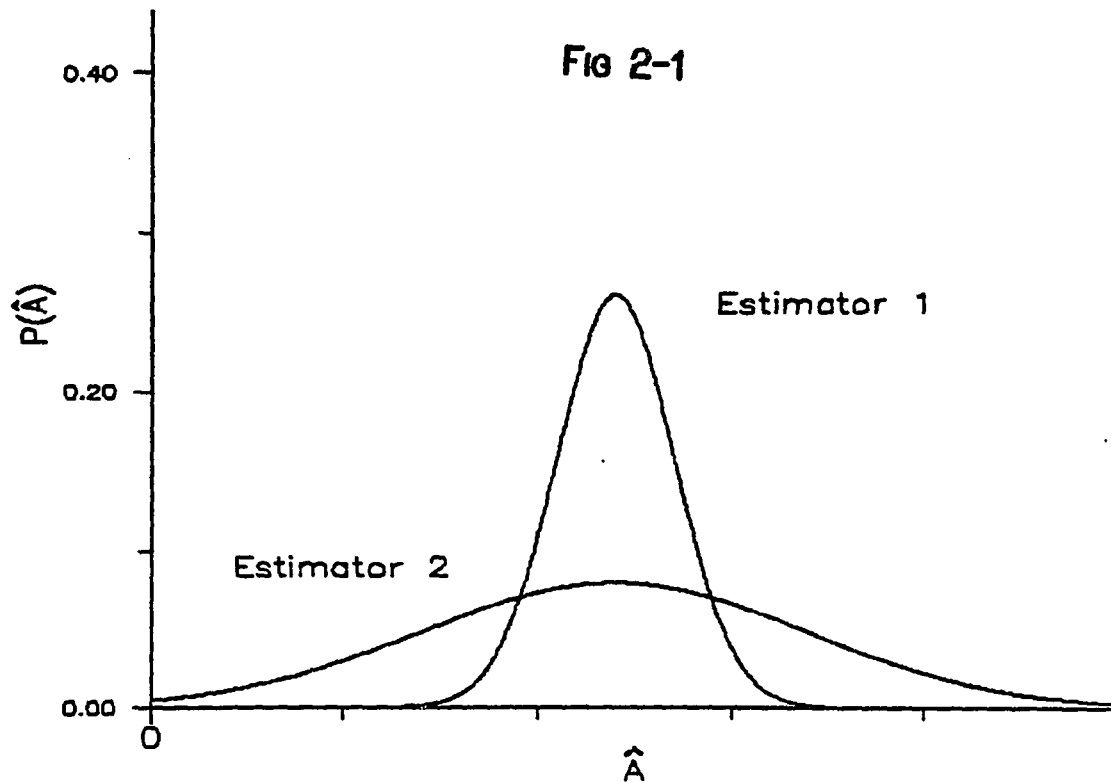
The power spectral density is given by

$$P_{xx}(w) = \sum_{m=-\infty}^{\infty} \gamma_{xx}(m) e^{-jwm} \quad (5)$$

Usually estimation of a parameter of random process is based on finite segment of a single sequence; i.e., we have  $N$  values  $x_n$ ,  $0 \leq n \leq N-1$ , from which we wish to estimate some parameter which we denote as "A". The estimate  $\hat{A}$  of the parameter  $A$  is a function of the random variables  $x_n$ ,  $0 \leq n \leq N-1$ , denoted by

$$\hat{A} = F(x_0, x_1, \dots, x_{N-1})$$

Therefore  $\hat{A}$  is also a random variable. The probability density function of  $\hat{A}$  will be denoted  $p_{\hat{A}}(\hat{A})$ . The shape of  $p_{\hat{A}}(\hat{A})$  will



depend on the choice of the estimator  $F(\ )$  and the probability densities of the random variable  $x_n$ , as indicated Fig 2-1. It is reasonable to characterize an estimator as being "good" if there is high probability that the estimate will be close to  $A$ . Generally speaking, it is plausible that for a good estimator the probability density function  $p_{\hat{A}}(\hat{A})$  should be narrow and concentrated around the true value, and we might compare different estimators on that basis. On this basis it is clear that estimator 1 in Fig-1 is superior to estimator 2 because the probability density of estimator 1 is more concentrated about the true value

A. In keeping this notion, two properties of estimators that are commonly used as a basis for comparison are the "bias" and "variance". The bias of an estimator is defined as the true value of the parameters minus the expected value of the estimate, i.e.,

$$\text{Bias} = A - E[\hat{A}]$$

An unbiased estimator is one for which the bias is 0. This is then means that the expected value of the estimate is the true value. Therefore, if the probability density  $p_{\hat{A}}(\hat{A})$  is symmetrical around A, then its center would be at the true value A. The variance of the estimator in effect measures the width of the probability density and is defined by

$$\text{Var}[\hat{A}] = E[(\hat{A} - E[\hat{A}])^2] = \sigma^2$$

A small variance suggests that the probability density  $p_{\hat{A}}(\hat{A})$  is concentrated around its mean value and hence  $E(\hat{A}) = A$  with a higher probability. If  $\hat{A} = A$ , unbiased estimator then small variance mean  $\hat{A} = A$  with high probability.

## 2. Conventional Methods of Spectral Estimation.[1],[2],[3],[4]

Traditional spectrum estimation, as currently implemented using the FFT, is characterized by many tradeoffs in an effort to produce statistically reliable spectral estimates. There are tradeoffs in windowing time-domain averaging, and frequency-domain averaging of the sampled data obtained from the random process in order to balance the needs to reduce sidelobes, to perform effective ensemble averaging, and to ensure adequate spectral resolution. Two spectral estimation techniques based on Fourier transform operation have evolved. The first is the Power Spectral Density estimate based on the indirect approach via an autocorrelation estimate, was popularized by Blackman and Turkey[3]. The other is the Power Spectral Density estimate, based on the direct approach via an FFT operation on the data directly which is typically referred to as "Periodogram".

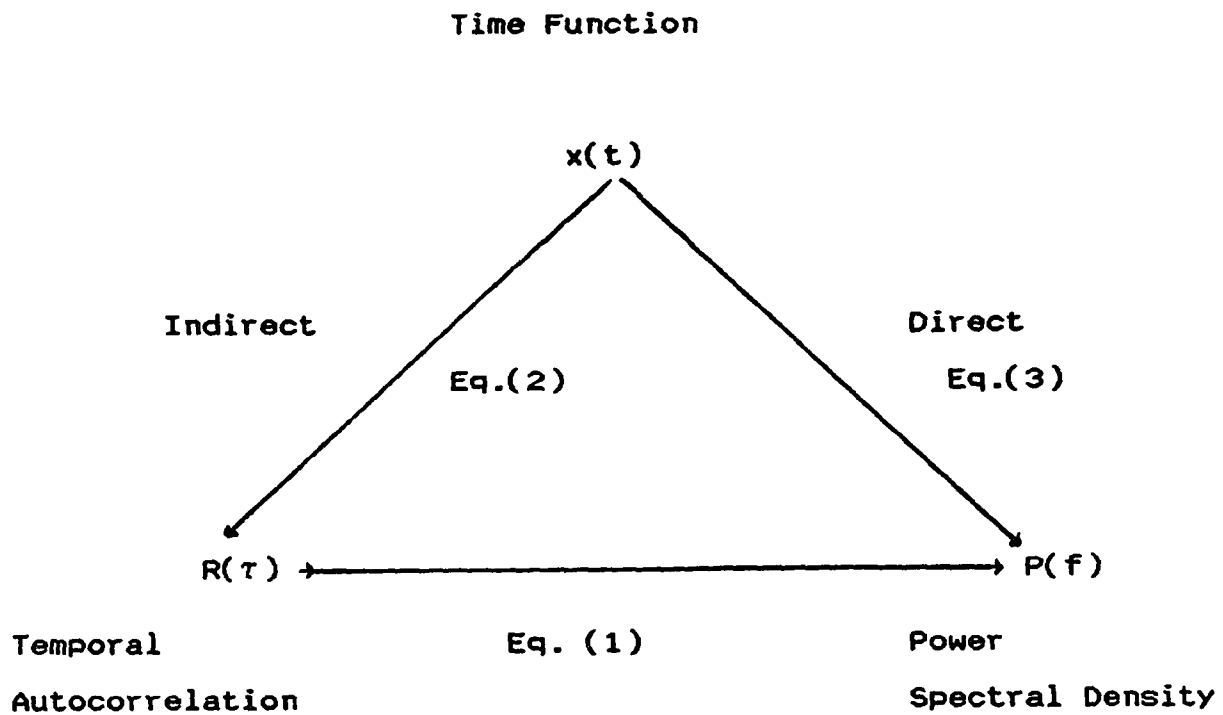


Fig 2-2. direct and Indirect methods to obtain PSD  
 (Stationary and Ergodic properties assumed)

Using the indirect approach, we first find  $R_{xx}(\tau)$

$$R_{xx}(\tau) = \lim_{T \rightarrow \infty} \frac{1}{2T} \int_{-T}^T x(t+\tau) x^*(t) dt \quad (6)$$

then obtain the power spectral density (PSD),



$$P(f) = \int_{-\infty}^{+\infty} R_{xx}(\tau) \exp(-j2\pi f\tau) d\tau \quad (7)$$

Using the direct approach we get the PSD by

$$P(f) = \lim_{T \rightarrow \infty} E \left[ \frac{1}{2T} \left| \int_{-T}^T x(t) \exp(-j2\pi ft) dt \right|^2 \right] \quad (8)$$

When only a finite data sequence is available, only a finite number of discrete autocorrelation function values, or lags, can be estimated. An obvious autocorrelation estimate, based on (6), is an unbiased estimator given by

$$\hat{R}_{xx}(m) = \frac{1}{N-m} \sum_{n=0}^{N-m-1} x_{n+m} x_n^* \quad (9)$$

for  $m=0,1,\dots,M$ , where  $M \leq N-1$ . Blackman and Turkey proposed to obtain the spectral estimate by

$$\hat{P}_{BT}(f) = \Delta t \sum_{m=-M}^M \hat{R}_{xx}(m) \exp(-j2\pi fm\Delta t) \quad (10)$$

The negative lag estimates are determined from the positive lag estimates as follows:

$$\hat{R}_{xx}(-m) = \hat{R}_{xx}(m) \quad (11)$$

The direct method of spectrum analysis is the modern version of periodogram. A sampled data version of expression (8), for which measured data are available only for samples  $x_0, x_1, \dots, x_{N-1}$ , is given by

$$\hat{P}_{PER}(f) = \frac{1}{N \Delta t} \left| \Delta t \sum_{n=0}^{N-1} x_n \exp(-j2\pi f n \Delta t) \right|^2 \quad (12)$$

defined for the frequency interval  $-1/(2\Delta t) \leq f \leq 1/(2\Delta t)$ . Notice that

$$\hat{P}_{PER}(f_m) = \frac{1}{N \Delta t} \left| X_m \right|^2 \quad (13)$$

where  $f_m = m\Delta f$  and  $X_m$  is the DFT of sequence  $x_n$ . Use of the FFT will permit evaluation of (12) at the discrete set of  $N$  equally spaced frequency  $f_m = m \Delta f$  Hz, for  $m=0,1, \dots, N-1$  and  $\Delta f$  is  $1/N\Delta t$ .  $\hat{P}_{PER}(f_m)$  is identical to the energy spectral density except for the division by the time interval of  $N\Delta t$  second, to make it power spectral density.

Many of the problems of these conventional methods of PSD

estimation techniques can be traced to the assumption made about the data outside the measurement interval. The use of only those windowed data implicitly assumes the unmeasured data to be zero, which is usually not the case. This multiplication of the actual time series by window function means the overall transform is the convolution of the desired transform with the transform of the window function. If the power of a signal is concentrated in a narrow bandwidth, this convolution operation will spread that power into adjacent frequency regions. This phenomena, termed 'leakage', is a consequence of the windowing inherent in the computation of the periodogram.

In summary, the conventional Blackman and Turkey(BT) and Periodogram approach to spectral estimation have the following advantage.

1) Computationally efficient if only a few lags are needed(BT) or if the FFT is used (Peridogram).

2) Power Spectrum Density estimate directly proportional to the power for sinusoid processes.

The disadvantage of these techniques are

1) Suppression of weak signal main-lobe responses by strong signal sidelobes.

2) Frequency resolution limited by the available data record duration independent of the characteristics of the data or its SNR.

3) Introduction of the distortion in the spectrum due to sidelobes leakage.

4) Need for some sort of pseudo ensemble averaging to obtain statistically consistent periodogram spectra.

### 3. Maximum Likelihood Spectral estimation.[5]

In maximum likelihood spectral estimation (MLSE), originally developed for seismic array frequency-wave number analysis, one estimates the power spectral density by effectively measuring the power out of a set of narrow band filters. MLSE is sometimes referenced as the "Capon spectral estimate". The difference between MLSE and the conventional BT/Periodogram spectral estimation is that the shape of the narrow band filters in MLSE are, in general, different for each frequency whereas they are fixed with the BT/Periodogram procedures. The filters in MLSE adapt to the process for which the PSD is sought. In particular,

the filters are Finite Impulse Response(FIR) types with  $p$  weights;

$$A = [ a_0, a_1, \dots, a_{p-1} ]^T \quad (14)$$

where T stand for transpose. The coefficients are chosen so that the frequency response of the filters at the frequency under consideration is unity(i.e., an input sinusoid at that frequency would be undistorted at the filter output) and the variance of the output process is minimized. Thus the filter should adjust itself to reject component of the spectrum not near frequency under consideration  $f_0$ , so that the output power is due mainly to frequency components close to  $f_0$ . To obtain this filter, one minimizes the output variance  $\sigma^2$ , given by

$$\sigma^2 = A^\dagger R_{xx} A \quad (15)$$

where  $R_{xx}$  is the covariance matrix of  $x_n$ , subject to the unity frequency response constraint (so that the sinusoid of frequency  $f_0$  is filtered without distortion). That is

$$E^\dagger A = 1 \quad (16)$$

where  $E$  is the vector

$$E = [ 1, \exp(j2\pi f_0 \Delta t), \dots, \exp(j2\pi(p-1)f_0 \Delta t) ]^T$$

and  $\dagger$  denotes the complex conjugate transpose. The solution for the filter weights is easily shown to be

$$A_{\text{opt}} = \frac{R_{xx}^{-1} E}{E^\dagger R_{xx}^{-1} E} \quad (17)$$

and the minimum output variance is then

$$\sigma_{\text{min}}^2 = \frac{1}{E^\dagger R_{xx}^{-1} E} \quad (18)$$

Notice that  $E_f^\dagger A_{\text{opt}}$  is the optimum filter response at  $f$ , where

$$E_f = [ 1, \exp(j2\pi f \Delta t), \dots, \exp(j2\pi f(p-1)\Delta t) ]^T$$

then

$$E^{\dagger} A_{\text{opt}} = \frac{E^{\dagger} R_{xx}^{-1} E}{E^{\dagger} R_{xx}^{-1} E} = 1$$

That is the optimum filter frequency response at  $f_0$  is unity. The filter characteristics depends on the underlying autocorrelation function  $R_{xx}$ . Since the minimum output variance is due to frequency components near  $f_0$ , then  $\sigma_{\text{min}}^2$  can be interpreted as PSD estimate. Thus, the MLSE PSD is defined as

$$\hat{P}_{\text{ML}}(f_0) = \frac{\Delta t}{E^{\dagger} R_{xx}^{-1} E} \quad (19)$$

To compute the spectral estimate, one only needs an estimate of the autocorrelation matrix.

#### 4. Spatial Spectrum Relation

The direction estimation problem is mathematically equivalent to the estimation of the spatial Fourier transform of the radiation field. The waveform measured at the spatial position  $z_i$

of the  $i$ 'th element is denoted by

$$x_i(t) = S\left(t + \frac{z_i \cdot k_0}{c}\right) + n_i(t) \quad (20)$$

where  $n_i(t)$  is an additive noise at the  $i$ 'th element and  $z_i \cdot k_0$  is the dot product of the position vector  $z_i$  to the  $i$ 'th element and  $k_0$  is the direction vector of the wave impinging on the array (here assumed a single source). The spatial Fourier transform

$$X_i(f, k_0) = e^{-j2\pi(f/c)(z_i \cdot k_0)} S(f) + N(f) \quad (21)$$

Using vector notation we will define

$$x(t) = S\left(t + \frac{z \cdot k_0}{c}\right) + n(t) \quad (22)$$

where  $z \cdot k_0$  is a vector whose elements are given by  $z_i \cdot k_0$ ,  $i=1,2,\dots,M$  ( $M$  is the number of array elements). Correspondingly the spatial Fourier transform vector is given by

$$X(f, k_0) = e^{-j2\pi(f/c)(z \cdot k_0)} S(f) + N(f) \quad (23)$$



If the array is linear then  $z_i = d_i e_0$ , where  $e_0$  is a unit vector in the direction of the array line position and  $d_i$  is the distance from the  $i$ 'th element to some reference point, and  $z_i \cdot k_0 = d_i \sin \theta_0$  where  $\theta_0$  is the angle between the direction of propagation and the array broadside. For this case

$$\begin{aligned} X(f, k_0) &= X(f, \theta_0) \\ &= S(f) a(\theta_0) + N(f) \end{aligned} \quad (24)$$

where

$$a(\theta_0) = [ \exp(-j2\pi f/c d_1 \sin \theta_0), \dots, \exp(-2\pi f/c d_M \sin \theta_0) ]^T$$

For the case of multi signal impinging on the array from direction  $\theta_k$ ,  $k=1,2,\dots,D$  we have,

$$x(t) = \sum_{i=1}^D s_k \left( t + \frac{z \cdot k_i}{c} \right) + n(t) \quad (26)$$

$$\begin{aligned} X(f, \underline{k}) &= \sum_{i=1}^D e^{-j2\pi(f/c)(z \cdot k_i)} s_i(f) + N(f) \\ &= \sum_{i=1}^D s_i(f) a(\theta_i) + N(f) \end{aligned} \quad (27)$$

Now

$$\begin{aligned}
 R &= E [ X(t) X(t)^\dagger ] \\
 &= E [ X(f, \underline{k}) X(f, \underline{k})^\dagger ] \quad (28)
 \end{aligned}$$

where  $R$  is the array output covariance matrix. Using (27) we get

$$\begin{aligned}
 R &= E \left[ \sum_{i=1}^D S_i(f) a(\theta_i) \sum_{j=1}^D S_j(f) a(\theta_j)^\dagger \right] + E [ N(f)N(f)^\dagger ] \\
 &= \sum_{i=1}^D E [ |S_i(f)|^2 ] a(\theta_i) a(\theta_i)^\dagger + \sigma^2 I \quad (29)
 \end{aligned}$$

where we assumed the signals  $S_i(t)$  are uncorrelated and that the noise at the elements is uncorrelated zero mean and with variance  $\sigma^2$ , where

$$a(\theta_k) = [ e^{-j2\pi(f/c)d_1 \sin\theta_k}, \dots, e^{-j2\pi(f/c)d_M \sin\theta_k} ]^T \quad (30)$$

If the array is uniform  $d_i = i \cdot d$  then

$$a(\theta_k) = [ 1, e^{-2\pi f/c d \sin\theta_k}, \dots, e^{-2\pi f/c (M-1)d \sin\theta_k} ] \quad (31)$$

where we also chose the reference point at the first element.

If the signal is narrowband centered at  $f_0$  then  $X(f)$  is a constant, and if we also take  $d = \lambda_0/2$  then

$$a(\theta_k) = [ 1, e^{-\pi \sin\theta_k}, e^{-2\pi \sin\theta_k}, \dots, e^{-(M-1)\pi \sin\theta_k} ] \quad (32)$$

Under these conditions

$$R = A E [ S(f) S(f)^\dagger ] A^\dagger + \sigma^2 I \quad (33)$$

where

$$A = [ a(\theta_1), a(\theta_2), \dots, a(\theta_D) ]$$

and

$$S(f) = [ s_1(f), s_2(f), \dots, s_D(f) ] \quad (34)$$

From (33) it is clear that if we take  $X = AS$  then  $R = E [XX^\dagger]$ . In fact  $S(f) S(f)^\dagger$  is a diagonal matrix whose elements are  $P_k$ ; the power of the different signals.

When we deal with plane wave propagations, narrowband signal and linear array, it is simple to obtain equation (33) directly in the time domain rather than to obtain it as a special case of the more general case we discussed in this section.

## 5. The Bartlett spatial Estimation.

If the signals  $x_i(t)$  of (20)  $i=1,2, \dots, M$ , we weigh and delay to from

$$y(t) = \sum_{i=1}^M a_i x_i(t - \tau_i) , \quad (35)$$

then its Fourier transform is

$$Y(f, \underline{k}) = \sum_{i=1}^M a_i \exp[ -j2\pi(f/c) \underline{z}_i \cdot \underline{k} ] X_i(f) \quad (36)$$

where  $\tau_i$  is given by the dot product  $(\underline{z}_i \cdot \underline{k})/c$ , whose angle represents a beam direction with respect to the array broadside is  $\theta$ , and  $\underline{z}_i = d_i \underline{e}_0$  where  $\underline{e}_0$ , as before a unit vector in the direction of the array line position, then

$$Y(f, \underline{k}) = Y(f, \theta) = \underline{\vartheta}^T X(f, \underline{k}) \quad (37)$$

where

$$\underline{\vartheta} = [ a_1 e^{-j2\pi(f/c) d_1 \sin\theta} , \dots , a_M e^{-j2\pi(f/c) d_M \sin\theta} ] \quad (38)$$

From (27) we can write

$$X(f, \underline{k}) = A S(f) \quad (39)$$

where

$$A = [ a(\theta_1), a(\theta_2), \dots , a(\theta_k) ] \quad (40)$$

The energy at the output of the weighing filter is given by  $\int |Y(f, \underline{k})|^2 df$ , and we must find  $\theta$  which will give a maximum. However if the signal is narrowband, centered at  $f_0$  then

$$\begin{aligned}
 P(\theta) &= |Y(f_0, k)|^2 = E [\theta X X^\dagger \theta^\dagger] \\
 &= \theta A E [S(f) S(f)^\dagger] A^\dagger \theta^\dagger \\
 &= \theta R \theta^\dagger \tag{41}
 \end{aligned}$$

where  $R = A E [S(f) S^\dagger(f)] A$  as before,

The equation

$$P(\theta) = \theta R \theta^\dagger \tag{42}$$

is called the *Bartlett estimate*.

## 6. High Resolution array Processing Using the Eigensystem.[6]

New signal processing methods for passive direction finding have emerged recently. They are called "High Resolution" method

because they have theoretically a better resolving power than conventional or adaptive beamforming, but they use a more complete modeling of the medium which needs knowledge on the background noise spatial coherence. They are based on the properties of the eigenvectors and eigenvalues of the cross-spectral density matrix of the signal received at the sensors of the array. They have theoretically an asymptotic( Infinite observation time) infinite resolving power.

The improvement in performance of the array processing, using eigensystem, is due to the use of a model for the medium, which is more complete than the one utilized for previous array processing. Adaptive array processing, just as conventional beamforming, relies on certain assumptions about sources and the propagation in the medium. The source are assumed point-like, perfectly spatially coherent, and the shape of the wavefront received at the array from a source, is assumed a known function of the source position. The receiving element transfer functions are also assumed to be perfectly known. Let  $x(t)$  be the vector representing the signal received on the  $M$  elements of the array:

$$x(t) = [ x_1(t), x_2(t), \dots, x_M(t) ] \quad (43)$$

where  $x_i(t)$ ,  $i=1,\dots,M$ , is the signal received at the  $i$ 'th element. The space correlation matrix of the received signal is defined by:

$$C(\tau) = E [ X(t) X^\dagger(t+\tau) ] \quad (44)$$

where  $E$  stands for mathematical expectation and  $X^\dagger(t)$ , as before, is the conjugate-transpose of  $X(t)$ . The cross-spectral density matrix  $\Gamma(f)$  is the fourier transform of  $C(\tau)$ . Under the previous assumptions, the cross-spectral density matrix of a single source is given by

$$\Gamma(f) = \gamma(f) d(f) d^\dagger(f) \quad (45)$$

$d(f)$  is the source position vector: it is composed of  $M$  transfer functions between the source and each element normalized by the transfer function between the source and a reference point on the array.  $\gamma(f)$  is the spectral density of the signal received from the source at the reference point. In the case of an isotropic propagation with negligible attenuation between the sensors,  $d(f)$  is the familiar steering vector of the conventional beamforming:

$$d(f) = [ e^{-j2\pi f\tau_1} , e^{-j2\pi f\tau_2} , \dots , e^{-j2\pi f\tau_M} ]^T \quad (46)$$

$\tau_i$  is the delay of the source signal between the  $i$ 'th element and the reference point; that is  $\tau_i = d_i \sin \theta$ ,  $d_i$  is the distance of the  $i$ 'th element from the reference point and  $\theta$  is the direction of the source. The rank of this matrix is unity, which is characteristic of the perfect coherence assumption about sources. If we also assume that the sources and the background noise are statistically independent, then the cross-spectral density matrix of the signals at the element outputs is expressed by:

$$\Gamma(f) = \Gamma_b(f) + \sum_{i=1}^D \gamma_i(f) d_i(f) d_i^\dagger(f) \quad (47)$$

where  $\Gamma_b(f)$  is the cross-spectral density matrix of the background noise and  $D$  is the number of sources. It is generally assumed that the background noise is partially incoherent (statistically independent between the sensors). Thus

$$\Gamma_b(f) = \sigma(f) I, \quad (48)$$

is the spatial coherence matrix of the background noise,  $\sigma(f)$  its spectral density and  $I$  is the identity matrix. High resolution methods also assumes that the noise field can be resolved, that is to say the number of sources  $D$  is less than the number of sensor  $M$ . therefore



$$\Gamma(f) = \Gamma_b(f) + \Gamma_s(f) = \alpha(f)I + \sum_{i=1}^{D \times M} \gamma_i(f) d_i(f) d_i^\dagger(f) \quad (49)$$

The hypothesis on the background noise is the key to the high resolution.

- High Resolution Method Principles.

High resolution methods are based on eigenvalue-eigenvector decomposition of the cross-spectral density matrix  $\Gamma(f)$ . It can be easily seen from the relation defining an eigenvector  $V(f)$  and related eigenvalue  $\lambda(f)$ ,

$$\Gamma(f)V(f) = \alpha(f)V(f) + \sum_{i=1}^{D \times M} \gamma_i(f) d_i(f) [d_i^\dagger(f) V(f)] = \lambda(f) V(f) \quad (50)$$

That is  $V(f)$  must be either orthogonal to all  $d_i(f)$ ,  $i=1, \dots, D$ , with corresponding eigenvalues  $\lambda(f) = \alpha(f)$  or  $V(f)$  is a linear combination of  $d_i(f)$ ,  $i=1, 2, \dots, D$  given by

$$V(f) = \frac{1}{\lambda_{si}(f)} \sum_{i=1}^{D \times M} \gamma_i(f) [d_i^\dagger(f) V(f)] d_i(f) \quad (51)$$

The cross-spectral density matrix  $\Gamma(f)$  has:

a)  $D$  eigenvectors  $V_i(f)$  are also eigenvectors of the sources alone cross-spectral density matrix  $\Gamma_S(f)$ . They correspond to the non-zero eigenvalues  $\lambda_{si}(f)$  of  $\Gamma_S(f)$  which clearly has rank  $D$ . The related eigenvalues are,

$$\lambda_i(f) = \lambda_{si}(f) + \alpha(f) \quad (52)$$

These eigenvectors form a basis of the  $D$  dimensional subspace spanned by the  $D$  source position vector  $d_i(f)$ . This subspace will be named the source subspace. The following important relation is proved in the appendix.

$$\sum_{i=1}^D \gamma_i(f) d_i(f) d_i(f)^\dagger = \sum_{i=1}^D [\lambda_i(f) - \alpha(f)] V_i(f) V_i(f)^\dagger \quad (53)$$

b)  $(M-D)$  eigenvectors  $V_i(f)$  which are orthogonal to the preceding eigenvectors have the fundamental property to be orthogonal to all the source position vectors: (see 50)

$$V_i^\dagger(f) d_j(f) = 0 \quad D+1 \leq i \leq M, 1 \leq j \leq D \quad (54)$$

They are a basis of the so-called orthogonal subspace. The eigenvalues corresponding to these eigenvectors are all equal to  $\alpha(f)$ , and consequently smaller than any of these source space eigenvalues. From these properties, high resolution methods are deduced;

a) From the eigenvalues, first the number of sources is determined: it is the number of elements minus the number of the smallest and equal eigenvalues. Then, the source subspace and the complementary orthogonal subspace are set up through a partitioning of the eigenvectors to those that do not correspond and those that do correspond to the smallest eigenvalues.

b) Different methods can be used to exploit the partitioning into the two subspaces in order to obtain the source location. But clearly it is necessary for that to use the source wavefront shape knowledge assumption, from which a position vector model is deduced:  $d(f, \theta)$ ;  $\theta$  stands for the source position. It is possible to use the orthogonal subspace or the source subspace.

c) when using the source space, basically the source parameter  $\theta_i$  and  $\gamma_i(f)$  are extracted from the identity between two matrices. One is a reconstruction from the source subspace, of the sources alone, cross-spectral density matrix;

$$\sum_{i=1}^D [\lambda_i(f) - \alpha(f)] v_i(f) v_i^\dagger(f) \quad (55)$$

The other is a model of the source alone cross-spectral density matrix using the model  $d(f, \theta)$

$$\sum_{i=1}^D \gamma_i(f) d(f, \theta_i) d^\dagger(f, \theta_i) \quad (56)$$

In the general case this identification cannot be achieved directly and adjustment algorithm have to be used.

d) When the orthogonal subspace is used, the source position results from a projection of the position vector model onto the orthogonal subspace according to:

$$G(f, \theta) = \sum_{i=D+1}^M |v_i^\dagger(f) d(f, \theta)|^2 \quad (57)$$

when  $\theta$  varies,  $G(f, \theta)$  produces a null every time  $\theta$  equals the position  $\theta_i$  of a source. The nulls of  $G(f, \theta)$  yield the source location. Knowing them, spectral densities are then at hand. Some authors (Schmidt) use a weighted sum of the square modulus.

The main property of the high resolution method is that its resolution is no longer limited by the signal to noise ratio of the sources as with adaptive array processing: it increases theoretically with the observation time up to infinity. Therefore, asymptotically as averaging time increases, two sources can be resolved no matter how close and how weak, as compared to the background noise.

## 7. MUSIC (Multiple Signal Classification)[7]

### 1) Data Model

The waveform received at the M array elements are a linear combination of the D incident wavefronts and noise that can be expressed as follows

$$\begin{bmatrix} X_1 \\ X_2 \\ \vdots \\ X_M \end{bmatrix} = \begin{bmatrix} a(\theta_1), a(\theta_2), \dots, a(\theta_D) \end{bmatrix} \begin{bmatrix} F_1 \\ F_2 \\ \vdots \\ F_D \end{bmatrix} + \begin{bmatrix} W_1 \\ W_2 \\ \vdots \\ W_M \end{bmatrix}$$

or,

$$X = A F + W \quad (58)$$

where  $a(\theta_i)$  as in (30).

The incident signals are represented in amplitude and phase at some arbitrary reference point by the complex quantities  $F_1, F_2, \dots, F_D$ . The noise whether sensed along the signal or generated internally, is given by the complex vector  $W$ . The element  $a(i,j)$  of the matrix  $A$  are a function of the signal arrival angles and the array element locations. That is,  $a(i,j)$  depends on the  $i$ 'th array element, its position relative to the origin, and its response to a signal incident from the direction of the  $j$ 'th signal.

## 2) The Covariance Matrix $R$

The  $M \times M$  covariance matrix of  $X$  vector is given by

$$R = \overline{X X^\dagger} = A \overline{F F^\dagger} A^\dagger + \overline{W W^\dagger} \quad (59)$$

or

$$R = A P A^\dagger + \lambda_{\min} R_0$$

where the overbar is used for the expectation. When the number of incident wavefronts  $D$  is less than the number of array elements  $M$ ,

then  $APA^\dagger$  is singular; it has a rank less than  $M$ . Therefore

$$|APA^\dagger| = |R - \lambda_{\min} R_0| = 0 \quad (60)$$

This equation is only satisfied with  $\lambda$  equal to one of the eigenvalues of  $R$  in the metric of  $R_0$ . But, for a full rank and  $P$  positive definite,  $APA^\dagger$  must be nonnegative definite. Therefore, any measured  $R = XX^\dagger$  matrix can be written

$$R = APA^\dagger + \lambda_{\min} R_0 \quad (61)$$

where  $\lambda_{\min}$  is the smallest solution to  $|R - \lambda R_0| = 0$ . Note that in the special case wherein the elements of the noise vector  $W$  have zero mean and variance  $\sigma$ , we have  $\lambda_{\min} R_0 = \sigma^2 I$ .

### 3) Calculating the Solution.

The rank of  $APA^\dagger$  is  $D$  and can be determined directly from the eigenvalues of  $R$  in the metric of  $R_0$ . That is, in the complete set of eigenvalues of  $R$  in the metric of  $R_0$ ,  $\lambda_{\min}$  will not always

be simple. In fact, it occurs  $N = M - D$  times. Therefore, the number of the incident signal estimator is

$$D = M - D$$

#### 4) The signal and Noise Subspace.

The  $M$  eigenvectors of  $R$  in the metric of  $R_0$  must satisfy  $R e_i = \lambda_i R_0 e_i, i=1,2,\dots,M$ . Since  $R = APA^\dagger + \lambda_{\min} R_0$ , we have  $APA^\dagger e_i = (\lambda_i - \lambda_{\min}) R_0 e_i$ . Clearly, for each of the  $\lambda_i$  that is equal to  $\lambda_{\min}$ , we must have  $APA^\dagger e_i = 0$  or  $A^\dagger e_i = 0$ . That is the eigenvector associated with  $\lambda_{\min}$  are orthogonal to the space spanned by the column of  $A$ ; the incident signal mode vectors.

#### 5) The algorithm

If  $E_N$  is defined to be the  $M \times M$  matrix whose column are the  $N$  noise eigenvectors, and the ordinary Euclidean distance from a vector  $Y$  to the signal subspace is  $d^2 = Y^\dagger E_N E_N^\dagger Y$  then  $d=0$  if  $Y$  is in the signal subspace. We can plot  $1/d^2$  for points along the  $a(\theta)$  as a function of  $\theta$ . That is



$$P_{MU}(\theta) = \frac{1}{a(\theta)^\dagger E_N E_N^\dagger a(\theta)} \quad (62)$$

when  $\theta = \theta_k$   $a(\theta)$  will be in signal subspace and  $P_{MU}(\theta)$  will have a peak.

Appendix:

From (27) we have

$$\sum_{i=1}^D v_i(f) d_i(f) [d_i(f)^\dagger v_j(f)] = \lambda_{si} v_j(f) \quad (A-1)$$

Multiplying by  $v_j^\dagger(f)$  we have after summation

$$\begin{aligned} & \sum_{i=1}^D \gamma_i(f) d_i(f) d_i^\dagger(f) \left( \sum_{j=1}^D v_j(f) v_j^\dagger(f) \right) \\ &= \sum_{j=1}^D \lambda_{sj} v_j(f) v_j^\dagger(f) \end{aligned} \quad (A-2)$$

Now

$$\sum_{i=0}^D \gamma_i(f) d_i(f) d_i^\dagger(f) v_j(f) v_j^\dagger(f) = 0$$

for  $j=D+1, \dots, M$

Hence

$$\sum_{i=1}^D \gamma_i(f) d_i(f) d_i^\dagger(f) \sum_{j=1}^M v_j(f) v_j^\dagger(f) = \sum_{j=1}^D \lambda_{s_j} v_j(f) v_j^\dagger(f)$$

Using the fact that  $\sum_{j=1}^M v_j(f) v_j^\dagger(f) = 1$

equation (30) follows.

#### References:

- [1] S. Kay, S. Marple, "Spectrum Analysis- A Modern Perspective,"  
Proceeding of IEEE, vol. 69, No. 11, Nov. 1981
- [2] M.S. Bartlett, "Periodogram analysis and continuous spectra,"  
Biometrika, vol. 37, pp 1-16, June 1950.
- [3] R. Blackman and Turkey, "The measurement of power Spectra from  
the point of view of communications Eng. New york: Dover 1959

[4] G. Carter, A. Nuttall, "Brief Summary of a generalized framework for power spectra estimation," Proc. IEEE, vol.68, pp. 1352-1354, Oct. 1980

[5] J. Capon, "high resolution Frequency-wave number spectrum analysis," Proc. IEEE, vol.57, Aug. 1969

[6] G. Bienvenu and L. Kopp, "Optimality of high resolution array processing using the eigen-system approach," IEEE Trans. Acousti., Speech, signal Processing, vol. ASSP-31, Oct. 1983

[7] R.O. Schmidt, "A signal subspace approach to emitter location and spectral estimation," Ph D. dissertation, Stanford Univ., Stanford, CA. Nov. 1981

### 3. MULTIPLE SOURCE DIRECTION FINDING WITH MINIMUM REDUNDANCY ARRAY.

#### 1. Introduction.

The uniform regular array, a linear array with its elements equally spaced (the distance is regularly taken to be  $\lambda/2$ ) was used intensively in direction finding as well as other array processing application. Different algorithms were used to process the output of this array, some of which are described in the previous section.

One of the important drawback of this array is its capability to resolve the maximum number of sources ( $D < M$ ) where  $M$  is the number of element. This fact is due to the dimension of the spatial covariance matrix at the output of the array. One important property of such covariance matrix is the fact of it is being Toeplitz Hermitian matrix. This fact plays an important role in using the uniform regular array in direction finding when implementing different algorithms.

The minimum redundancy array introduced in [1] and used in [2] for direction finding is to be discussed in this chapter. Its property is to be presented and some results of multi-source direction finding simulation are shown.

## 2. Array geometry

For  $D$  waves impinging on a nonuniform linear array, the signal received at the  $i$ 'th element

$$x_i(t) = \sum_{k=1}^D F_k(t) \exp[-j2\pi f_0(d_i/c) \sin\theta_k] + n_i(t) \quad i=1, \dots, M \quad (1)$$

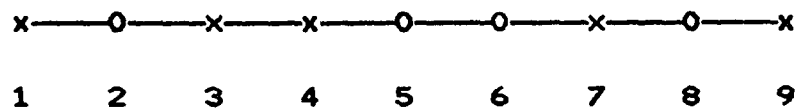
where  $M$  is the number of element,  $\theta_k$   $k=1, \dots, D$ , are the direction of the source with respect to broadside,  $F_k(t)$  is the complex envelope of the  $k$ 'th signal,  $c$  is the speed of light and  $n_i(t)$  are the noise sources which are assumed independent.

The  $i, j$ 'th entry of the covariance matrix will be given by

$$\begin{aligned} R_{ij} &= E \left[ \sum_{k=1}^D F_k(t) \exp[-j2\pi(d_i/\lambda) \sin\theta_k] \right. \\ &\quad \left. \cdot \sum_{m=1}^D F_m(t) \exp[-j2\pi(d_j/\lambda) \sin\theta_m] \right] \\ &= \sum_{k=1}^D P_k \exp[-j2\pi \left( \frac{d_i - d_j}{\lambda} \right) \sin\theta_k] + \sigma^2 \delta(i-j) \quad (2) \end{aligned}$$

where  $P_k = E [ |F_k(t)|^2 ]$  and the different source were assumed uncorrelated. Also we used  $\lambda f = c$ .

For the non-uniform array we will use the following representation and notation: For example 5 element array located as follows



where  $x$  signifies the location of the elements and  $0$  signifies empty location where array element would have been if the array is uniform. We call the integers that correspond to the location of the array elements "index of location". Let us assume that  $D=6$ , then we use the notation

$$\begin{bmatrix} x_1 \\ x_3 \\ x_4 \\ x_7 \\ x_9 \end{bmatrix} = [ a(\theta_1) \ a(\theta_2) \dots a(\theta_6) ] \begin{bmatrix} F_1(t) \\ F_2(t) \\ F_3(t) \\ F_4(t) \\ F_5(t) \\ F_6(t) \end{bmatrix} + \begin{bmatrix} n_1(t) \\ n_2(t) \\ n_3(t) \\ n_7(t) \\ n_{10}(t) \end{bmatrix} \tag{3}$$

where

$$a(\theta_i) = [ e^{-j(2\pi/\lambda)d_1 \sin\theta_i} , e^{-j(2\pi/\lambda)d_3 \sin\theta} , e^{-j(2\pi/\lambda)d_4 \sin\theta} , e^{-j(2\pi/\lambda)d_7 \sin\theta} , e^{-j(2\pi/\lambda)d_9 \sin\theta} ]^T \quad (4)$$

In such notation the covariance matrix R:

$$E [XX^\dagger] = \begin{bmatrix} \overline{X_1 X_1^*} & \overline{X_1 X_3^*} & \overline{X_1 X_4^*} & \overline{X_1 X_7^*} & \overline{X_1 X_9^*} \\ \overline{X_3 X_1^*} & \overline{X_3 X_3^*} & \overline{X_3 X_4^*} & \overline{X_3 X_7^*} & \overline{X_3 X_9^*} \\ \overline{X_4 X_1^*} & \overline{X_4 X_3^*} & \overline{X_4 X_4^*} & \overline{X_4 X_7^*} & \overline{X_4 X_9^*} \\ \overline{X_7 X_1^*} & \overline{X_7 X_3^*} & \overline{X_7 X_4^*} & \overline{X_7 X_7^*} & \overline{X_7 X_9^*} \\ \overline{X_9 X_1^*} & \overline{X_9 X_3^*} & \overline{X_9 X_4^*} & \overline{X_9 X_7^*} & \overline{X_9 X_9^*} \end{bmatrix} + \sigma^2 I \quad (5)$$

where overbar means expectation, I is identity matrix and  $\sigma^2$  is the power of noise. If we choose  $d_i = i\lambda/2$  then (2) becomes,

$$R(i-j) = \sum_{k=1}^D P_k \exp[ -j\pi(i-j)\sin\theta_k ] + \sigma^2 \delta(i-j) \quad (6)$$

$i, j \in \{\text{index of location}\}$

With this (5) becomes

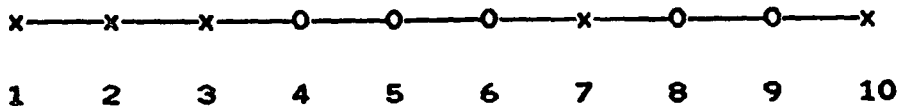
$$R = \begin{bmatrix} R(0) & R(2) & R(3) & R(6) & R(8) \\ R(2)^* & R(0) & R(1) & R(4) & R(6) \\ R(3)^* & R(1)^* & R(0) & R(3) & R(5) \\ R(6)^* & R(4)^* & R(3)^* & R(0) & R(2) \\ R(8)^* & R(6)^* & R(5)^* & R(2)^* & R(0) \end{bmatrix} \quad (7)$$

Notice that this matrix is Hermitian but not toeplitz. Hence it has less redundancy than Uniform Regular Array (URA). It has one entry with R(1) instead of four of these, in a corresponding 5x5 Toeplitz matrix, two entries with R(2) instead of three in a corresponding Toeplitz. Two R(3) and one R(4) as in Toeplitz. One R(5),R(6) and R(8) which could not occur in URA with five elements.

Minimum redundancy Array is a non-uniform array whose covariance is Hermitian wherein the entries above the diagonal has no multiplicity (redundancy). Obviously if, such a case exists, we will have for MRA  $M(M-1)/2$  different R(i).

If for example we distribute the element as follows,





Then the new X vector;

$$X = [X_1, X_2, X_3, X_7, X_{10}]^T$$

and (1,2,3,7,10) is the set of index of location. The corresponding covariance matrix;

$$R_M = \begin{bmatrix} R(0) & R(1) & R(2) & R(6) & R(9) \\ R(1)^* & R(0) & R(1) & R(5) & R(8) \\ R(2)^* & R(1)^* & R(0) & R(4) & R(7) \\ R(6)^* & R(5)^* & R(4)^* & R(0) & R(3) \\ R(9)^* & R(8)^* & R(7)^* & R(3)^* & R(0) \end{bmatrix} \quad (8)$$

This matrix has all covariance lags  $R(i)$   $i=1, \dots, 9$  repeated just ones except  $R(1)$  which is repeated twice.

Now we are in a position to state the requirement on

allocating the array elements so that we get minimum redundancy. From (2), if such a geometry exist then the difference in the index of locations  $(i-j)$  for  $i, j \in \{ \text{set of index of location} \}$   $i \neq j$  span the set of integers  $(1, 2, \dots, M(M-1)/2)$ . Unfortunately such set of index of location does not always exist. Instead for a given  $M$  elements array there exist an  $L \leq M(M-1)/2$  such that the difference of locations  $(i-j)$  for  $i, j \in \{ \text{set of index of location} \}$  span the set of integer  $(1, 2, \dots, L)$ . Notice that for any MRA the highest covariance lag,  $L$  with covariance matrix entry  $R(L)$  and the corresponding array aperture is  $(\lambda/2)L$  (assuming minimum distance between any two element is  $\lambda/2$ ).

One can prove that if there exists an MRA with  $(\lambda/2)L$  aperture then there is another MRA with smaller aperture that is  $(i-j)$  spans the integer  $(1, 2, \dots, L')$ ;  $L' < L$ . Obviously array with  $L'(\lambda/2)$  aperture would have higher redundancy.

It is obvious that if the aperture of the MRA is  $(\lambda/2)(M)(M-1)/2$  then it is unique. If the aperture is smaller, then it is possible to find different "location indices" with the same amount of redundancy except, possibly, different covariance lags are repeated.

Table 3-1

M	L	MRA sequence	redundancy
3	4	0 1 3	None
4	6	0 1 4 6	None
5	9	0 1 2 6 9	1(2)
		0 1 4 7 9	3(2)
6	13	0 1 2 6 10 13	1,4(2)
		0 1 4 5 11 13	1,4(2)
		0 1 6 9 11 13	2,5(2)
7	17	0 1 2 3 8 13 17	2,5(2),1(3)
		0 1 2 6 10 14 17	1,8(2),4(3)
		0 1 2 8 12 14 17	1,2,6,12(2)
		0 1 2 8 12 15 17	1,2,7,15(2)
		0 1 8 11 13 15 17	4,7(2),2(3)
8	23	0 1 2 11 15 18 21 23	1,2,3,10 21(2)
		0 1 4 10 16 18 21 23	2,3,5,6 17(2)
9	29	0 1 2 14 18 21 24 27 29	1,2,6,13 27(2),3(3)
		0 1 3 6 13 20 24 28 29	1,3,4,5,7 23,28(2)
		0 1 4 10 16 22 24 27 29	2,3,5,12 23,28(2)
			1,3,4,5 14,30,35(2)
10	36	0 1 3 6 13 20 27 31 35 36	1,3,4,5 14,30,35(2)
11	43	0 1 3 6 13 20 27 34 38 42	1,3,4,5,21 37,42(2) 14(3),7(4)

Exhaustive computer program was written to find  $L$  for a given  $M$  element array and the corresponding indices locations of the MRA. The program also specify the redundancy element and their multiplicity. Table 3-1 presents these results for MRA with 3 to 11 elements.

Notice that image index location with reference point at the higher end is principally the same array. That is  $\{0\ 1\ 4\ 7\ 9\}$  and  $\{0\ 2\ 5\ 8\ 9\}$  are principally the same array.

From this table we see that(except for the image)  $M=3$  and  $M=4$  are unique with  $L = M(M-1)/2$ . Arrays with higher number of elements result in  $L < M(M-1)/2$  and hence possibly more than one index location for each. Particularly when  $M=7$  there are six different array location arrangements, all with  $L = 17$ .

### 3. The augmented matrix of MRA.

This is an  $(L+1) \times (L+1)$  Toeplitz matrix generated from the entries of the covariance matrix of the MRA, in such a way that  $R(1)$  is used in the first diagonal above the main diagonal,  $R(2)$  in the second diagonal, etc.  $R(L)$  in the higher corner. If we are

dealing with asymptotic case(infinitely many samples are used to obtain R)

$$R = \frac{1}{N} \sum X(n) X(n)^{\dagger}$$

then the covariance lags which are repeated more than ones will be equal with probability one and there is no difference which one to use in the augmented matrix. However if only a limited number of samples, N, are used to obtain R then these covariance lags may differ, so that it is advisable to take the arithmetic average of them.

As an example the augmented matrix generated from (5) is given by

$$R_{aug} = \begin{bmatrix} R(0) & R(1) & R(2) & & R(9) \\ R(1)^* & R(0) & R(1) & & R(8) \\ \vdots & & & & \\ & & & & \\ R(9)^* & & & & R(0) \end{bmatrix} \quad (9)$$

where R(1) is taken as,

$$R(1) = 1/2 \left\{ \frac{1}{N} \sum_{n=1}^N ( X_1(n)X_2(n)^* + X_2(n)X_3(n)^* ) \right\} \quad (10)$$

#### 4. Multi-Source Direction Finding using

the augmented matrix.

The augmented matrix is an  $(L+1) \times (L+1)$  and hence if it is used with any direction finding algorithm, it is capable to resolve  $L$  source direction. For this we must augment the direction vector to contain  $L+1$  elements that is instead

$$a(\theta) = [ 1, \exp[-j\pi(d_2-1)\sin\theta], \dots, \exp[-j(d_M-1)\sin\theta] ] \quad (11)$$

where  $(d_2, d_3, \dots, d_M)$  are the location index set, we must use an augmented direction vector:

$$a_{\text{aug}}(\theta) = [ 1, \exp[-j\pi \sin\theta], \dots, \exp[-j\pi L \sin\theta] ] \quad (12)$$

where in these direction vectors we used the first element of the array as a reference and assumed the array element located at integer multiples of  $\lambda/2$ . If we define the null spectrum  $S(\theta)$  for example

$$S(\theta) = a_{\text{aug}}^\dagger(\theta) \left[ \sum_{i=D+1}^{L+1} e_i e_i^\dagger \right] a_{\text{aug}}(\theta)$$

where  $e_i$ ,  $i = D+1, \dots, L+1$  are the noise eigenvectors of the augmented matrix (assumed  $N$  is very large) then from the peaks of

$$P(\theta) = \frac{1}{S(\theta)}$$

we get the direction  $\theta_k$ ,  $k=1,2, \dots, D$  of the different sources.

## 5. Simulation Results.

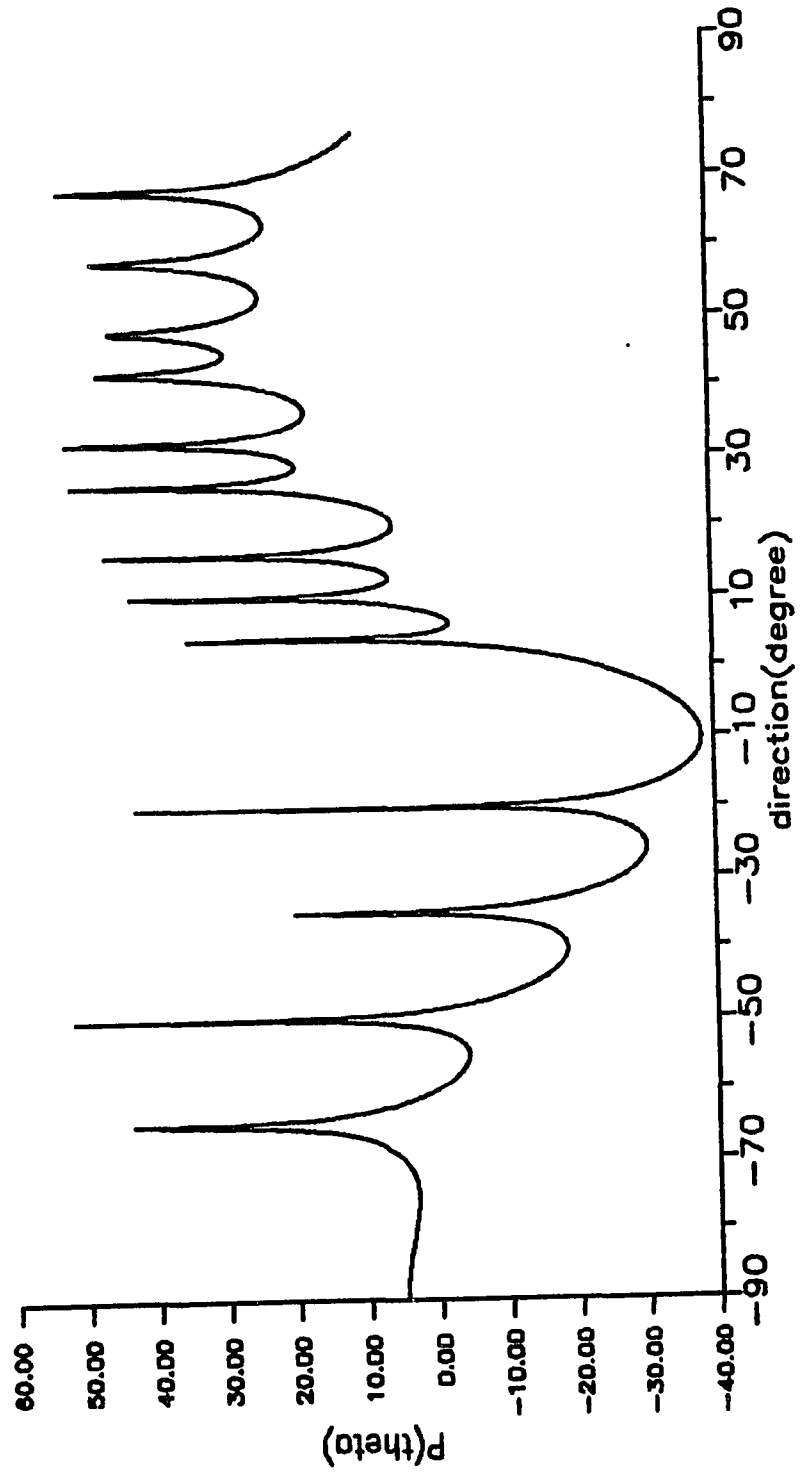
To show the maximum capability of 6 elements array with 13 sources located at direction  $4^\circ, 10^\circ, 16^\circ, 26^\circ, 32^\circ, 42^\circ, 48^\circ, 58^\circ, 68^\circ, -65^\circ, -50^\circ, -35^\circ, -20^\circ$  and  $\text{SNR} = 20$  dB, we used each of the MRA whose location indices are  $(0,1,2,6,10,13)$ ,  $(0,1,4,5,11,13)$  and  $(0,1,6,9,11,13)$ . Asymptotically  $P(\theta)$  is same for the three different formation and the results is shown in fig. 3-1.

**References:**

- [1] A. T. Moffet, "Minimum-Redundancy Linear Array" IEEE Trans. AP. Vol AP-16 No. 2 March, 1968
- [2] S. Pillai, Y. Bar-Ness and F. Haber, "A new approach to array geometry for improved Spatial Spectrum Estimation," Proceeding of IEEE, Vol. 23 No. 10 Oct. 1985



FIG 3-1



#### 4. EFFECTS OF RANDOM DISPLACEMENT OF THE ARRAY ELEMENTS ON THE PERFORMANCE OF DIRECTION FINDING.

##### -UNIFORM REGULAR ARRAY V.S. MINIMUM REDUNDANCY ARRAY-

###### 1. Introduction.

Uniform Regular Array(URA); that is an array whose  $M$  elements are located at an equal distances(customarily  $= \lambda/2$ ) from each other, was intensively used in the literature for direction finding of multi-sources. Different algorithms were used to extract the directions of these sources, Some are known as classical power methods, like the Bartlett estimator[1], others are classified as superresolution methods. Among the latter are, the linear prediction method[2],the maximum likelihood method[3] and the eigenstructure methods. The most popular of the eigenstructure approach is the MUSIC algorithm[4].

With the Minimum Redundancy Array(MRA), the elements are distributed nonuniformly along a line (linear array). [5]

The position of these elements either for URA or MRA can't be accurate. This might be due to the variations in mechanical structure or environmental effects. The best that one can assume about the actual location is that it is at a certain nominal position with some additive random variation which has some known distribution.

Effects of such random displacement of the array elements has been considered in the literature dealing with the interference cancellation problem[6]. To the best of our knowledge, the effects of such displacement on the performance of the direction finder, particularly the one using MRA, has not yet been considered. It is obvious that element displacement from a nominal location will cause perturbations of the covariance matrix elements. This perturbation may cause an error in the estimation of the direction of the signals, particularly if the correlation matrix is obtained from the mean of finite number of snapshots.

The purpose of this chapter is to study the effect of these perturbation on the entries of the covariance matrix and conclude on the effect of these on the performance of a direction finder. In the next sections we will derive the values of the perturbations of the asymptotic covariance matrix entries, due to

one dimensional random displacement uniformly distributed, two dimensional random displacement uniformly distributed, and two dimensional random displacement Gaussian distributed. These results are compared to one another. The resultant perturbed covariance matrix is found in section(5) and the conclusion about the meaning of the difference between perturbed and nominal matrix and their effect on direction estimation is stated. In section (6) the definition of the statistical randomly perturbed covariance matrix is presented and in section (7) simulation results are shown and discussed.

## 2. Random perturbation in one dimension, uniform probability distribution.

For the linear array we assume the elements are nominally located at the x axis at a distance  $d_i$ ,  $i=1,\dots,M$  from some reference point, regularly taken as integer multiple of  $\lambda/2$  i.e  $d_i = l_i \lambda/2$ ,  $l_i$  are integers( see Fig 4-1). The received signal at the  $i$ 'th location is

$$X_i(t) = \sum_{k=1}^D F_k(t) \exp[ j\omega_0(t - \frac{d_i}{c} \sin \theta_k) ] + n_i(t)$$

$$i = 1, \dots, M \quad (1)$$

when D is the number of signals impinging on the array assumed uncorrelated and narrow-band.  $\theta_k$ ,  $k=1, \dots, D$  are the directions of these sources with respect to broadside.  $F_k(t)$  is the complex envelope of the k'th signal, c is the speed of light and  $n_i(t)$  are noise source which are assumed independent, delta correlated with variance  $\sigma_n^2$ , and independent of the signals. Considering the perturbation of the location, we define

$$d_i = (l_i \frac{\lambda}{2} + u_i(t) ) \quad (2)$$

where  $u_i(t)$  are independent random variable uniformly distributed between  $-\delta$  to  $+\delta$  and its pdf is  $f_{u_i}(u) = 1/2\delta$  for  $|u| \leq \delta$ ,  $\delta$  is the maximum displacement.

Defining the received signal in a vector form, then the covariance matrix of X; the received vector, is given by

$$R' = E [ X(t) X(t)^\dagger ] \quad (3)$$

$E [ ]$  is the expectation and

$$x(t) = [ x_1(t), x_2(t), \dots, x_M(t) ]^T \quad (4)$$

with  $x_i(t)$  defined in (1).

The  $i, j$ 'th entry of covariance matrix  $R'$

$$\begin{aligned} R'_{ij} &= E [ x_i(t) x_j(t) ] \\ &= E \left( \left[ \sum_{k=1}^D F_k(t) \exp [j\omega_0(t - \frac{d_i}{c} \sin\theta_k)] + n_i(t) \right] \times \right. \\ &\quad \left. \left[ \sum_{m=1}^D F_m^*(t) \exp [-j\omega_0(t - \frac{d_j}{c} \sin\theta_m)] + n_j^*(t) \right] \right) \end{aligned}$$

substituting for  $d_i$  from (2) we get after some manipulation

$$\begin{aligned} R'_{ij} &= \sum_{k=1}^D \sum_{m=1}^D E \left\{ F_k(t) F_m^*(t) \exp [ -jk_0(l_i \frac{\lambda}{2} + u_i) \sin\theta_k(t) ] \right. \\ &\quad \left. \exp [ jk_0(l_j \frac{\lambda}{2} + u_j) \sin\theta_m(t) ] \right\} + \sigma_n^2 \delta(i-j) \end{aligned} \quad (5)$$

where we used the fact that the signal sources and the additive noise are independent also  $k_0 = \omega_0/c$ . Rearranging (5) we get

$$R'_{ij} = \sum_{k=1}^D \sum_{m=1}^D E \left[ F_k(t) e^{-jk_0 l_i \frac{\lambda}{2} \sin \theta_k} F_m^*(t) e^{jk_0 l_j \frac{\lambda}{2} \sin \theta_m} e^{-jk_0 u_i \sin \theta_k} e^{jk_0 u_j \sin \theta_m} \right] + \sigma_n^2 \delta(i-j) \quad (6)$$

The expected value inside the parenthesis could be obtained using the equation

$$E_{F_k F_m} [ \quad ] = E_{u_i u_j} [ E_{F_k F_m} ( \quad | u_i u_j ) ]$$

We are only handling the case of uncorrelated sources then the term in (6) becomes after performing the conditional expectation

$$E [ x_i(t) x_j(t) | u_i, u_j ] = \sum_{k=1}^D P_k \exp [jk_0 (l_j - l_i) \frac{\lambda}{2} \sin \theta_k] \exp [jk_0 (u_j - u_i) \sin \theta_k] + \sigma_n^2 \delta(i-j) \quad (7)$$

where  $P_k = E [ | F_k(t) |^2 ]$  is the power of the  $k$ 'th signal.

Clearly from (7)

$$R'_{ij} = E [ E [ x_i(t) x_j(t) | u_i, u_j ] ]$$

$$= \sum_{k=1}^D P_k \exp [ jk_0(l_j - l_i) \frac{\lambda}{2} \sin \theta_k ]$$

$$E [ \exp [ jk_0(u_j - u_i) \sin \theta_k ] ] + \sigma_n^2 \delta(i-j) \quad (8)$$

Now

$$E [ \exp(jk_0 u_j \sin \theta_k) ] = \int_{-\delta}^{\delta} \exp(jk_0 u \sin \theta_k) f_{u_j}(u) du$$

$$= \frac{1}{2\delta} \int_{-\delta}^{\delta} \exp(jk_0 u \sin \theta_k) du$$

$$= \frac{\sin(k_0 \delta \sin \theta_k)}{k_0 \delta \sin \theta_k}$$

$$\equiv \eta_k \quad (9)$$

It is reasonable to assume that the perturbation at different location are independent, leading to:



$$\begin{aligned}
E [ e^{jk_0(u_j - u_i)\sin\theta_k} ] &= E [ e^{jk_0 u_j \sin\theta_k} ] E [ e^{-jk_0 u_i \sin\theta_k} ] \\
&= \eta_k^2 && \text{for all } i \neq j \\
&= 1 && \text{for } i = j \qquad (10)
\end{aligned}$$

$u_i$  has the same distribution as  $u_j$  and it is easy to show that the second term in (10) leads to the same result of (9), despite the negative sign in the exponent.

Finally substituting (10) together with (9) in (8) we end up with

$$\begin{aligned}
R'_{ij} &= \sum_{k=1}^D P_k \exp [ jk_0(l_j - l_i) \frac{\lambda}{2} \sin\theta_k ] \eta_k^2 && \text{for } i \neq j \\
&= \sum_{k=1}^D P_k + \sigma_n^2 && \text{for } i = j
\end{aligned} \qquad (11)$$

We define an error in the elements of the covariance matrix caused by the perturbation by

$$\Delta R_{ij} = | R'_{ij} - R_{ij} |$$

where  $R_{ij}$  is the  $i, j$ 'th entry of the covariance matrix under

unperturbed condition, i.e when the elements at their nominal location with  $\delta = 0$  and hence  $\eta_k = 0$  for all  $k=1, \dots, D$ . Then obviously

$$\Delta R_{ij} = \left| \sum_{k=1}^D P_k \exp \left[ j k_0 (l_j - l_i) \frac{\lambda}{2} \sin \theta_k \right] (1 - \eta_k^2) \right|$$

for  $i \neq j$

$$= 0 \quad \text{for } i = j$$

(12)

Notice that  $\eta_k$  is a function of  $\sin \theta_k$ , in a way that when  $\theta_k = 0$ ; the source is broadside to the array, then  $\Delta R_{ij} = 0$ . That is no error is caused by the random perturbation of the array element location.

### 3. Random Perturbation in two dimensions, uniform distribution.

We assume that beside the perturbation in the x axis, there exists another perturbation orthogonal to the x axis in a plane that contains the x-axis and the source( this assumption makes

sense since we are considering direction in one plane, azimuth for example). Fig.4-2 depicts the second dimensional perturbation. From it we notice that due to the perturbation  $v_i$  the delay of the wave is changed from  $d_i \sin \theta_k$  for the nominal location to  $d_i \sin \theta_k + v_i \cos \theta_k$  ( $v_i$  consider a positive perturbation if it is toward the source in the plane previously mentioned).

Taking this fact into consideration we have for the two dimensional perturbation instead of (8)

$$R'_{ij} = \sum_{k=1}^D P_k \exp \left[ jk_0(l_j - l_i) \frac{\lambda}{2} \sin \theta_k \right] \cdot E \left[ \exp \left[ jk_0 \left( (u_j - u_i) \sin \theta_k + (v_j - v_i) \cos \theta_k \right) \right] \right] + \sigma_n^2 \delta(i-j) \quad (13)$$

As before:

$$E \left[ \exp( jk_0 v_j \cos \theta_k ) \right] = \frac{\sin (k_0 \delta \cos \theta_k)}{k_0 \delta \cos \theta_k} \quad (14)$$

Where we assumed the second dimensional perturbation is also uniform  $(-\delta, \delta)$ . Again if perturbation of the different element locations, as well as in different dimensions are independent then

$$\begin{aligned}
& E \left[ \exp \left[ jk_0 \left( (u_j - u_i) \sin \theta_k + (v_j - v_i) \cos \theta_k \right) \right] \right] \\
&= \frac{\sin^2(k_0 \delta \sin \theta_k)}{(k_0 \delta \sin \theta_k)^2} \times \frac{\sin^2(k_0 \delta \cos \theta_k)}{(k_0 \delta \cos \theta_k)^2} \\
&\equiv \eta_k'^2 && i \neq j && (15) \\
&= 1 && i = j
\end{aligned}$$

where we also used (9).

Comparing (9) with (15) we conclude the following inequality

$$\eta_k'^2 \leq \eta_k^2 \leq 1 \quad (16)$$

#### 4. Random Perturbation with Gaussian Distribution.

The only difference in this case is the probability density function,

$$\begin{aligned}
E \left[ \exp(jk_0 u_j \sin \theta_k) \right] &= \frac{1}{\sqrt{2\pi\sigma^2}} \int_{-\infty}^{+\infty} \exp(jk_0 u \sin \theta_k) e^{-u^2/2\sigma^2} du \\
&= e^{-\frac{\sigma^2}{2} k_0^2 \sin^2 \theta_k} && (17)
\end{aligned}$$

The last step was derived in the appendix. Similarly,

$$E [ \exp( jk_0 v_j \cos\theta_k ) ] = e^{-\frac{\sigma^2}{2} k_0^2 \cos^2\theta_k} \quad (18)$$

Also notice from the derivation in the appendix that the result, does not change for  $E [ \exp( -jk_0 u_j \sin\theta_k ) ]$  or  $E [ \exp( -jk_0 v_j \cos\theta_k ) ]$ . Therefore

$$\begin{aligned} & E \left[ \exp \left[ jk_0 \left( (u_j - u_i) \sin\theta_k + (v_j - v_i) \cos\theta_k \right) \right] \right] \\ &= \left( e^{-\frac{\sigma^2}{2} k_0^2 (\sin^2\theta_k + \cos^2\theta_k)} \right)^2 \\ &= e^{-\sigma^2 k_0^2} \quad (\equiv \eta_k^*) \quad \text{for} \quad i \neq j \\ &= 1 \quad \text{for} \quad i = j \quad (19) \end{aligned}$$

To try to relate  $\eta_k^*$  to  $\eta_k^*$ ; we first notice from Appendix . 2 equation (A-2) that

$$\eta_k^* \approx 1 - \frac{k_0^2 \delta^2}{6} + \frac{1}{120} k_0^4 \delta^4 + \dots \quad (20)$$

and from (A-3), if we take  $\sigma^2 = \delta^2/3$  that

$$\eta_k^* \approx 1 - \frac{k_0^2 \delta^2}{6} + \frac{1}{72} k_0^4 \delta^4 + \dots \quad (21)$$

Therefore

$$\eta_k'^2 \leq \eta_k^{*2} < 1 \quad (22)$$

5. Variation of the Covariance Matrix due to perturbation in the element location.

From (11) we can write for the entries of the covariance matrix

$$\begin{aligned} R_{ij}' &= \sum_{k=1}^D P_k \exp [ jk_0(l_j - l_i) \frac{\lambda}{2} \sin \theta_k ] \xi_k^2 & i \neq j \\ &= \sum_{k=1}^D P_k + \sigma_n^2 & i = j \end{aligned} \quad (23)$$

where  $\xi_k$  represents the different kinds of perturbation :

$$1. \quad \eta_k = \frac{\sin(k_0 \delta \sin \theta_k)}{k_0 \delta \sin \theta_k} \quad (24)$$

for one dimensional uniform distribution  $(-\delta, \delta)$  as in (9)

$$2. \quad \eta_k^* = \frac{\sin(k_0 \delta \sin \theta_k)}{k_0 \delta \sin \theta_k} \times \frac{\sin(k_0 \delta \cos \theta_k)}{k_0 \delta \cos \theta_k} \quad (25)$$

For two dimensional uniform distribution  $(-\delta, \delta)$  as in (15)

$$3. \quad \eta_k^* = e^{-\sigma^2 k_0^2 / 2} \quad (26)$$

for two dimensional Gaussian distribution  $\mathcal{N}(0, \sigma^2)$  as in (19).

Now let us define

$$a(\theta_k) = [ 1, \exp(-jk_0 l_2 \frac{\lambda}{2} \sin \theta_k), \dots, \exp(-jk_0 l_M \frac{\lambda}{2} \sin \theta_k) ] \quad (27)$$

when we took  $l_1 = 0$ ; that is the reference point is at the first element. If we are considering URA then in (24)  $l_i = i-1$   $i=1, 2, \dots, M$  and the covariance matrix is  $M \times M$ . For the MRA we must form the augmented matrix which is a Toeplitz matrix whose entries along the different diagonals are given by,

$$\sum_{k=1}^D P_k \exp \left[ jk_0 \frac{i\lambda}{2} \sin \theta_k \right] \quad i=1, 2, \dots, L$$

where  $L \leq M(M-1)/2$  and the matrix is  $(L+1) \times (L+1)$ .

From (23) with  $l_1 = 0$  and (27) we write for the perturbed covariance matrix

$$R' = \sum_{k=1}^D \xi_k^2 P_k a(\theta) a(\theta)^\dagger + \sum_{k=1}^M P_k (1 - \xi_k^2) I + \sigma_n^2 I \quad (28)$$

$$= S' + N' + N$$

where

$$S' = \sum_{k=1}^D \xi_k^2 P_k a(\theta_k) a(\theta_k)^\dagger \quad (29)$$

$$N' = \sum_{k=1}^D P_k (1 - \xi_k^2) I \quad (30)$$

$$N = \sigma_n^2 I \quad (31)$$

$S'$ ,  $N'$  and  $N$  are the signal, the perturbation and the additive noise covariance matrices, respectively. For the unperturbed array the covariance matrix is given by

$$R = \sum_{k=1}^D P_k a(\theta_k) a(\theta_k)^\dagger + \sigma_n^2 I \quad (32)$$

$$= S + N$$



where

$$S = \sum_{k=1}^D P_k a(\theta_k) a(\theta_k)^{\dagger} \quad (33)$$

and

$$N = \sigma_n^2 I \quad (34)$$

$$\begin{aligned} R' - R &= S' - S + N' \\ &= \sum_{k=1}^D (\xi_k^2 - 1) P_k a(\theta_k) a(\theta_k)^{\dagger} + \sum_{k=1}^D (1 - \xi_k^2) P_k I \end{aligned} \quad (35)$$

$\xi_k^2 \leq 1$  hence (28) means that due to perturbation the effective powers of the different signal decrease by a factor =  $\xi_k^2$  and an extra noise  $N'$  is generated which is equivalent to an additive noise whose variance

$$\sigma_{n'}^2 = (1 - \xi_k^2) P_k \quad (36)$$

This is to say that as an effect of perturbation the resultant signal-to-noise ratio reduced. The effect of this on errors in direction finding depends on the algorithm used. If a superresolution method is used for example then such perturbation has no effect(see appendix 3). We emphasize that in calculating

the matrices  $R$  and  $R'$  we used an expectation which is, with ergodic assumption, equivalent to using  $N$  ( $N \rightarrow \infty$ ) snapshots or what is termed asymptotic covariance matrices.

## 6. Statistical Randomly Perturbed Covariance Matrix.

Let the received vector at the  $n$ 'th snapshot be defined by

$$X(n) = \sum_{k=1}^D F_k(n) a_n(\theta_k) + n(n) \quad (37)$$

$$\theta_k = 1, 2, \dots, D$$

where

$$a_n(\theta_k) = \left[ 1, \exp \left[ -jk_0 \left( l_2 \frac{\lambda}{2} + u_{2n} \right) \sin \theta_k \right], \right. \\ \left. \dots, \exp \left[ -jk_0 \left( l_M \frac{\lambda}{2} + u_{Mn} \right) \sin \theta_k \right] \right]^T \quad (38)$$

$F_k(n)$  is the sample at the  $n$ 'th snapshot of the complex envelope of the  $k$ 'th signal,  $u_{in}$   $i=1, \dots, M$ , is the sample at the  $n$ 'th snapshot of the random perturbation. The statistical covariance matrix is given by

$$R^* = \frac{1}{N} \sum_{n=0}^N X(n) X(n)^{\dagger} \quad (39)$$

Each entry of  $R^*$  will be the average of  $N$  snapshots of terms like (5). Calculating the effect of perturbation directly from this equation is impossible. Instead numerical simulation is the way used to obtain the results and draw conclusions.

## 7. Simulation Results

Many simulation runs were performed to examine the effects of the array random displacements on the direction finding performance of the arrays. Both uniform regular array and minimum redundancy array structures were used. As a direction finding algorithm the MUSIC was implemented. The emphasis was mostly on statistical behavior with a finite number of snapshots. In some cases a large number of snapshots were used, so that we learned about the asymptotic behavior as well.

With 5 element URA and three sources impinging on the array from  $10^\circ$ ,  $20^\circ$  and  $30^\circ$  off broadside, we depict in Fig 4-3 the average error in direction (i.e sum of errors divided by number of sources) versus the number of snapshots. As expected errors are larger when we use two dimensional, instead of one dimensional perturbation or when we increase the maximum value of perturbation

$\delta$ . Also it is clear from this curve as well as from others that errors go to zero asymptotically as was concluded in the text. Particularly worth noticing, that when we include two dimensional perturbation the direction finding estimator becomes very poor when we use a small number of snapshots. Not as bad, when only one dimensional perturbations are taken into account, Fig 4-4 is similar to Fig 4-3 except the comparison is now done for two dimensional uniform to two dimensional Gaussian perturbation.

In obtaining the result in Fig 4-5 we used an MRA instead of URA and compare the performance of the first when one dimensional and two dimensional uniform perturbations are used. Fig 4-6 compares the performance of MRA when the perturbations are two dimensional uniform versus when the perturbation are two dimensional Gaussian. Using  $\delta = 0.1\lambda$ , the average error of MRA with only one dimensional perturbation converge to almost asymptotic value(zero) with only 100 snapshots. It is very clear from these figures that despite perturbation MRA outperforms the URA. Direct comparison of these two arrays performances are shown in Fig 4-7. The superiority of the MRA on URA becomes questionable when we restrict ourselves to small number of snapshots, particularly when  $\delta = 0.25\lambda$ . This fact is clearly depicted in Fig

4-8 and Fig 4-9. The cross over point, that is the number of snapshots below which URA performs better than MRA are different in these figures. This is due to the fact that the equivalent noise due to perturbation depends on the direction of sources which are taken  $25^\circ, 45^\circ$  in Fig 4-9 and  $30^\circ, 45^\circ$ , instead, in Fig 4-9. In Fig 4-10, on the other hand such cross-over does not occur. This is because in obtaining the result of this figure with URA we used three sources instead of two and hence the noise vector subspace has dimension two instead of three, a loss of large percentage in smoothing capability. For MRA the dimension of the noise vector subspace is 7 instead of 8. This is not a very big difference.

To show the effect of redundancy in the covariance matrix entries on the performance we compare in Fig 4-11 the average error in direction when we use the entries of the covariance matrix as they result from measurement (unaveraged covariance matrix), together with the case when all entries along any diagonal is first averaged and then used (averaged covariance matrix). Fig 4-12 is the same as Fig 4-11 except for the difference in direction of one of the sources. Notice that the larger  $\theta_k$  ( $30^\circ$  instead of  $25^\circ$ ) larger the effective noise caused

by perturbation and the larger is the direction estimation error. This fact can be concluded from comparing the result of these two figures (Fig 4-12 versus Fig 4-11). In Fig 4-13 and Fig 4-14 we added for comparison to the result already depicted in Fig 4-11 and Fig 4-12 the average direction estimation error obtained with 5 element MRA.

## 8. Conclusion.

The effect of random displacements of array location, on the performance of direction finding was studied in this chapter. Different probability density functions were used; one dimensional uniform, two dimensional uniform and two dimensional Gaussian distribution. It was found that in the steady state (i.e. when number of snapshot used are infinitely large), such perturbation is equivalent to an added white noise and a reduction in signal power. Two dimensional perturbations caused large effect than one dimensional. Also two dimensional uniform perturbation causes more degradation than Gaussian distribution. In all cases degradation depends on the direction of sources; worse when the source is further away from broadside.

Since these perturbation only reduce signal-to-noise ratio, it is expected that superresolution methods, if used, will not suffer degradation in the steady state (This was shown by simulation). Nevertheless, when only limited number of snapshots were used, simulation shows error in estimating the direction of source worse when signal-to-noise ratio is worse. Many results of this kind of simulation are given in this chapter.

Simulating perturbations effect on minimum redundancy array elements depicts superior performance of this array in comparison to the regular uniform array, despite the fact that the later exploits redundancy in getting more precise covariance matrix. This is due to the fact the MRA is using more eigenvectors to resolve the source direction.

Appendix 1

$$E = \frac{1}{\sqrt{2\pi\sigma^2}} \int_{-\infty}^{+\infty} e^{jk_0 u \sin \theta_k} e^{-u^2/2\sigma^2} du$$

$$= e^{-k_0^2 \frac{\sigma^2}{2} \sin^2 \theta_k} \frac{1}{\sqrt{2\pi\sigma^2}} \int_{-\infty}^{+\infty} \exp\left[-\left(\frac{u^2}{2\sigma^2} + jk_0 u \sin \theta_k - k_0^2 \sigma^2 \sin^2 \theta_k / 2\right)\right] du$$

when we in fact completed to a square the argument of the exp.

Rewriting the last integral we have

$$E = e^{-k_0^2 \frac{\sigma^2}{2} \sin^2 \theta_k} \int_{-\infty}^{+\infty} \frac{1}{\sqrt{2\pi\sigma^2}} \exp\left[-(u + jk_0 \sin \theta_k \sigma^2)^2 / 2\sigma^2\right] du$$

The integrant of this integral is a Gaussian probability density function with mean equals  $-jk_0 \sin \theta_k \sigma^2$  and variance  $\sigma^2$ . therefore value of this integral is unity and

$$E = e^{-\left(\frac{\sigma^2}{2} k_0^2 \sin^2 \theta_k\right)} \quad (A-1)$$



Appendix 2

let from (15)

$$\eta_k^s = \frac{\sin X}{X} \times \frac{\sin Y}{Y}$$

where

$$X = K_0 \delta \sin \theta_k$$

and

$$Y = k_0 \delta \cos \theta_k$$

Now

$$\frac{\sin X}{X} \times \frac{\sin Y}{Y} \approx \frac{1}{XY} ( X - X^3/3! + X^5/5! - X^7/7! + \dots )$$

$$( Y - Y^3/3! + Y^5/5! - Y^7/7! + \dots )$$

$$\approx \frac{1}{XY} [ XY - \frac{X Y^3}{3!} + \frac{X Y^5}{5!} - \frac{X Y^7}{7!} + \dots$$

$$- \frac{Y X^3}{3!} + \frac{X^3 Y^3}{(3!)^2} - \frac{X^3 Y^5}{3!5!} + \frac{X^3 Y^7}{3!7!} + \dots$$

$$+ \frac{Y X^5}{5!} - \frac{X^5 Y^3}{3!5!} + \frac{X^5 Y^5}{(5!)^2} + \dots$$

$$- \frac{X^7 Y}{7!} + \frac{X^7 Y^3}{3!7!} + \dots$$

$$\begin{aligned}
&\approx 1 - \frac{Y^2 + X^2}{3!} + \frac{Y^4 + X^4}{5!} + \frac{X^2 Y^2}{(3!)^2} - \dots \\
&\approx 1 - \frac{k_0^2 \delta^2 (\cos^2 \theta_k + \sin^2 \theta_k)}{6} \\
&\quad + \frac{1}{120} ( k_0^4 \delta^4 \cos^4 \theta_k + k_0^4 \delta^4 \sin^4 \theta_k + \\
&\quad \quad \quad \frac{120}{36} k_0^2 \delta^2 \sin^2 \theta_k \cos^2 \theta_k ) + \dots
\end{aligned}$$

$$\eta_k^* \approx 1 - k_0^2 \delta^2 / 6 + \frac{1}{120} k_0^4 \delta^4 \tag{A-2}$$

From (19)

$$\begin{aligned}
\eta_k^* &= e^{-\sigma^2 k_0^2 / 2} \\
&\approx 1 - \frac{\sigma^2 k_0^2}{2} + \frac{(\sigma^2 k_0^2)^2}{8} + \dots
\end{aligned}$$

taking  $\sigma^2 = \delta^2 / 3$  we get

$$\eta_k^* \approx 1 - \frac{\delta^2 k_0^2}{6} + \frac{\delta^4 k_0^2}{72} + \tag{A-3}$$

### Appendix 3

If  $\theta_i$   $i = D+1, \dots, M$  is an eigenvector which belong to the noise subspace, then from (32), using the fact that  $\mathbf{e}_i$  is orthogonal to  $\mathbf{a}(\theta_k)$   $k=1,2,\dots,D$  we get

$$\begin{aligned} R \mathbf{e}_i &= \sum_{k=1}^D P_k \mathbf{a}(\theta_k) \mathbf{a}(\theta_k)^\dagger \mathbf{e}_i + \sigma_n^2 \mathbf{I} \mathbf{e}_i \\ &= \sigma_n^2 \mathbf{e}_i \end{aligned} \quad \text{A-4}$$

as expected.

Now using (28)

$$\begin{aligned} R' \mathbf{e}_i &= \sum_{k=1}^D \xi_k P_k \mathbf{a}(\theta_k) \mathbf{a}(\theta_k)^\dagger \mathbf{e}_i + \left( \sum_{k=1}^D P_k (1-\xi_k)^2 + \sigma_n^2 \right) \mathbf{I} \mathbf{e}_i \\ &= \left( \sum_{k=1}^D P_k (1-\xi_k)^2 + \sigma_n^2 \right) \mathbf{I} \mathbf{e}_i \end{aligned} \quad \text{A-5}$$

That if  $\mathbf{e}_i$  is noise eigenvectors for  $R$  corresponds to  $\sigma_n^2$  then it is also noise eigenvector (orthogonal to signal direction) which correspond to  $\lambda_i = \sum_{k=1}^D P_k (1-\xi_k)^2 + \sigma_n^2$

## References

- [1] M.S. Bartlett, "Peridogram analysis and continuous spectra," *biometrika*, vol. 37, pp 1-16 June 1950
- [2] M. Morf, B. Dickenson, T. Kailath and A. Viterbi, "Efficient solution of Covariance equation for Linear prediction, IEEE Trans, Acoust. speech signal processing., vol. ASSP-25, pp. 429-433, Oct. 1977
- [3] J. Capon, "High-resolution frequency-wavenumber spectrum analysis," in *Proc. IEEE*, vol. 57 pp 1408-1418, Aug. 1969
- [4] R.O. Schmidt, "Multiple emitter location and signal parameter estimation," in *Proc. RADC spectral Est. Workshop*, Griffis AFBS, NY 1979
- [5] S. Pillai, Y. Bar-ness and F. Haber, "A new Approach to Array Geometry for improved Spatial Spectrum estimation," *Proceeding of the IEEE* vol 23 No 10 oct. 1985
- [6] C. Yeh, F. Haber, Y. Bar-Ness, "Effect of Random Amplitude and Steering Phase Error on the Behavior of the Hybrid Array" *The Globcom 84*, Conference paper 7.3, Atlanta, Georgia, Nov. 26-29, 1983.

FIG 4-1

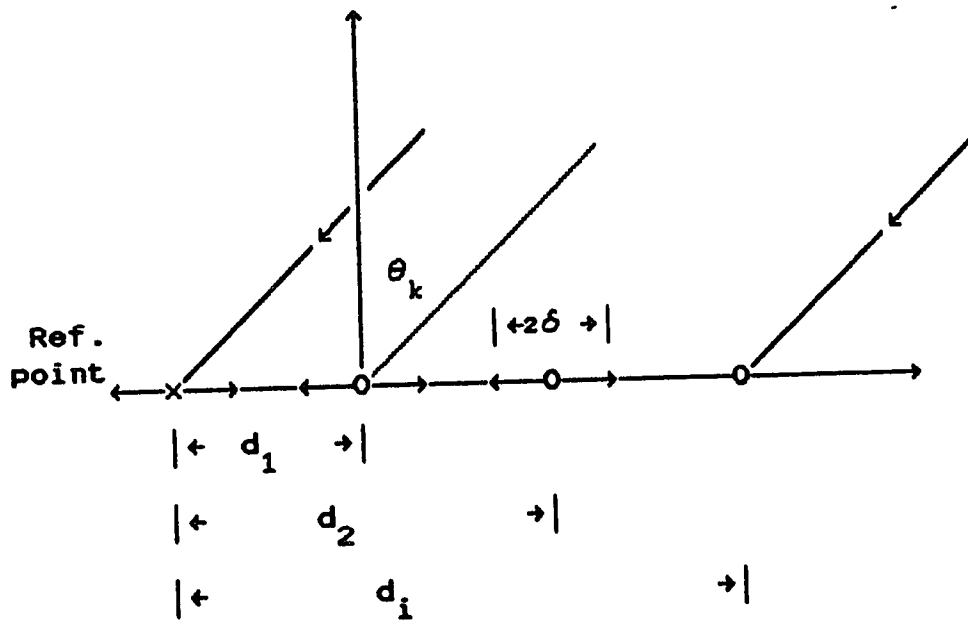


FIG 4-2

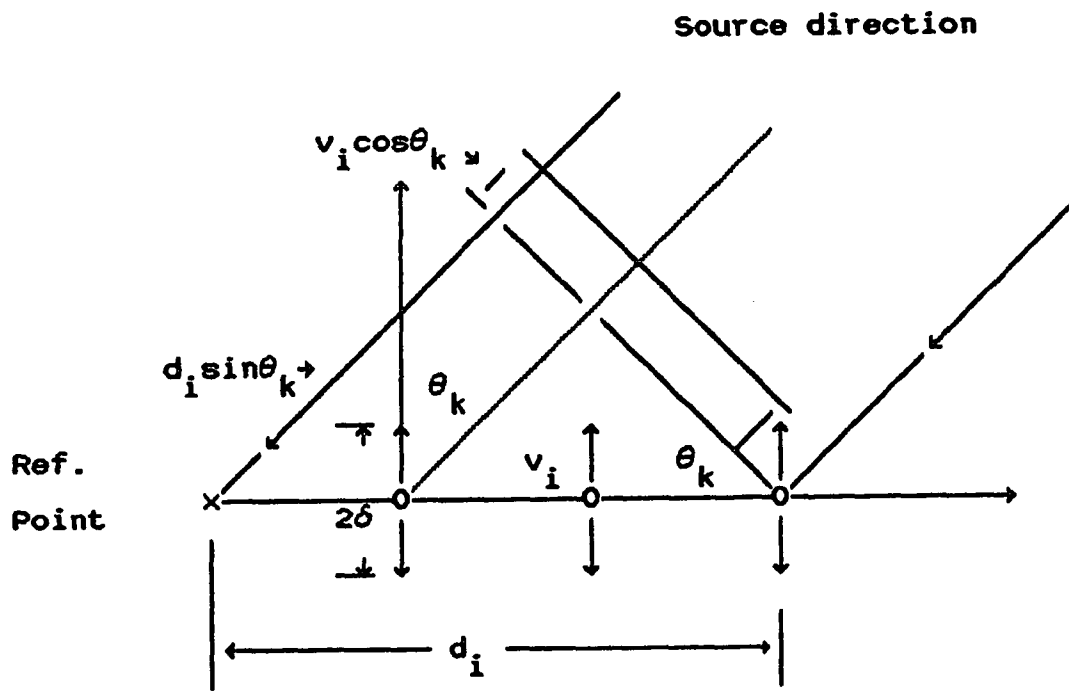


FIG 4-3

5 elements URA.  
Solid: 2 dim. Unif. pert. Dashed: 1 dim. Unif. pert.  
Upper:  $\delta = 0.125$  lamda lower:  $\delta = 0.1$  lamda

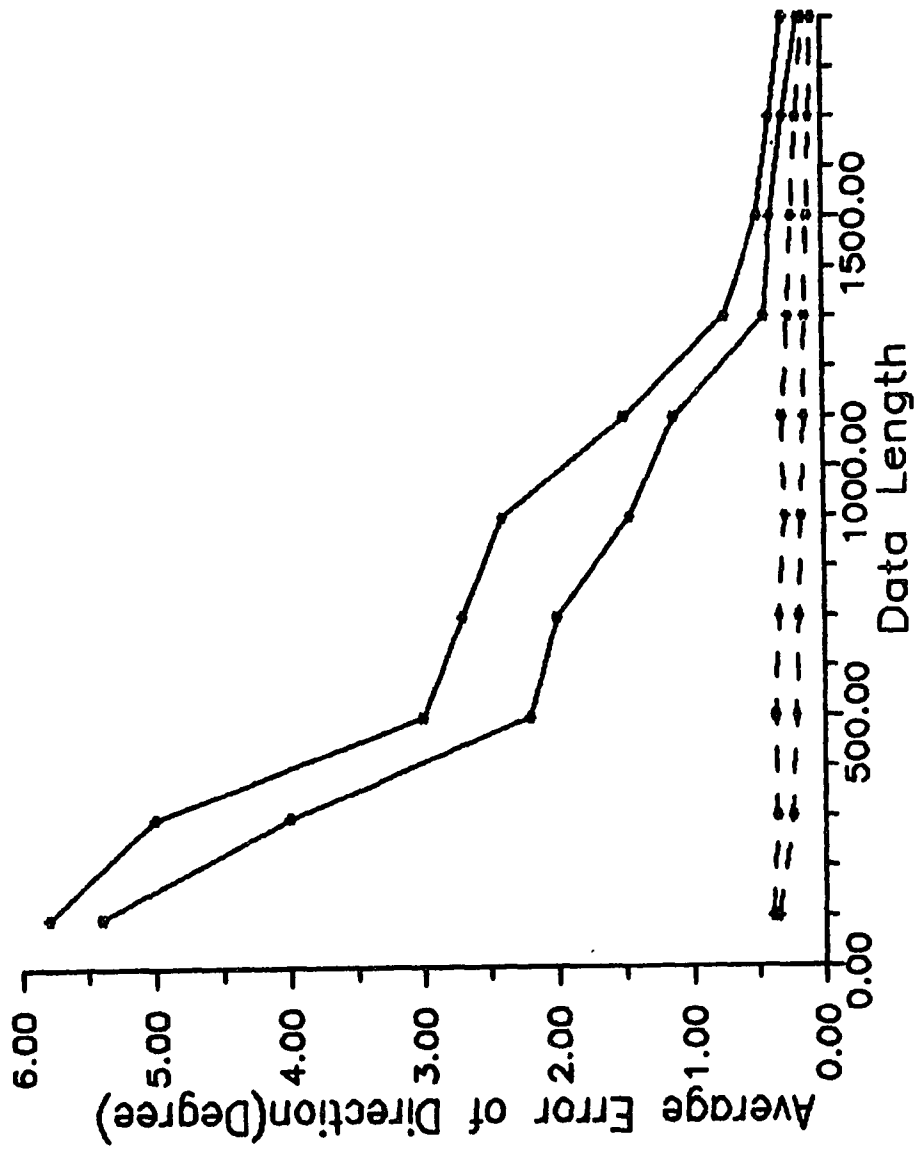


FIG 4-4

5 elements URA.  
Solid: 2 dim. Unif. pert. Dashed: 2 dim. Gaus. pert.  
Upper:  $\delta = 0.125$  lamda lower:  $\delta = 0.1$  lamda (UNIF.)  
Upper:  $\sigma = 0.07$  lamda lower:  $\sigma = 0.05$  lamda (GAUS.)

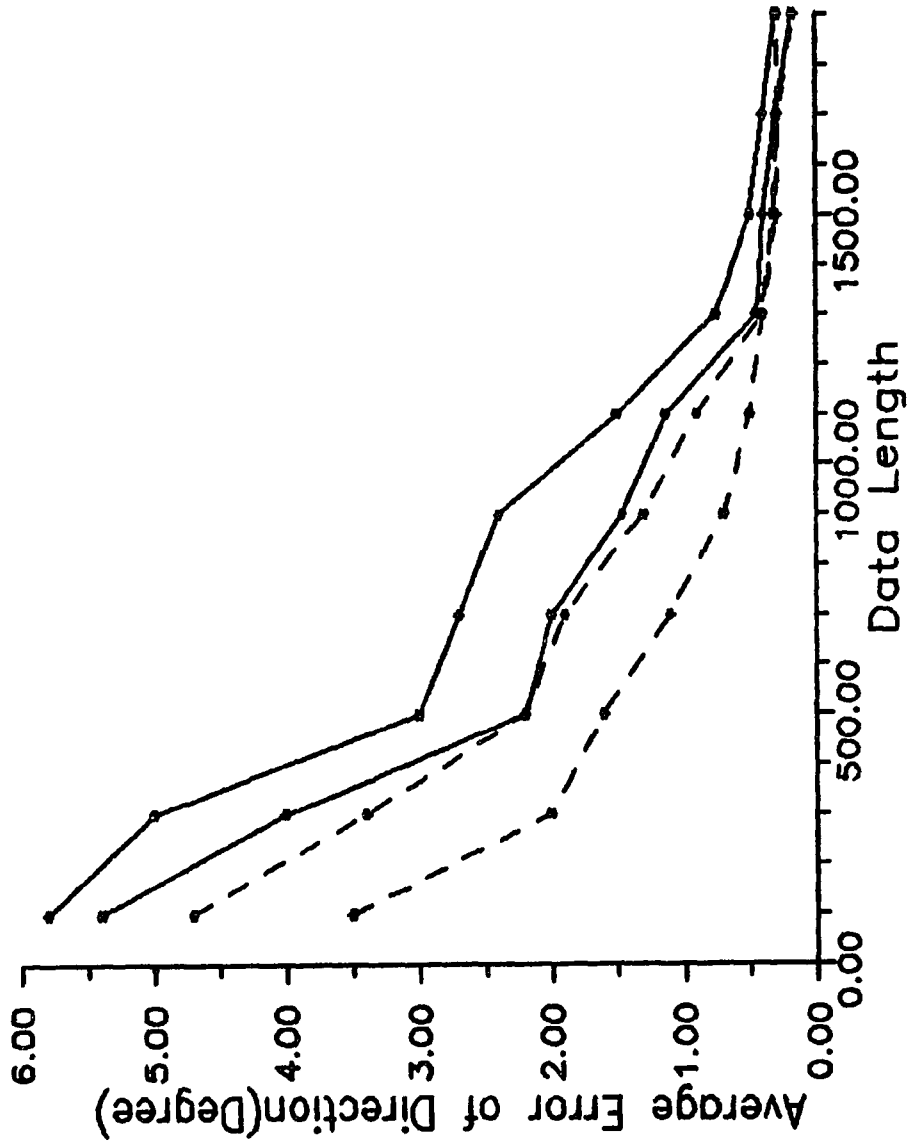
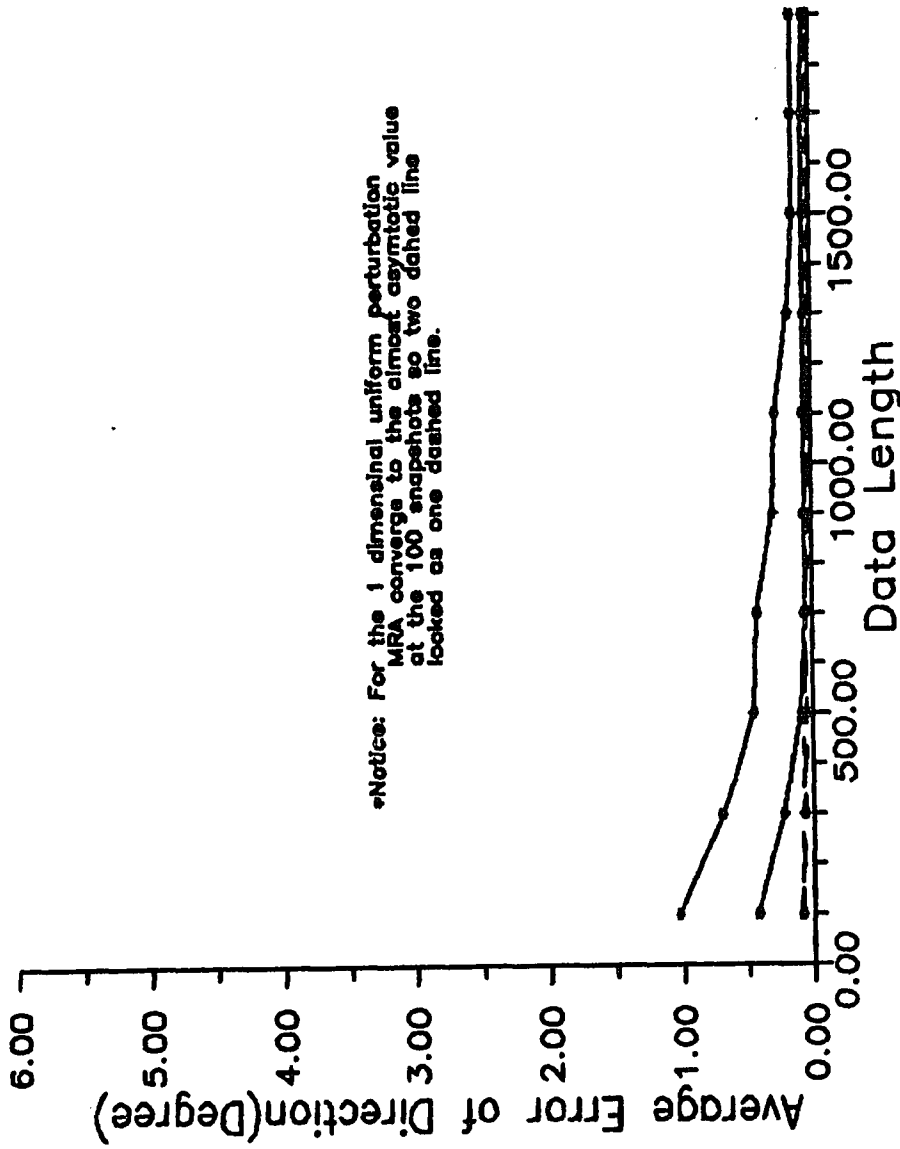




FIG 4-5

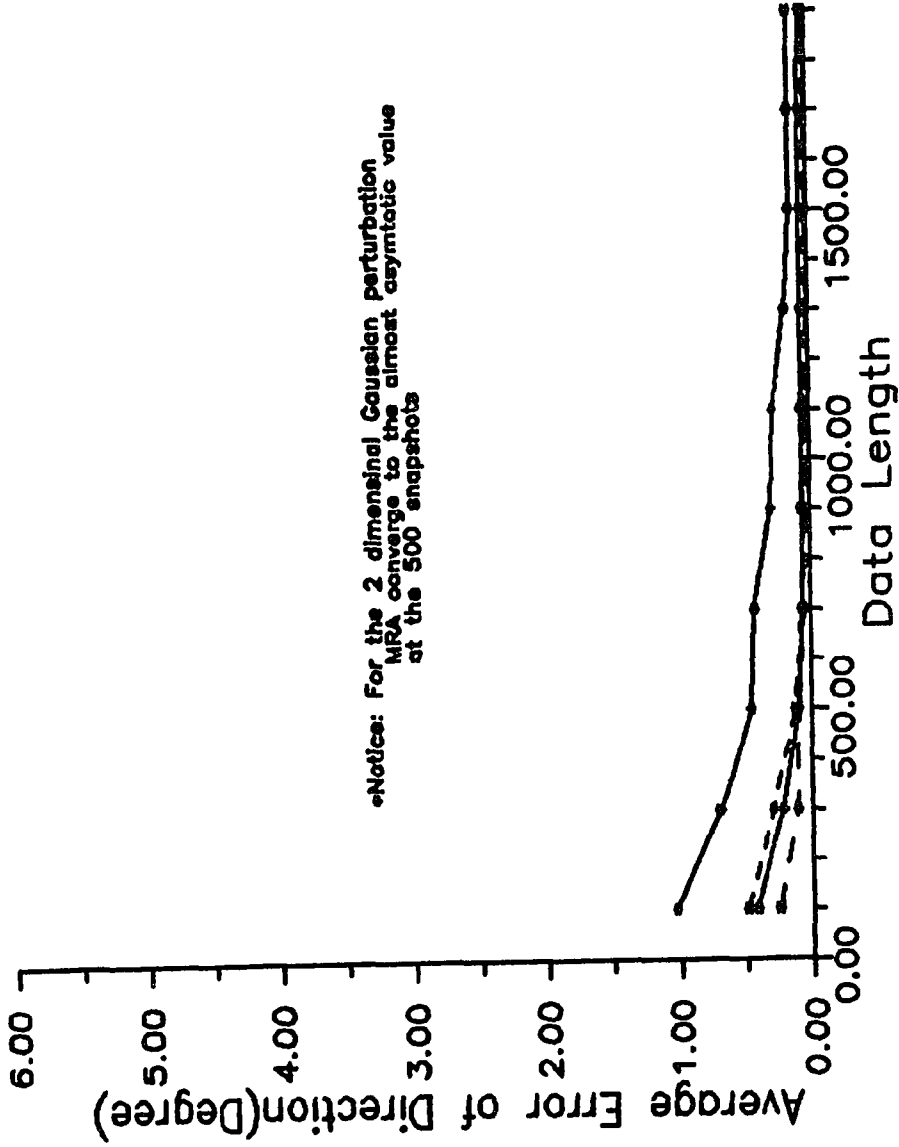
5 elements MRA.  
Solid: 2 dim. Unif. pert. Dashed: 1 dim. Unif. pert.  
Upper:  $\delta = 0.125$  lamda lower:  $\delta = 0.1$  lamda



Notice: For the 1 dimensional uniform perturbation MRA converge to the almost asymptotic value at the 100 snapshots so two dashed line looked as one dashed line.

Fig 4-6

5 elements MRA  
 Solid: 2 dim. Unif. pert. Dashed: 2 dim. Gaus. pert.  
 Upper:  $\delta = 0.125$  lamda lower:  $\delta = 0.1$  lamda (UNIF.)  
 Upper:  $\sigma = 0.07$  lamda lower:  $\sigma = 0.05$  lamda (GAUS.)



•Notice: For the 2 dimensional Gaussian perturbation MRA converge to the almost asymptotic value at the 500 snapshots

FIG 4-7

Solid: 2 dim. pert. Dashed: 1 dim. pert.  
Upper: URA Lower: MRA  
Delta = 0.125 lamda

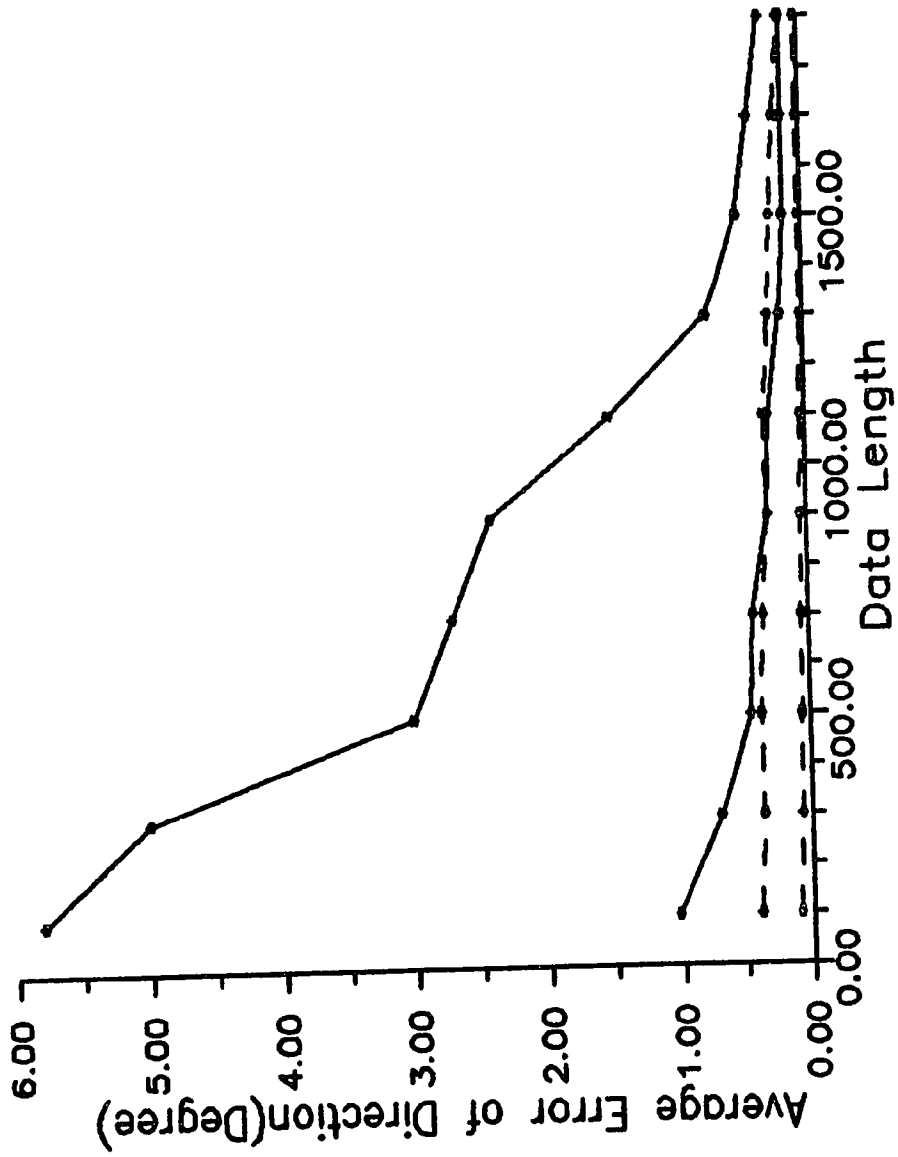


FIG 4-8

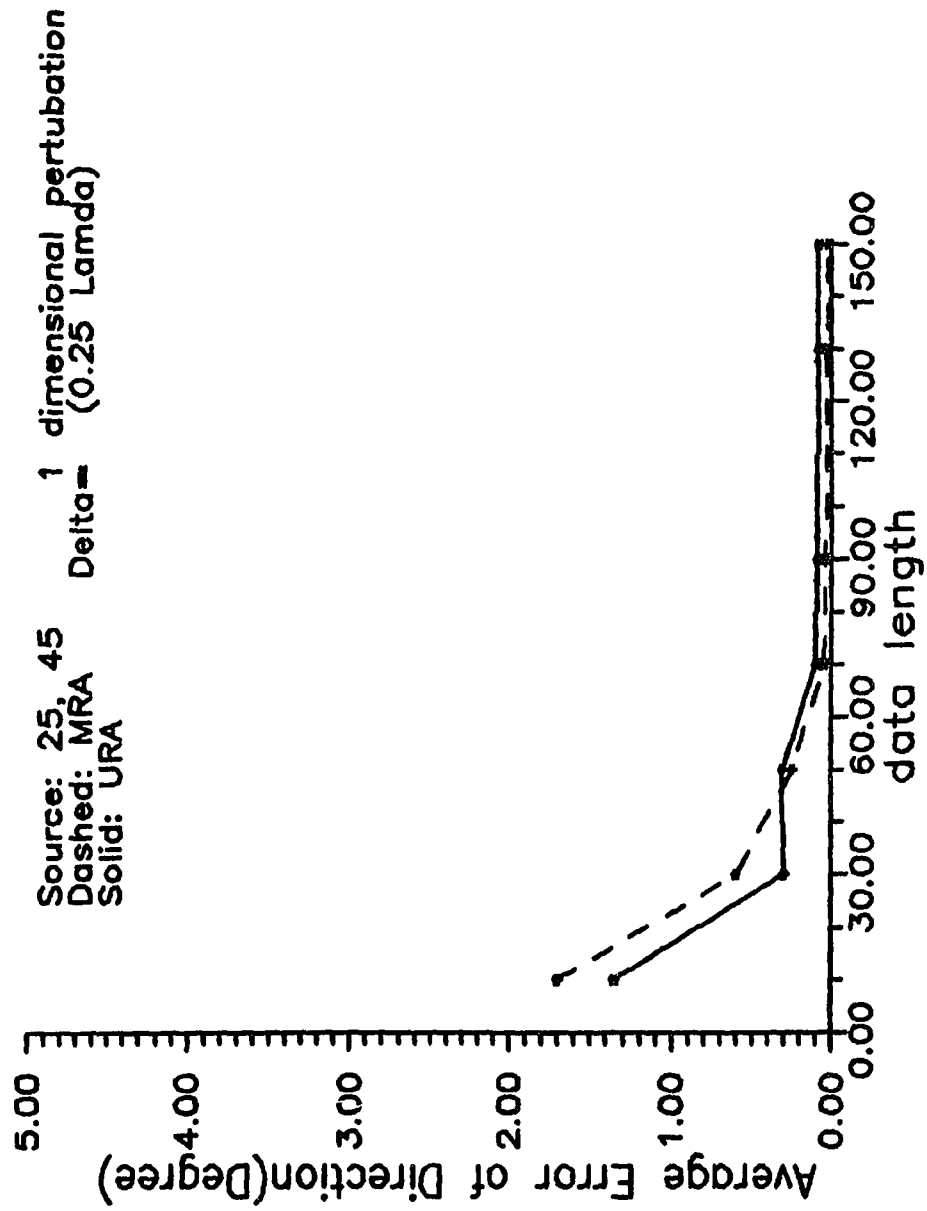


FIG 4-9

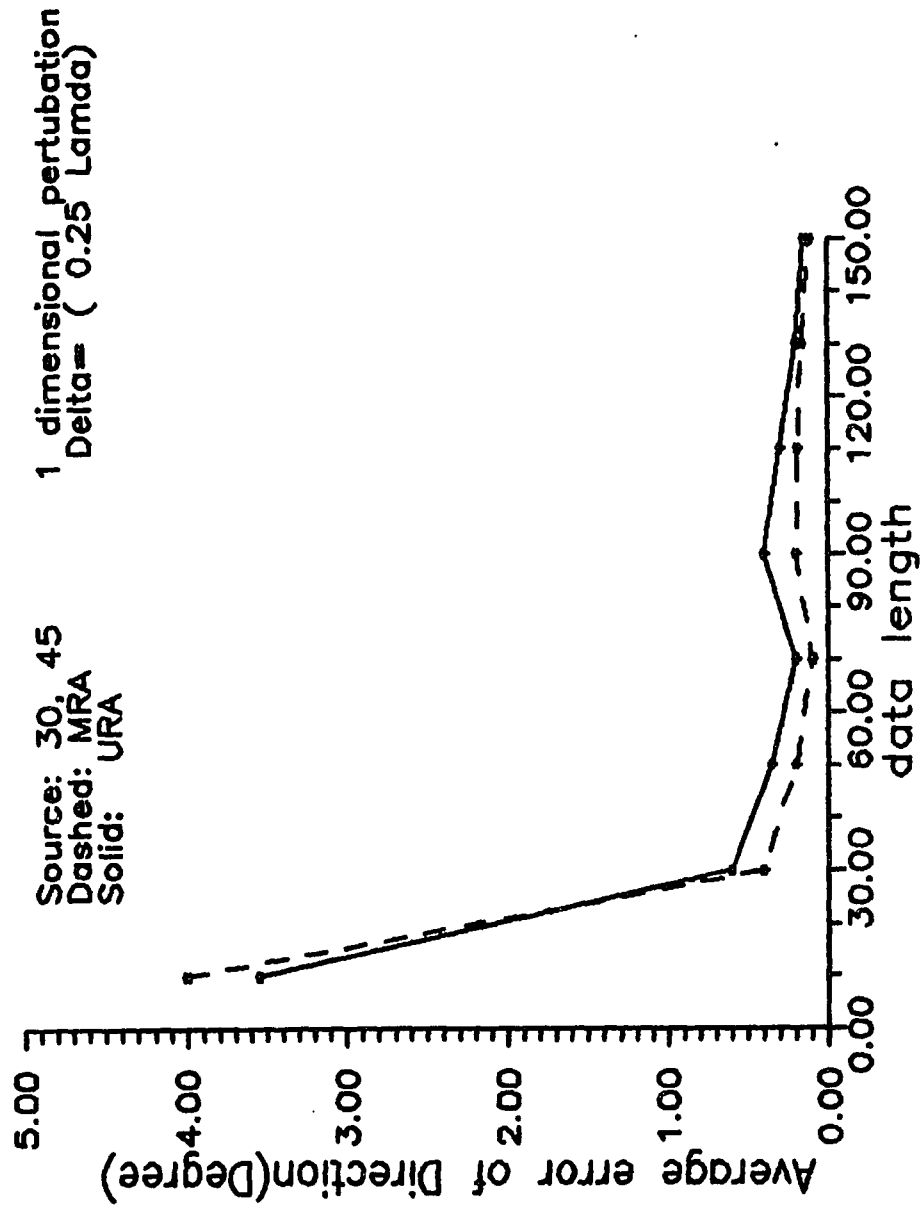


FIG 4-10

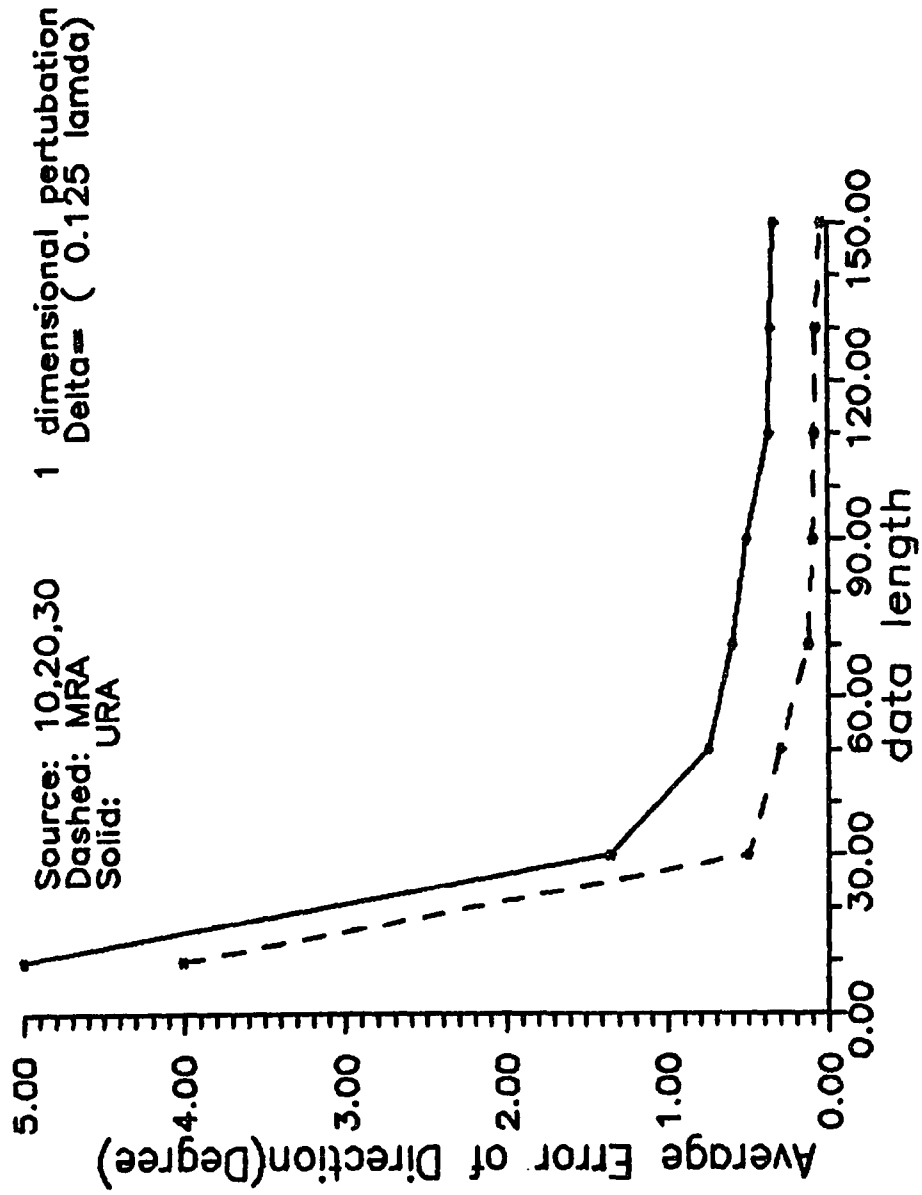


FIG 4-11

Source: 25, 45 1 dimensional perturbation  
Solid: URA (Averaged covariance matrix)  
Dashed: URA(Unaveraged covariance matrix)  
Delta= (0.25 lamda)

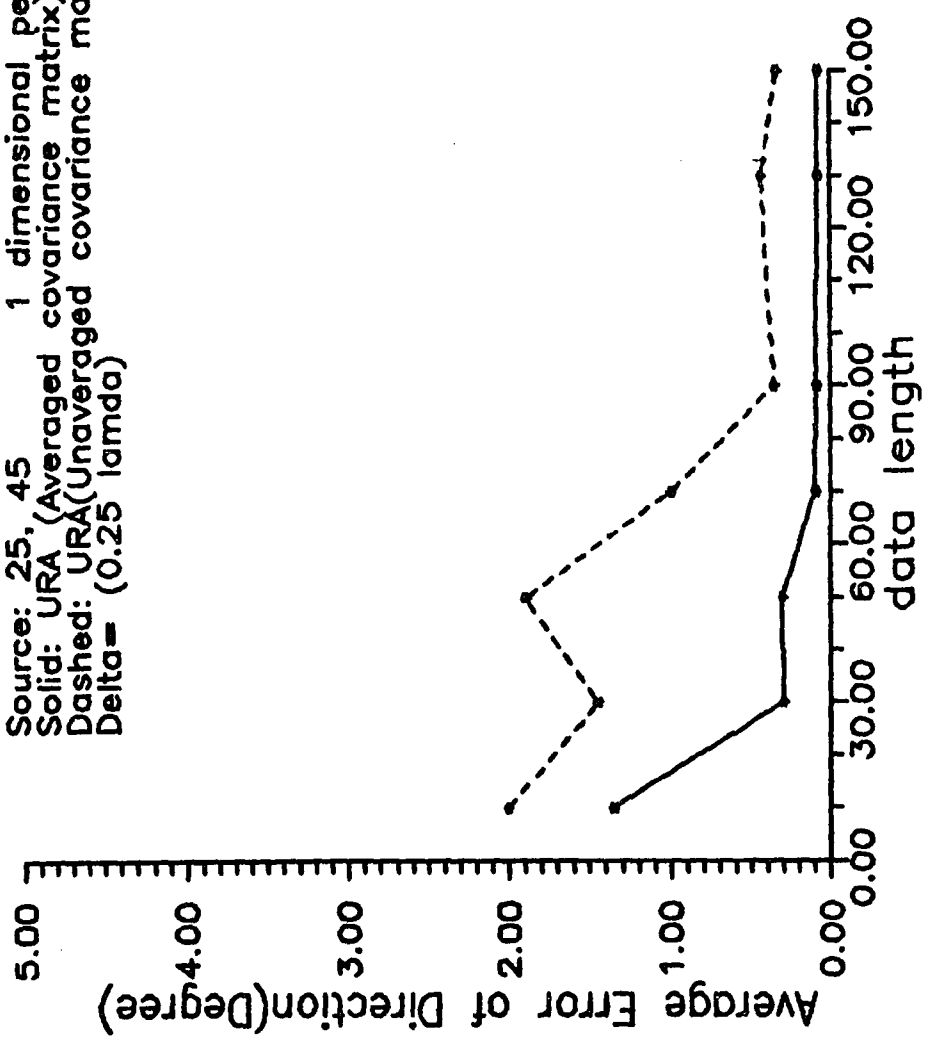


FIG 4-12

Source: 30, 45  
Solid: URA(Averaged covariance matrix)  
Dashed: URA(Unaveraged covariance matrix)  
Delta = (0.25 lamda)

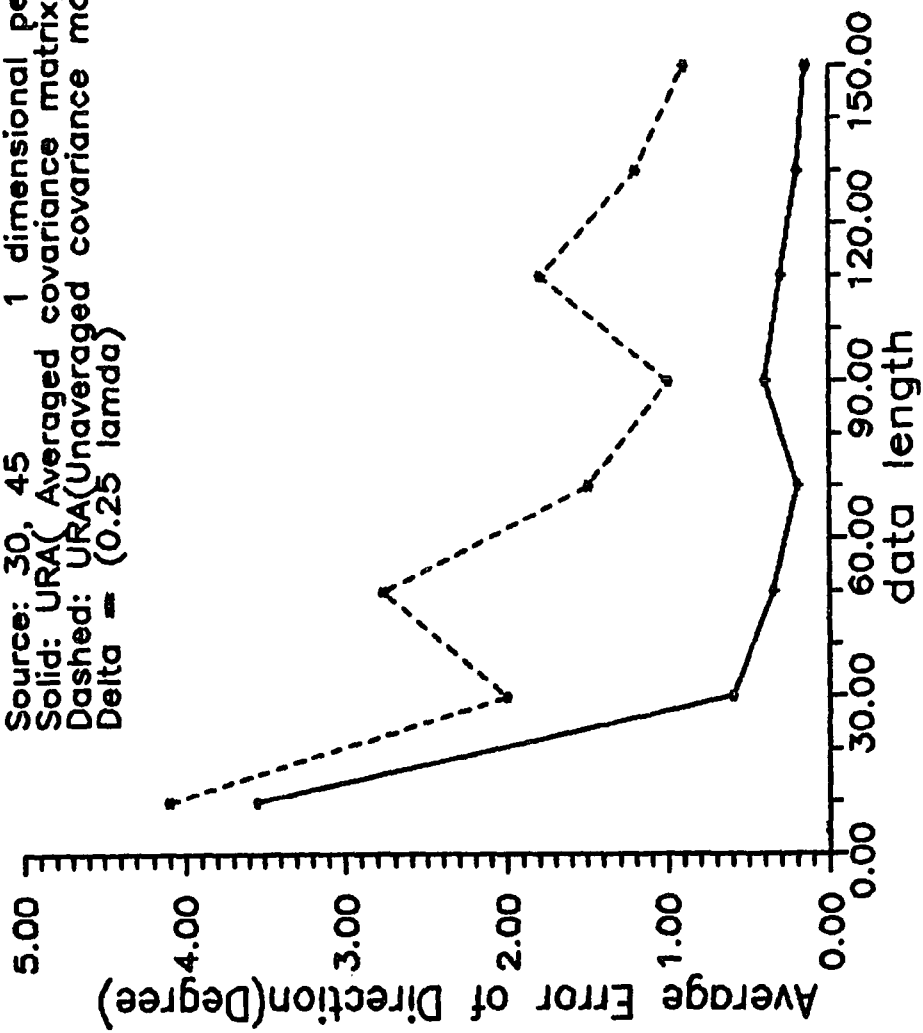




FIG 4-13

Source: 25, 45 1 dimensional pertubation  
(0.25 Lamda)

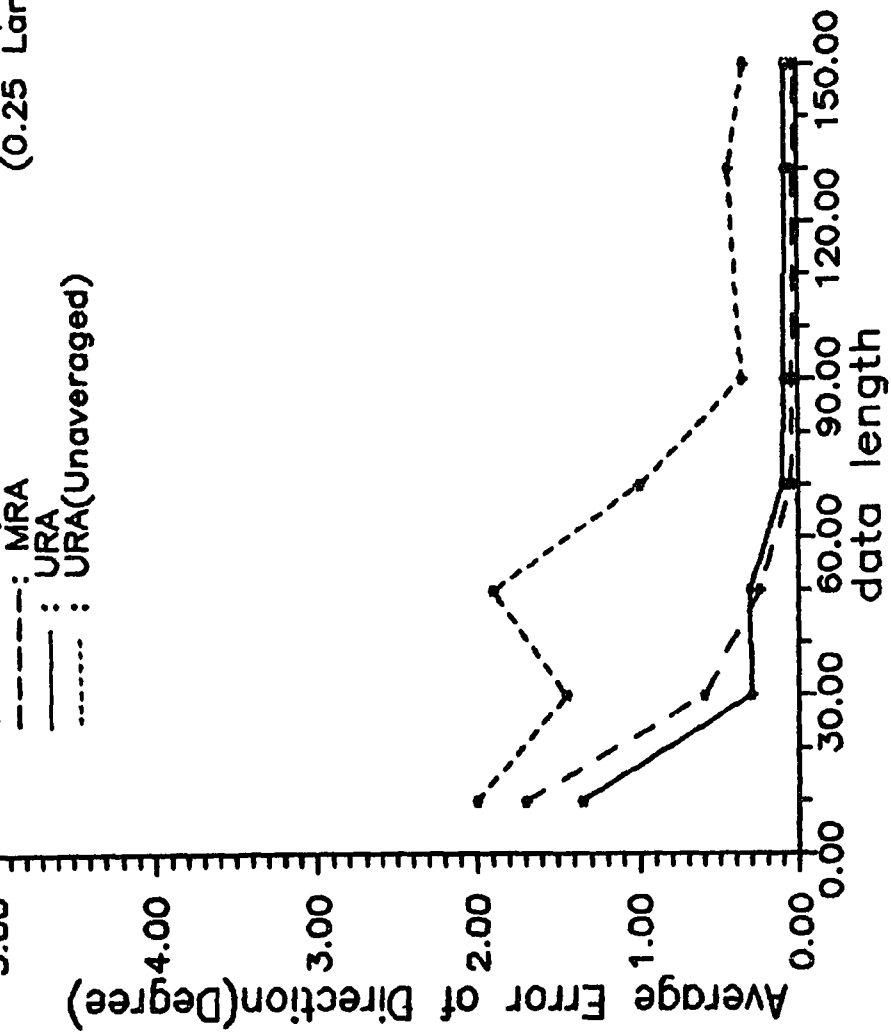
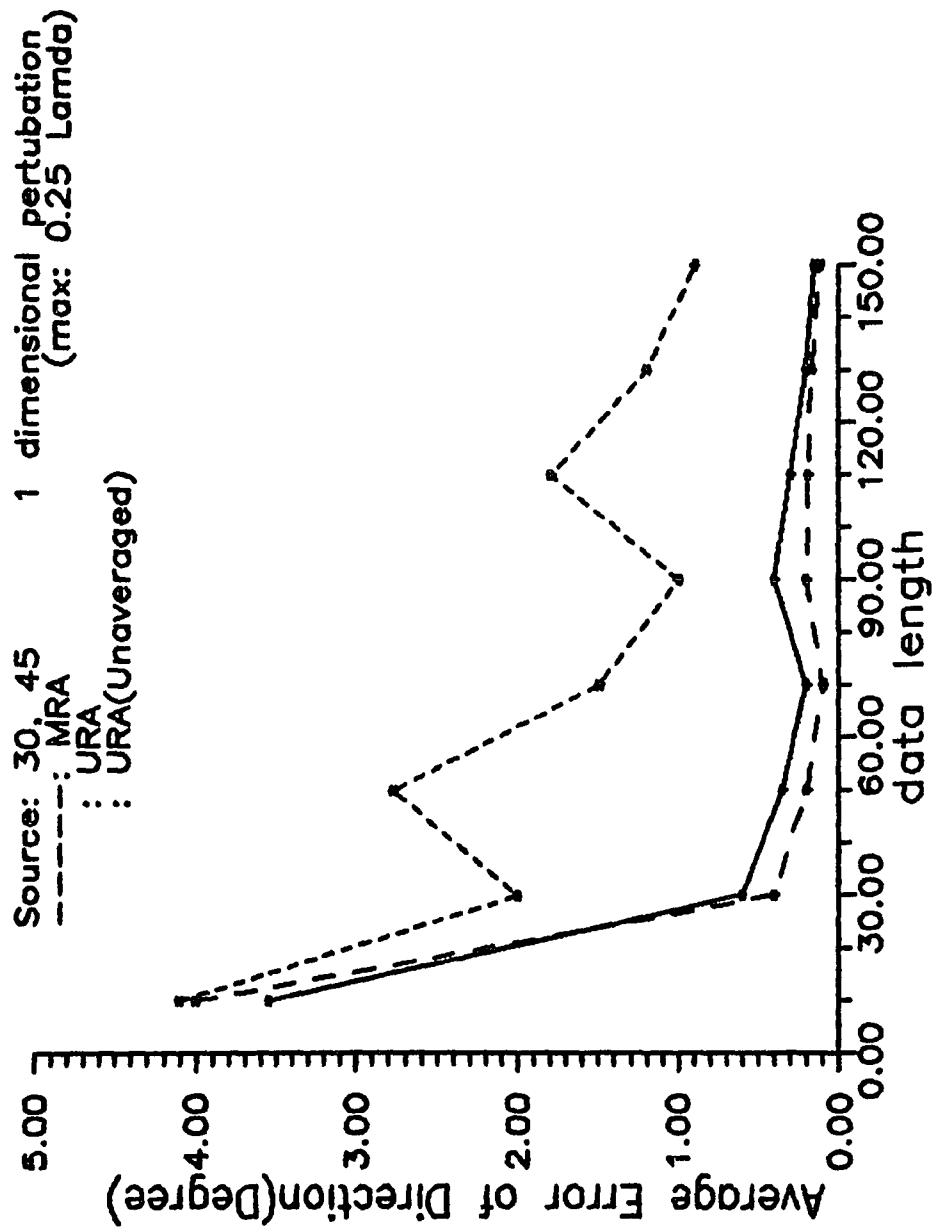


FIG 4--14



## 5. PERFORMANCE OF THE UNIFORM REGULAR ARRAY AND THE MINIMUM REDUNDANCY ARRAY USING MUSIC AND MINIMUM-NORM ALGORITHM.

### 1. Introduction.

The minimum redundancy array(MRA) was first proposed in [1] and implemented for direction finding using eigen system structure in [2]. The structure of the MRA, in fact, causes the removal of most, if not all the redundancy, in the correlation between the array elements. Such redundancy clearly exists in the conventional uniform regular array (URA).This redundancy in the URA may be explored to obtain a better estimate of the correlation,with the same number of snapshots. Nevertheless, since with the MRA the same number of elements are distributed nonuniformly,the aperture of the first is much larger than the latter, making it possible to get a larger dimension for  $\hat{R}$ . Larger dimension of  $\hat{R}$  means larger dimension for the noise subspace,given that the number of signal sources impinging on the array is the same. Since in any superresolution method the null spectrum depends on the number of noise eigenvector used, one might expect

the MRA to be superior. Therefore there are different properties of each of arrays; redundancy in the URA and larger dimension in the MRA, which provides either with an advantage on the other.

The purpose of this chapter is to use each of these arrays for direction finding and compare their performance. Two superresolution method would be studied; the MUSIC and the Minimum Norm. Each of these algorithm may be used in defining the null spectrum either the noise subspace [3], or the source subspace[4]. The usage of either of these two subspace has its advantages and drawbacks. While using the source subspace requires extra computations, it converges to the actual signal direction faster and with less sample snapshots. It is also more tractable analytically. Conversely when using the noise subspace, the convergence to the nominal value require, longer data and the estimated eigenvalues and their corresponding eigenvectors have larger variations causing statistical characterization of these eigenvector to be untractible analytically. In this chapter we will concentrate on using noise subspace only.

In the next section we will present the structure of the MRA for different number of elements and use a computer algorithm designed to generate the actual element locations for MRA with a

given number of element  $M$ . An example of MRA will also be presented. The section will be concluded by comparing the estimation error in the correlation matrices obtained with MRA and URA. In section 3 we will derive the basic formulae needed for both MUSIC and Minimum Norm algorithms. In section 4 we present the simulation results to evaluate the performances of the two arrays.

## 2. MRA array geometries and their covariance matrix $\hat{R}$ .

For any linear array with  $M$  elements the received signal at each element is given by

$$x_i(t) = \sum_{k=1}^D F_k(t) e^{-jk_0 d_i \sin \theta_k} + n_i(t) \quad (1)$$

$$i = 1, \dots, M$$

where  $D$  is the number of signals impinging on the array assumed uncorrelated and narrow-band,  $\theta_k$ ,  $k=1, \dots, D$  are the directions of these sources with respect to broadside,  $d_i$  represent the location of the  $i$ 'th element with respect to a reference point (regularly taking as integer multiple of  $\lambda/2$ ),  $F_k(t)$  is the complex envelope of the  $k$  signal.  $k_0$  represents the wave number common to all

sources,  $n_i(t)$  are noise sources which are assumed independent, delta correlated with variance  $\sigma^2$ .

Equation (1) can be written in vector notation as

$$X(t) = A F(t) + n(t)$$

where

$$X(t) = [ X_1(t), X_2(t), \dots, X_M(t) ]^T$$

$$F(t) = [ F_1(t), F_2(t), \dots, F_M(t) ]^T$$

$$n(t) = [ n_1(t), n_2(t), \dots, n_M(t) ]^T$$

T stands for transpose

$$A = [ a(\theta_1), a(\theta_2), \dots, a(\theta_D) ] \quad (2)$$

A is an MxD and  $a(\theta_k)$  is a M dimensional vectors each given by;

$$a(\theta_k) = [ e^{-jk_0 d_1 \sin \theta_k}, e^{-jk_0 d_2 \sin \theta_k}, \dots, e^{-jk_0 d_M \sin \theta_k} ]$$

$$k = 1, \dots, D, d_i \text{ are integers} \quad (3)$$

The correlation matrix of the received signal is given by

$$R = E [ X(t)X(t)^\dagger ] = A E [ F(t)F(t)^\dagger ] A^\dagger + E n(t)n(t)^\dagger$$

$E [ F F^\dagger ]$  is an MxM diagonal matrix whose diagonal terms,  $P_k$  represents the signal power of the k source. With this

$$R = \sum_{k=1}^D P_k a(\theta_k) a(\theta_k)^{\dagger} \quad (4)$$

using (3) we write

$$a(\theta_k) a(\theta_k)^T = \begin{bmatrix} e^{-jk_0 d_1 w_k} \\ e^{-jk_0 d_2 w_k} \\ \vdots \\ e^{-jk_0 d_M w_k} \end{bmatrix} \left[ e^{jk_0 d_1 w_k}, \dots, e^{jk_0 d_M w_k} \right] \quad (5)$$

where for expediency we used  $w_k = \sin \theta_k$ . Substituting (5)

in (4) we get for the  $i, j$  element of  $R$

$$R_{ij} = \sum_{k=1}^D P_k e^{-jk_0 (d_i - d_j) w_k} + \sigma^2 \delta(i-j) \quad (6)$$

$$i, j = 1, \dots, M$$

If the array is uniform then  $d_{i+1} - d_i$  are the same for each  $i$ . That is the distance between successive elements, usually taken to be  $\lambda/2$ , then  $d_i - d_j$  will be the same: 1, 2, 3, ..., etc., whenever  $j = i-1, j = i-2, j = i-3$ , etc., causing the term on any diagonal to be

the same and hence Toeplitz structure. On the other hand if  $d_i$  are chosen such that  $d_i - d_j = m$  ( $i, j = 1, 2, \dots, M$ ), and  $m$  spans the integer set  $\{0, 1, \dots, L\}$ , where  $L \leq M(M-1)/2$  then the terms above the diagonal will contain exactly  $L$  different correlation lags  $r(i)$ ,  $i=1, \dots, L$  and  $(M(M-1)/2) - L$  terms possibly equal to some other  $r(i)$ . That is instead of (6) we have for this case

$$r_{ij} = r(i-j) = r(m) = \sum_{k=1}^D P_k e^{-jk_0^m w_k} + \sigma^2 \delta(m) \quad (7)$$

$$m = 0, 1, 2, \dots, L$$

This way of selecting the elements location make the array what we call Minimum Redundancy Array(MRA).

As an example we take the case of 5 elements uniform regular array; then

$$a(\theta_k) = \begin{bmatrix} 1 \\ e^{-jk_0 w_k} \\ e^{-jk_0 2w_k} \\ e^{-jk_0 3w_k} \\ e^{-jk_0 4w_k} \end{bmatrix} \quad (8)$$



is the steering vector for the k'th signal, while for the case of 5 elements minimum redundancy array the steering vector for the k'th signal is

$$a(\theta_k) = \begin{bmatrix} 1 \\ e^{-jk_0 w_k} \\ e^{-jk_0 4w_k} \\ e^{-jk_0 7w_k} \\ e^{-jk_0 9w_k} \end{bmatrix} \quad (9)$$

Using the notation of (7) the covariance matrices for the URA and MRA respectively are

$$R = \begin{bmatrix} r(0) & r(1) & r(2) & r(3) & r(4) \\ & r(0) & r(1) & r(2) & r(3) \\ & & r(0) & r(1) & r(2) \\ \text{conj.} & & & r(0) & r(1) \\ \text{symmetric} & & & & r(0) \end{bmatrix} \quad (10)$$

for URA

and

$$R = \begin{bmatrix} r(0) & r(1) & r(4) & r(7) & r(9) \\ & r(0) & r(3) & r(6) & r(8) \\ & & r(0) & r(3) & r(5) \\ \text{conjg.} & & & r(0) & r(2) \\ \text{symmetric} & & & & r(0) \end{bmatrix} \quad (11)$$

for MRA.

Notice that covariance matrix for the URA is Toeplitz and the MRA is only Hermitian. Also the MRA has  $L+1$  different elements where

$$L = 9 = \frac{M(M-1)}{2} - 1 < \frac{M(M-1)}{2}$$

Table 5-1 depicts the configuration of the MRA for different number of elements. The number in the configuration column shows the distance of the different elements from their adjacent elements normalized to  $\lambda/2$ . The dimension of the array shows the aperture size in  $\lambda/2$ , 1 is given in these column, when  $\lambda/2$  is the minimum distance between any two adjacent elements.

Number of Ant. Elemen	Dim. of the URA	Dim. of the MRA	Configuration
5	4	9	0.1.3.3.2
6	5	13	0.1.5.3.2.2
7	6	17	0.1.3.6.2.3.2
8	7	23	0.1.3.6.6.2.3.2
9	8	29	0.1.3.6.6.6.2.3.2
10	9	36	0.1.2.3.7.7.7.4.4.1
11	10	43	0.1.2.3.7.7.7.7.4.4.1

Table 5-1

For the 5 elements array ,for example, we have that the element are located at  $[0, \lambda/2, 4\lambda/2, 7\lambda/2, 9\lambda/2]$  which corresponds to distances :  $[0, \lambda/2, 3\lambda/2, 3\lambda/2, 2\lambda/2]$  from their adjacent elements. This is shown in the last column of the table as 0,1,3,3,2. If we refer these distances to the reference element( which could be at any extreme side) we get by summing all distance,  $9\lambda/2$ . This is the total aperture( which is called at

column 3 of table 5-1 dim.). In fact such structure is not unique. It is only so if the dimension =  $[ M \times (M-1)/2 ]$  where  $M$  is the number of the array elements. Such a unique case is possible only if  $M=4$  and the dimension is six ( see [2] ). The location of the elements of the MRA as they are presented in the configuration column of table 5-1 were generated by a special search computer program.

For processing the signals of the MRA we must first generate what we term Augmented Matrix. This is a Toeplitz matrix which we obtain from the Hermitian covariance matrix of the array by repeating  $r(m)$  along the different diagonals;  $r(0)$  along the main diagonal,  $r(1)$  along the second diagonal, and so on. Therefore the dimension of the augmented matrix is  $(L+1) \times (L+1)$

$$R_{aug} = \begin{bmatrix} r(0) & r(1) & r(2) & \dots & r(L) \\ & r(0) & r(1) & \dots & r(L-1) \\ \text{conjg.} & & \dots & & \vdots \\ \text{symmetric} & & & & r(1) \\ & & & & r(0) \end{bmatrix} \quad (12)$$

Up to this point, in calculating the covariance matrix  $R$ , we used the ensemble expected value. In practice this is impossible. Instead we collect  $N$  snapshots of  $X(n)X(n)^\dagger$ , where  $X(n)$  is a sample of the vector at time  $nT$  (where  $T$  is the sampling period), and average on all these snapshots to obtain an estimate for  $R$

$$\hat{R} = \frac{1}{N} \sum_{n=1}^N [X(n)X(n)^\dagger] \quad (13)$$

Obviously each entry of  $\hat{R}$  is a random variable.

For the URA there are few entries at each diagonal which represents the same correlation lag. (that is, exist some redundancy). We explore this redundancy by generating  $\tilde{R}$  from  $\hat{R}$  as follows:

For the 5 elements we take

$$\tilde{r}(1) = 1/4 \{ \hat{r}(2-1) + \hat{r}(3-2) + \hat{r}(4-3) + \hat{r}(5-4) \}$$

$$\tilde{r}(2) = 1/3 \{ \hat{r}(3-1) + \hat{r}(4-2) + \hat{r}(5-3) \}$$

$$\tilde{r}(3) = 1/2 \{ \hat{r}(4-1) + \hat{r}(5-2) \}$$

$$\tilde{r}(4) = \hat{r}(5-1)$$

$$\tilde{r}(0) = 1/5 \{ \sum \text{all elements along the diagonal} \}$$

For the augmented MRA matrix we use all the estimated elements of (11) as they are without averaging except for

$$\tilde{r}(3) = 1/2 \{ \hat{r}(4-1) + \hat{r}(7-4) \}$$

$$\tilde{r}(0) = 1/5 \{ \sum \text{all elements along the diagonal.} \}$$

To observe the effect of these averaging on  $\hat{R}$  for both MRA and URA we find the difference  $\Delta \hat{R}$

$$\Delta \hat{R} = \| \tilde{R}(n) - R(n) \| \quad (14)$$

where the norm  $\|A\|$  of an  $M \times M$  matrix is defined;

$$\|A\| = \frac{1}{M^2} \sum_i \sum_j a_{ij}$$

Fig 5-1 presents  $\Delta \hat{R}$  as a function of the data length (snapshots used in calculating  $\hat{R}$ ).

### 3. Formulation of direction finding algorithm formulas.

#### a) MUSIC

The MUSIC algorithm[3] is a way to estimate the direction of signal impinging on an array. It exploits the orthogonal property of the noise subspace eigenvector to the source direction vectors. If a vector  $d$

$$d = [ d_1, d_2, \dots, d_M ] \quad (15)$$

has the property

$$a^\dagger(\theta_k) d = 0 \quad k = 1, 2, \dots, D \quad (16)$$

then the polynomial

$$s(z) = \sum_{k=0}^{M-1} d_{k+1} z^{-k} \quad (17)$$

will have zeros at  $z = e^{-jk_0 w_k}$   $k = 1, 2, \dots, D$ . From these zeros the direction of the signals can be found. Notice, however, that beside the  $D$  zeros which correspond to the signal directions, there are other  $M-D$  zeros termed extraneous zeros. Due to the orthogonality property of the noise eigenvector subspace and source direction vectors, mentioned before, any of the  $L-D$  noise eigenvector will have the property of the vector  $d$  mentioned in (16). This was first proposed by Pisarenko [5] for his direction finding approach.

We define

$$s(\theta) = \sum_{k=0}^{M-1} e_{i,k+1} z^{-k} \quad (18)$$

where  $e_i$   $i = D+1, D+2, \dots, M$  are eigenvectors corresponding to the smallest eigenvalues of the covariance matrix  $R$ ;  $R = E\{X(t)X(t)^\dagger\}$ ,  $(\lambda_1 \geq \lambda_2 \geq \dots \lambda_D, \lambda_{D+1}, \dots, \lambda_M)$ .  $s(\theta)$  in (18) usually called the null spectrum. Define  $P(\theta)$ ;

$$P(\theta) = \frac{1}{s(\theta)} \quad (19)$$

will have a high peaks at  $\theta_k$ ,  $k=1,2,\dots,D$ ; the signal directions. Now if the covariance matrix is only an estimate obtained from a finite samples  $X(n)$  as in (13), then noise eigenvectors  $e_i$ ,  $i = D+1, \dots, M$  and so is the directions obtained will be not sufficiently accurate unless the SNR is very high. In such case one might utilize not only one eigenvector as in (18) but all  $L-D$  eigenvectors and define the null spectrum by

$$\hat{s}(\theta) = a^\dagger(\theta) \left( \sum_{k=D+1}^M \hat{e}_i \hat{e}_i^\dagger \right) a(\theta) \quad (20)$$

$$P(\theta) = \frac{1}{\hat{s}(\theta)}$$



where  $\hat{e}_i$   $i=D+1, \dots, M$  are the estimate of the noise eigenvectors such an approach of using all noise eigenvectors was first used by Schmidt[6] who called it MUSIC. Obviously it results in some sort of smoothing in estimating errors of the noise eigenvectors and causes better estimate of  $e^{jk} w_k$  and the direction of the signals. Many others followed Schmidt's approach.

Let  $E_S$  be the  $M \times D$  matrix constructed from the signal subspace eigenvectors, i.e. eigenvectors which correspond to the largest eigenvalues  $\lambda_i$   $i=1, 2, \dots, D$ . That is

$$E_S = [ e_1, e_2, \dots, e_D ] \quad (21)$$

where  $e_i$  are the eigenvector given by

$$e_i = [ e_{1i}, e_{2i}, \dots, e_{Mi} ]^T \quad (22)$$

$i= 1, 2, \dots, D$

and let  $E_N$  be the  $M \times (M-D)$  matrix consisting of the noise subspace eigenvectors; i.e. eigenvectors which correspond to the smallest eigenvalues  $\lambda_i$   $i= D+1, \dots, M$ . That is ;

$$E_N = [ e_{D+1}, e_{D+2}, \dots, e_M ] \quad (23)$$

Because these subspace are orthogonal then

$$[E_S \mid E_N] [E_S \mid E_N]^\dagger = I \quad (24)$$

Hence

$$a^\dagger(\theta) [E_S \mid E_N] \begin{bmatrix} E_S^\dagger \\ \dots \\ E_N^\dagger \end{bmatrix} a(\theta) = M$$

or

$$a^\dagger(\theta) [E_S E_S^\dagger + E_N E_N^\dagger] a(\theta) = M$$

Using both (21) and (23) we end up with

$$a^\dagger(\theta) \left( \sum_{i=D+1}^M \hat{e}_i \hat{e}_i^\dagger \right) a(\theta) = M - a^\dagger(\theta) \left( \sum_{i=1}^D \hat{e}_i \hat{e}_i^\dagger \right) a^\dagger(\theta) \quad (25)$$

Therefore using (20) we can also have for the null spectrum,

$$\hat{S}(\theta) = M - a^\dagger(\theta) \left( \sum_{i=D+1}^M \hat{e}_i \hat{e}_i^\dagger \right) a(\theta) \quad (26)$$

i.e.  $\hat{S}(\theta)$  is defined by the signal subspace instead of, by the noise subspace (20). Clearly for the noise subspace we have to find only one eigenvalue (the smallest) which must have

multiplicity  $M-D$ . This is simpler than finding all the different  $D$  eigenvalues and their corresponding eigenvector when using signal subspace. Nevertheless, the estimates of these eigenvectors are better than the estimates of the eigenvector which belong to noise subspace. This in turn results in much better direction estimates when using signal subspace. Notice from (20) and (26) that whenever  $a(\theta)$  is in the direction of the signal direction vector  $a(\theta_k)$  the estimate of the null space  $\hat{S}(\theta_k)$  vanishes.

#### B) Minimum Norm Algorithm

Instead of choosing  $d$  as noise eigenvectors or signal eigenvectors to generate the null spectrum for the MUSIC algorithm, Kumaresan and Tufts [7] proposed to choose  $d$  as follows

1. Its first element to be unity
2. Its Euclidian Length to be minimum

The second requirement is the reason for the name Minimum Norm algorithm.

Let us first partition the subspaces of (21) and (23) as follows

$$E_S = \begin{bmatrix} g^T \\ \dots\dots\dots \\ E'_S \end{bmatrix} \quad (27)$$

and

$$E_N = \begin{bmatrix} c^T \\ \dots\dots\dots \\ E'_N \end{bmatrix} \quad (28)$$

where  $g$  and  $c$  are in fact composed of the first elements of the signal and noise subspace eigenvectors, respectively. Then  $E'_S$  and  $E'_N$  are  $(M-1) \times D$  and  $(M-1) \times (M-D)$  matrices respectively obtained from  $E_S$  and  $E_N$  by deleting their first rows:

$$g = [ e_{1,1}, e_{2,1}, \dots, e_{D,1} ] \quad (29)$$

$$c = [ e_{D+1,1}, e_{D+2,1}, \dots, e_{M,1} ] \quad (30)$$

$$d = [ d_1, d_2, \dots, d_M ] \quad (31)$$

Since  $d$  has to be in the range of  $E_N$  (see 16) it will be orthogonal to the column of  $E_S$ , i.e.

$$E_S^\dagger d = 0 \quad (32)$$

or equivalently

$$\left[ g^* \mid E_S'^\dagger \right] \begin{bmatrix} 1 \\ d' \end{bmatrix} = 0 \quad (33)$$

where we took  $d_1 = 1$  and  $d' = [d_2, d_3, \dots, d_M]^T$ . From (32) we can write

$$E_S'^\dagger d' = -g^* \quad (34)$$

$E_S^\dagger$  is an  $D \times (M-1)$  matrix and we in fact have  $D$  equations with  $M-1$  unknown, which can be solved for  $d'$  by using pseudo inverse of  $E_S'^\dagger$ .

By the requirement of the minimum norm of  $d'$

$$\|d\| = \sum_{i=2}^M |d_i|^2 \quad \text{is minimum,}$$

the pseudo inverse matrix can be obtained by the singular value decomposition of  $E_S'^\dagger$ . Such a solution give

$$d = \left[ \begin{array}{c} 1 \\ \hline E'_S g^* / 1 - g^\dagger g \end{array} \right] \quad (35)$$

Combining the two matrices  $E_S$  and  $E_N$  from (27) and (28) and multiply by their transpose conjugate we get the identity matrix. This is because these two matrices contain all the eigenvectors of  $R$  which is Hermitian. Therefore

$$\left[ \begin{array}{c|c} g^T & c^T \\ \hline E'_S & E'_N \end{array} \right] \left[ \begin{array}{c|c} g^* & E'_S{}^\dagger \\ \hline c^* & E'_N{}^\dagger \end{array} \right] = I \quad (36)$$

which lead to

$$\begin{aligned} g^T g^* + c^T c^* &= 1 \\ E'_S g^* + E'_N c^* &= 0 \end{aligned} \quad (37)$$

by using (37) in (35) we have

$$d = \left[ \begin{array}{c} 1 \\ \hline E'_N c^* / c^\dagger c \end{array} \right] \quad (38)$$

Equations (35) and (38) depicts the fact that the required vector  $d$

can be obtained by using either the eigenvectors of the noise or the signal spaces.

Finally we must remark on the fact that the minimum norm algorithm has advantage of leading to[7]

1. More accurate estimate of  $w_k$  even with relatively low SNR
2. The M-D, extraneous zeros of  $S(\theta)$  tends to have less effect for causing false sources.

#### 4. Simulation Results

A number of simulation runs were performed to examine the behavior of the URA and the MRA and compare them. In these experiments different level of signal-to-noise ratio (SNR) were used. The effect of number of samples on the performance of the array was also examined. Two different noise sources were considered; additive random noise independent of the signal source, and noise caused by small random perturbations of the element locations.

In Fig 5-2 we present the case of a five element URA or MRA. Four sources of SNR were located at 5, 20, 45, 75 degree. This figure depicts, the average of the absolute errors in estimating

the directions of these four signals as a function of data length( Number of samples used in calculating  $\hat{R}$  ). Due to the dimension of  $\hat{R}$  only one noise vector was used in defining the null spectrum for the URA. For the sake of comparison only one noise vector was used for the MRA even though many more noise eigenvectors are obviously available. It is observed that MRA outperforms the URA down to a very small data length. The point of error with more than 4 degree depicted for the URA indicates a "false peak"

The effect of perturbation noise is examined in Fig 5-3 (Maximum perturbation of  $0.25\lambda$  was considered), Five element array were used with only one signal source and employing one noise eigenvector. The direction of the source was varied and for each direction the absolute value of error was found. Fig 5-4 presents the Cramer-Rao bound due to aperture length. That is for 5 element and 10 element (The aperture size of 5 element MRA). Comparing Fig 5-3 and Fig 5-4 we notice that the MRA performance presented in Fig 5-3 close to the bound for 10 element as it was shown Fig 5-4. Hence we might conjecture that the 5 element MRA performs almost like 10 element URA and that the larger aperture of the MRA is the dominant factor in achieving the improved performance.

The effect of the higher dimension of the augmented



covariance matrix for MRA and the resulted larger number of eigenvectors that could be used in MUSIC we show in Figure 5-5, 5-6 and 5-7 the effect of using one two or three noise eigenvector in defining the null spectrum of equation (20). notice how  $P(\theta) = 1/S(\theta)$  of (20) become sharper and sharper at  $\theta_k = 5, 20, 45$  and  $75$  (degree) the actual direction of the signal source as we use more and more eigenvector. Important to emphasis that such possibility of using more noise vector does not exist for the 5 element URA with 4 signal sources.

The effect of adding extra noise eigenvector in defining  $S(\theta)$  is compared again in Fig 5.8 as a function of data length. Notice that with small data length( Less than approximately 50 samples) there appear a false peak(indicated by average error greater than 4 degree), when only one noise eigenvector was used. This false peak readily disappear when another eigenvector was added in defining  $S(\theta)$ . In fact with two eigenvectors no such false peak was found even with at little as 10 samples. Figures 5-9 and 5-10 depict the false peak in  $P(\theta)$  in the first figure and its disappearance in the second when two noise eigenvectors were used in defining  $S(\theta)$ . Using the minimum norm algorithm we compare in Fig 5-11 the performance of the URA and the MRA as a function of

data length. From the procedure of this algorithm only one vector  $d$  is used to define the null spectrum. Notice how the MRA outperforms the URA particularly for small data length. Also notice the smoothness of the curve for URA in this figure in comparison to the fluctuation in errors as a function of data length when the MUSIC is used. This fact is due to the way the vector  $d$  is chosen among all vector which are orthogonal the signal space it has the minimum norm.

## 5. Conclusion

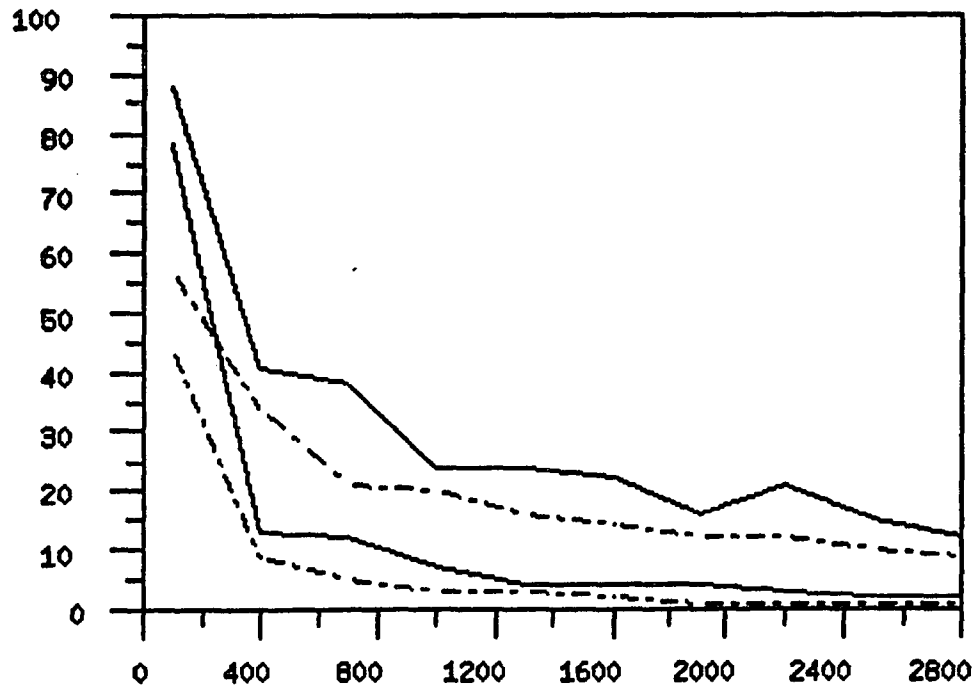
The MRA was shown to outperform the URA, when using either of MUSIC or Minimum-Norm algorithms. Two reason could cause these results; Larger aperture length and the fact that the MRA covariance matrix when augmented, has larger dimension and hence larger number of noise eigenvector to be used in superresolution algorithm. The effect of increasing the number of eigenvectors on the performance of both arrays was studied and shown to support this conjecture. The effect of different aperture length on the performance was examined by using perturbation noise and comparing performance with Cramer-Rao bound.

Important to emphasize that the MRA outperforms the URA despite the facts the latter contains redundancy in its covariance matrix entries which regularity exploited to smooth the data and cause reduction in the number of snapshot required for processing.

#### References

- [1] A. T. Moffet "Minimum-Redundancy Linear Array" IEEE Trans. AP. vol AP-16 No2 March, 1968
- [2] S.U. Pillai, Y. Bar-Ness and Fred Haber "A new Approach to Array Geometry for improved Spatial Spectrum Estimation" Proceeding of the IEEE vol 23 No 10 Oct. 1985
- [3] M. Kaveh , A.J. Barabell "The statistical Performance of the MUSIC and the Minimum-Norm Algorithm in resolving Plane waves in Noise" IEEE Transaction on Acoustics,Speech,and Signal Processing vol ASSP-34 No 2 April 1986
- [4] S.S. Reddi "Multiple Source Location- A Digital Approach" IEEE Transaction on Aerospace and Electronic System Vol AES-15 No 1 Jan. 1979
- [5] Pisarenko, V.F. "The retrieval of harmonics from a covariance function" Geophysics J. Roy. Astron Soc. 33 (1972)
- [6] R.O. Schmidt "Multiple emitter location and signal parameter estimation," in Proc. RADC spectral Est. Workshop, Griffis AFBS, NY 1979.
- [7] R. Kumaresan, D.W. Tufts "Estimating the angles of Arrival of Multiple Plane Waves" IEEE Transaction on AES Vol. AES 19 No1 Jan. 1983

FIG 5-1



———— MRA

..... URA

above SNR= 11 dB

below SNR= 32 dB

X axis: Data Length

Y axis:  $\Delta R \times 10^3$

$$\Delta R = \frac{|R(n) - \hat{R}(n)|}{R(n)}$$

$R(n)$ : Exact value

$\hat{R}(n)$ : Estimated value

FIG 5-2

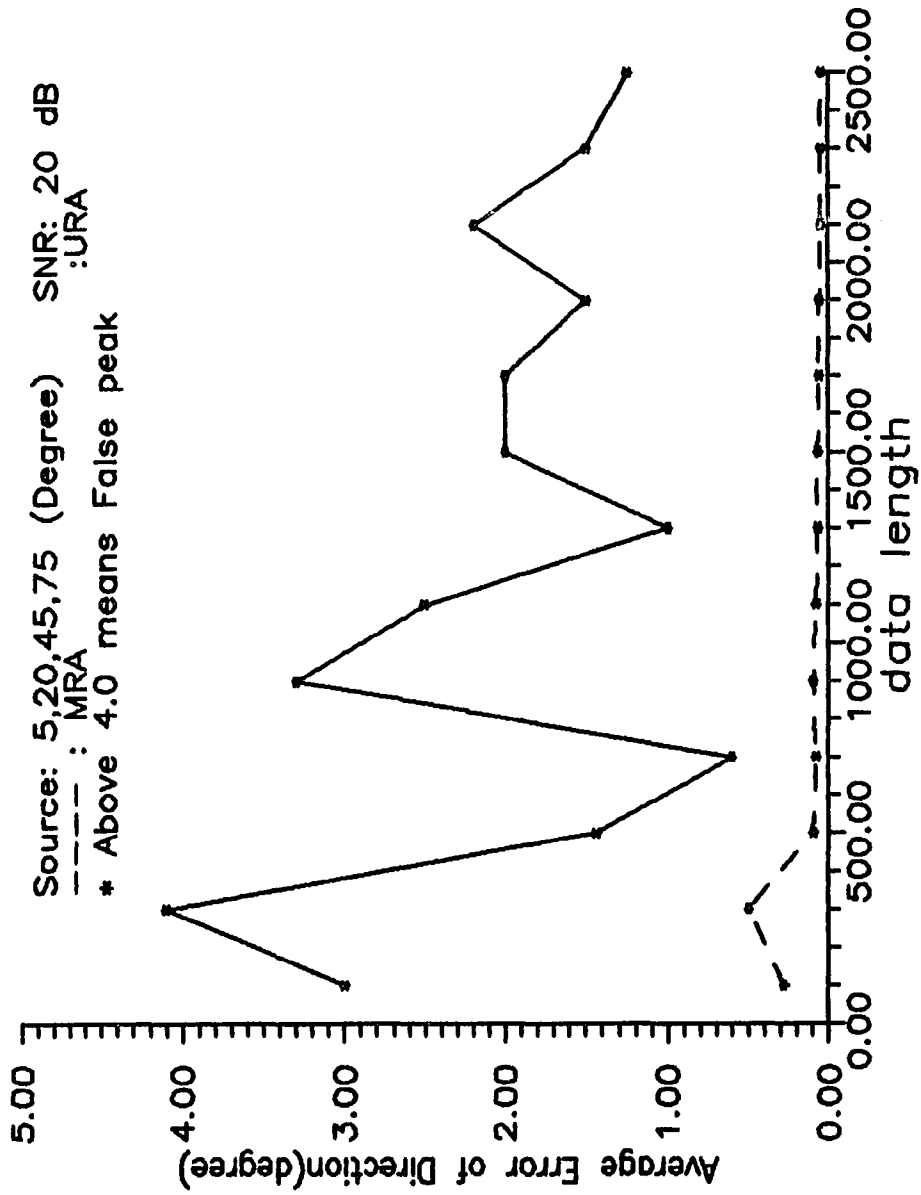


FIG 5-3

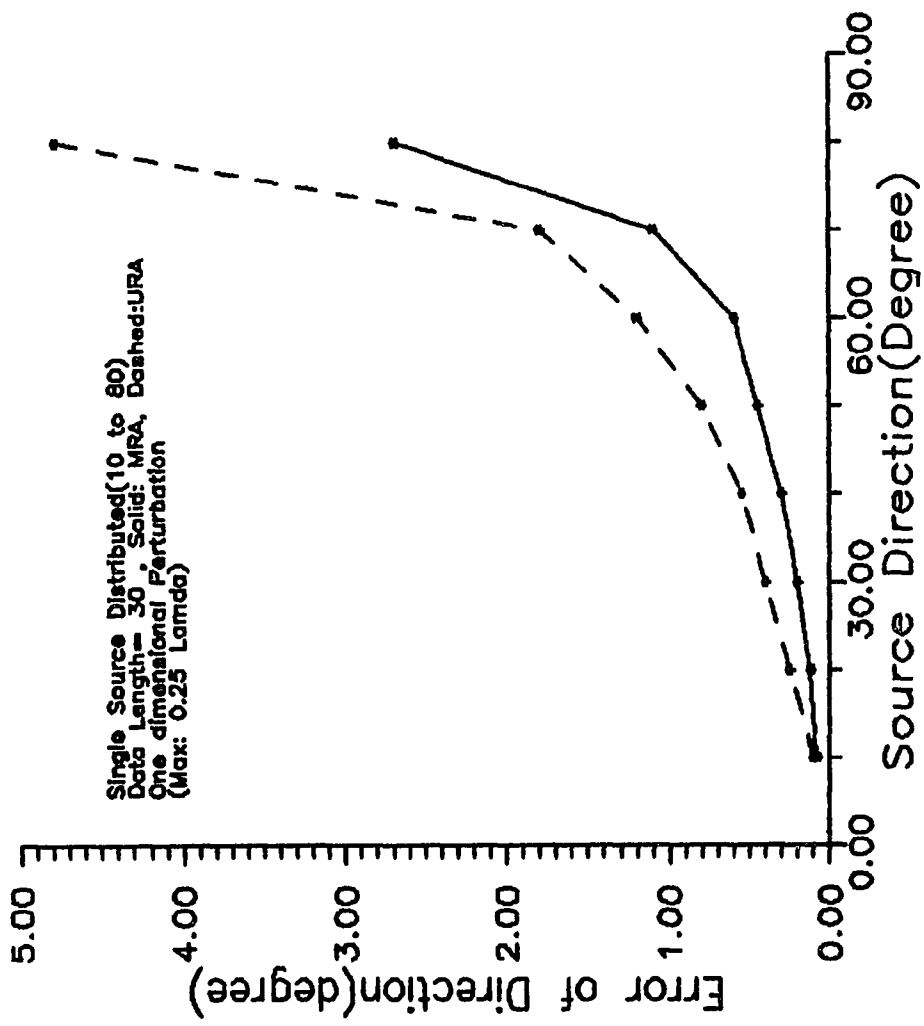


Fig 5-4

Cramer-Rao Bound of Random Perturbation

Solid: 10 elements URA

Dashed: 5 elements URA

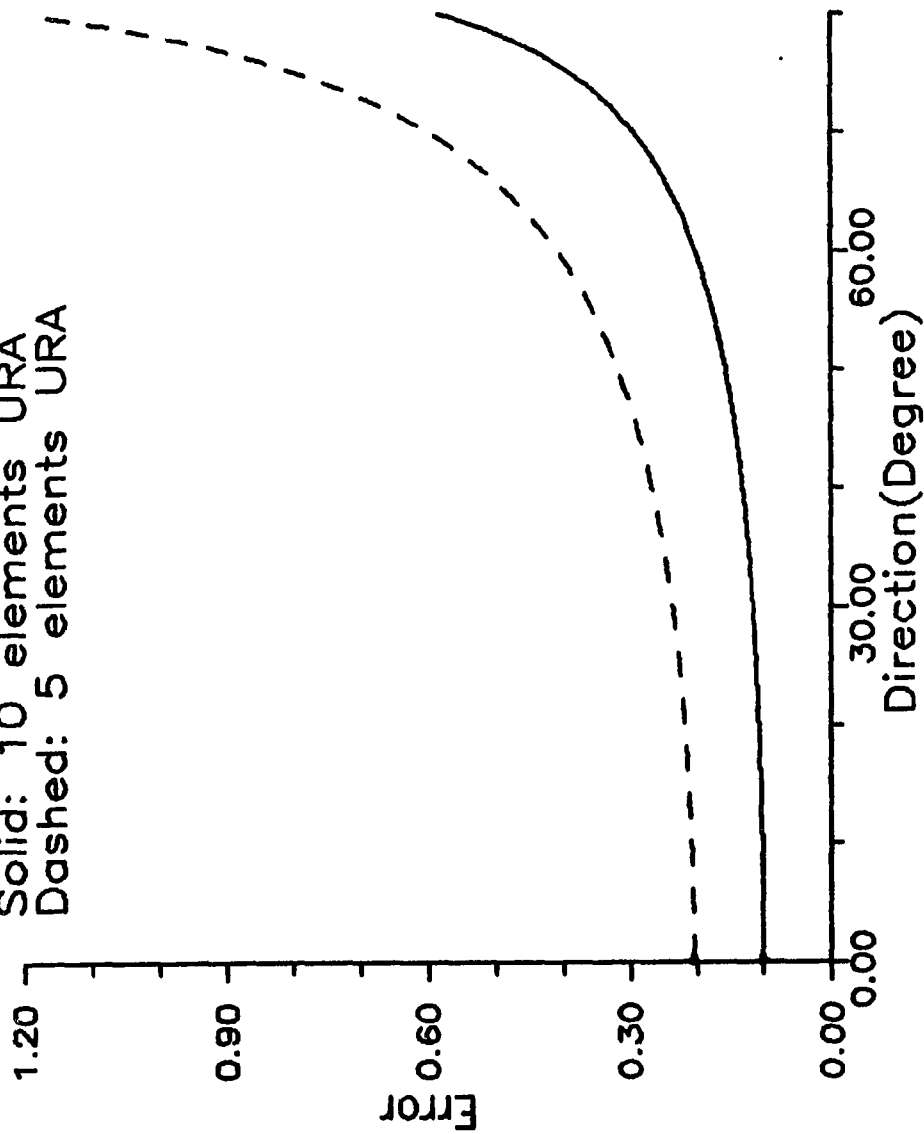


Fig 5-5

Direction: 5,20,45,75 SNR: 20 dB  
5 element MRA  
Data Length: 110  
# of Noise vector used:1

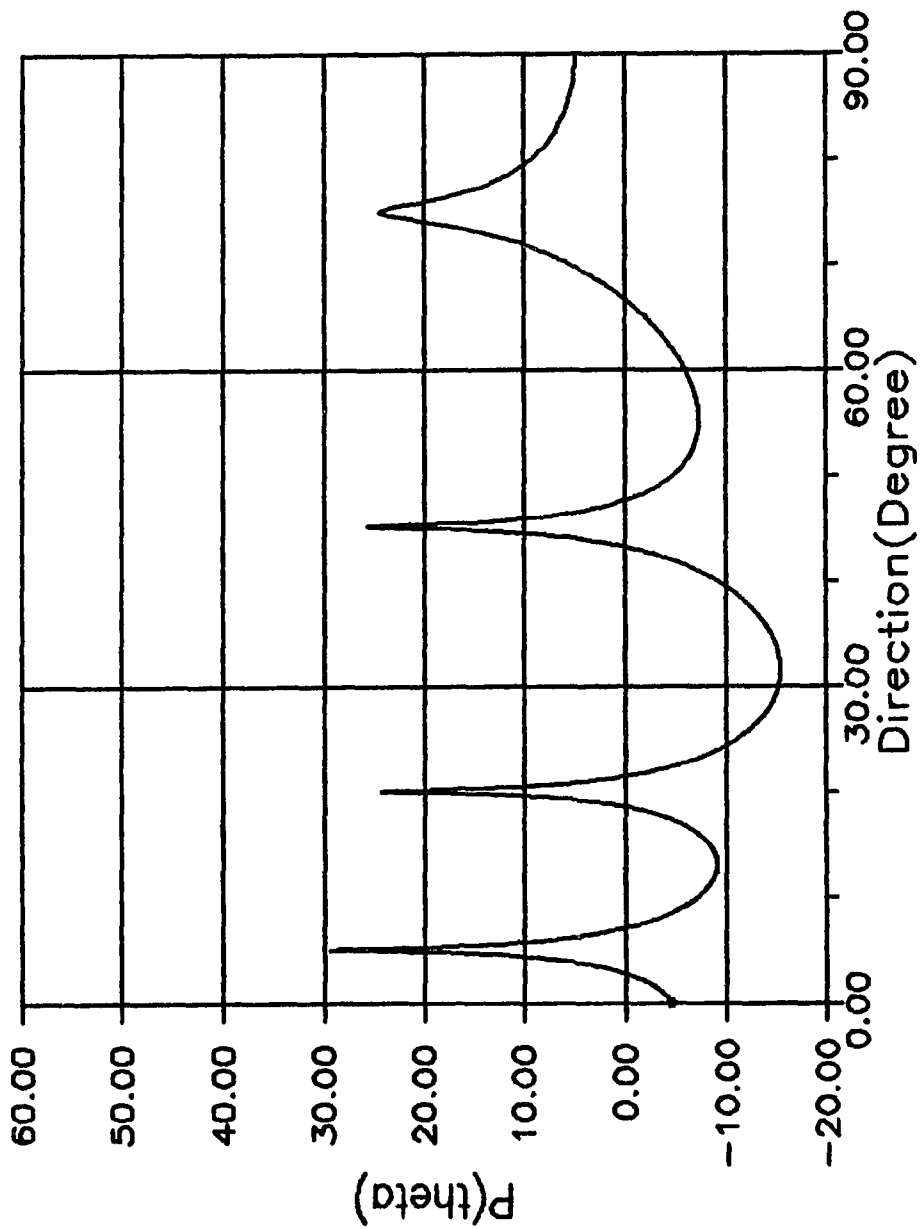




FIG 5-6

Direction: 5,20,45,75 SNR: 20 dB  
5 element MRA  
Data Length: 110  
# of Noise vector used:2

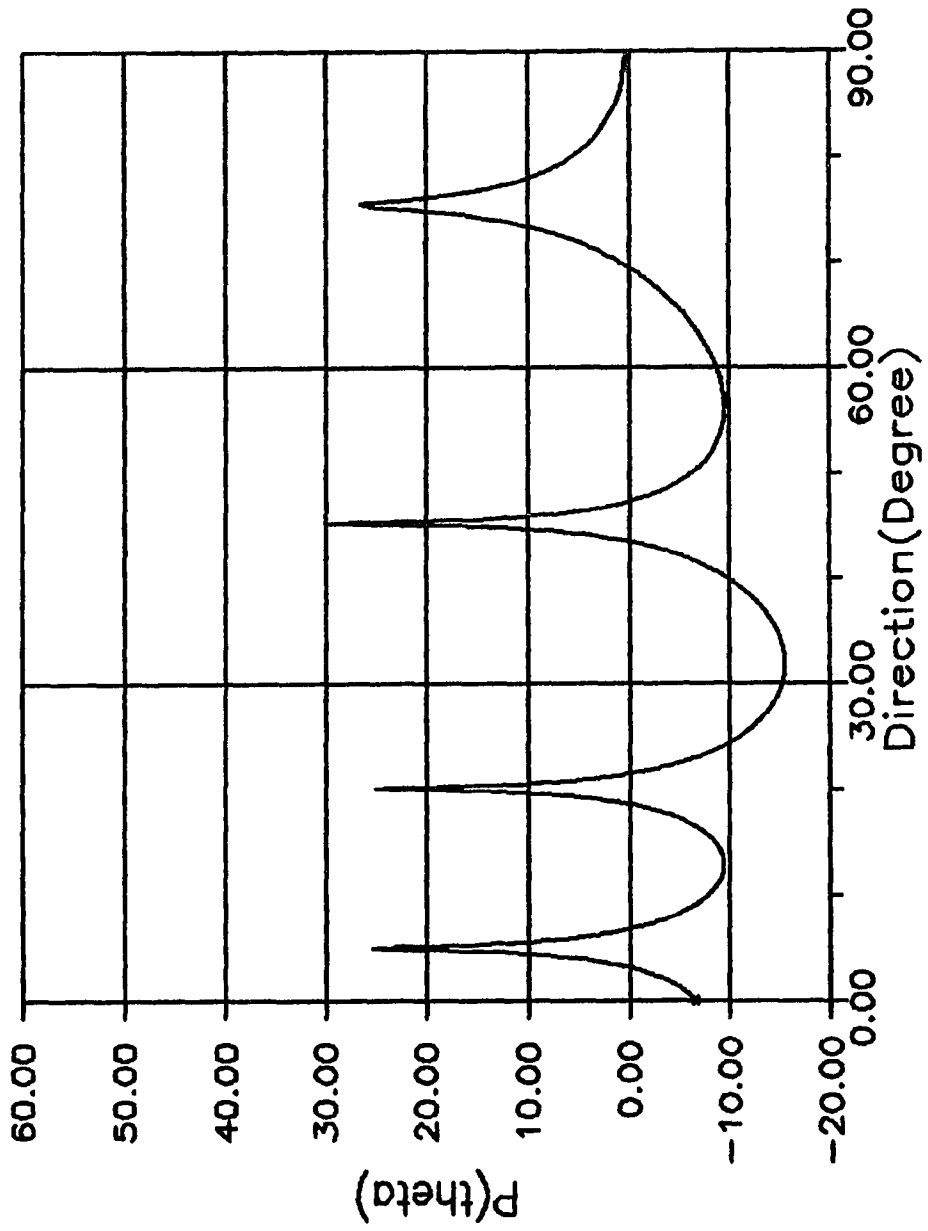


Fig 5-7

Direction: 5,20,45,75 SNR: 20 dB  
5 element MRA  
Data Length: 110  
# of Noise vector used:3

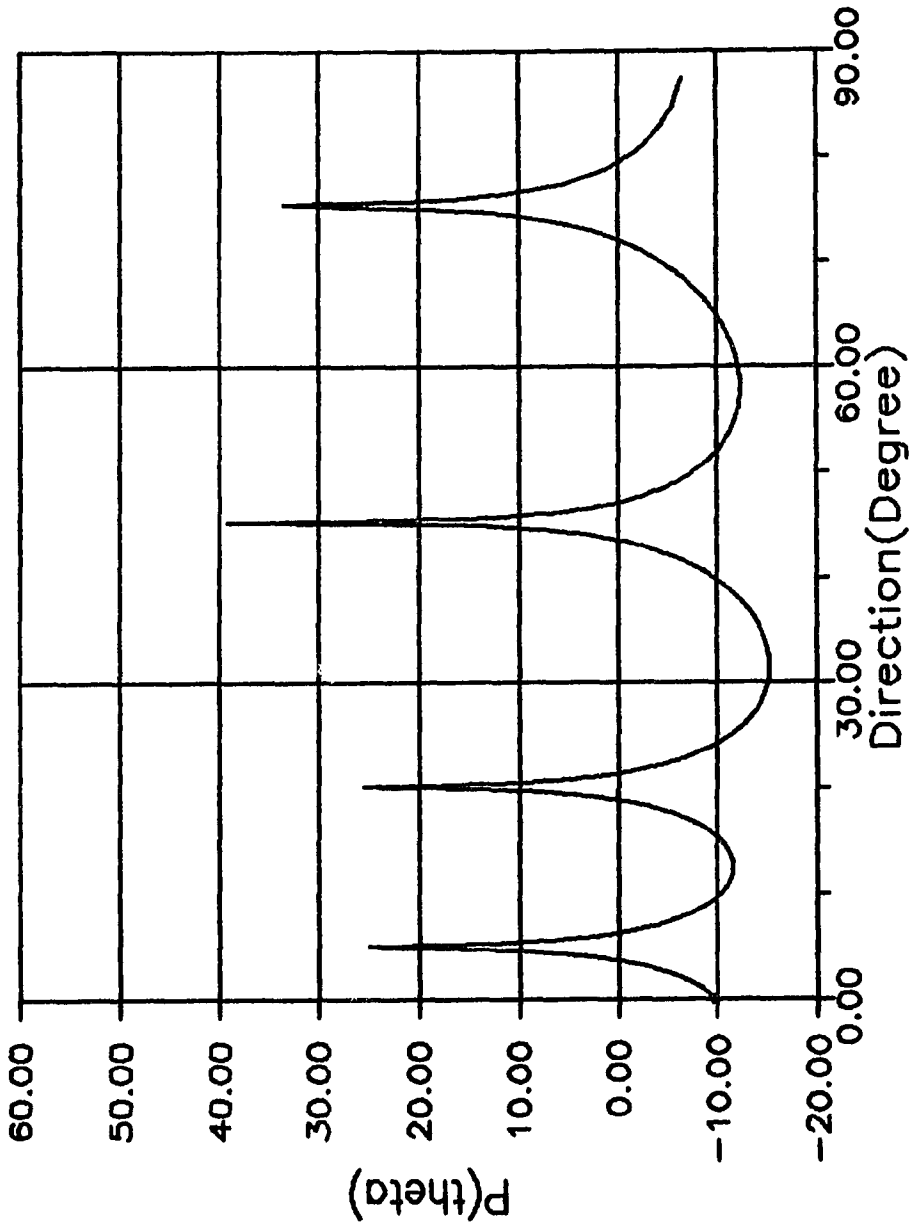


FIG 5-8

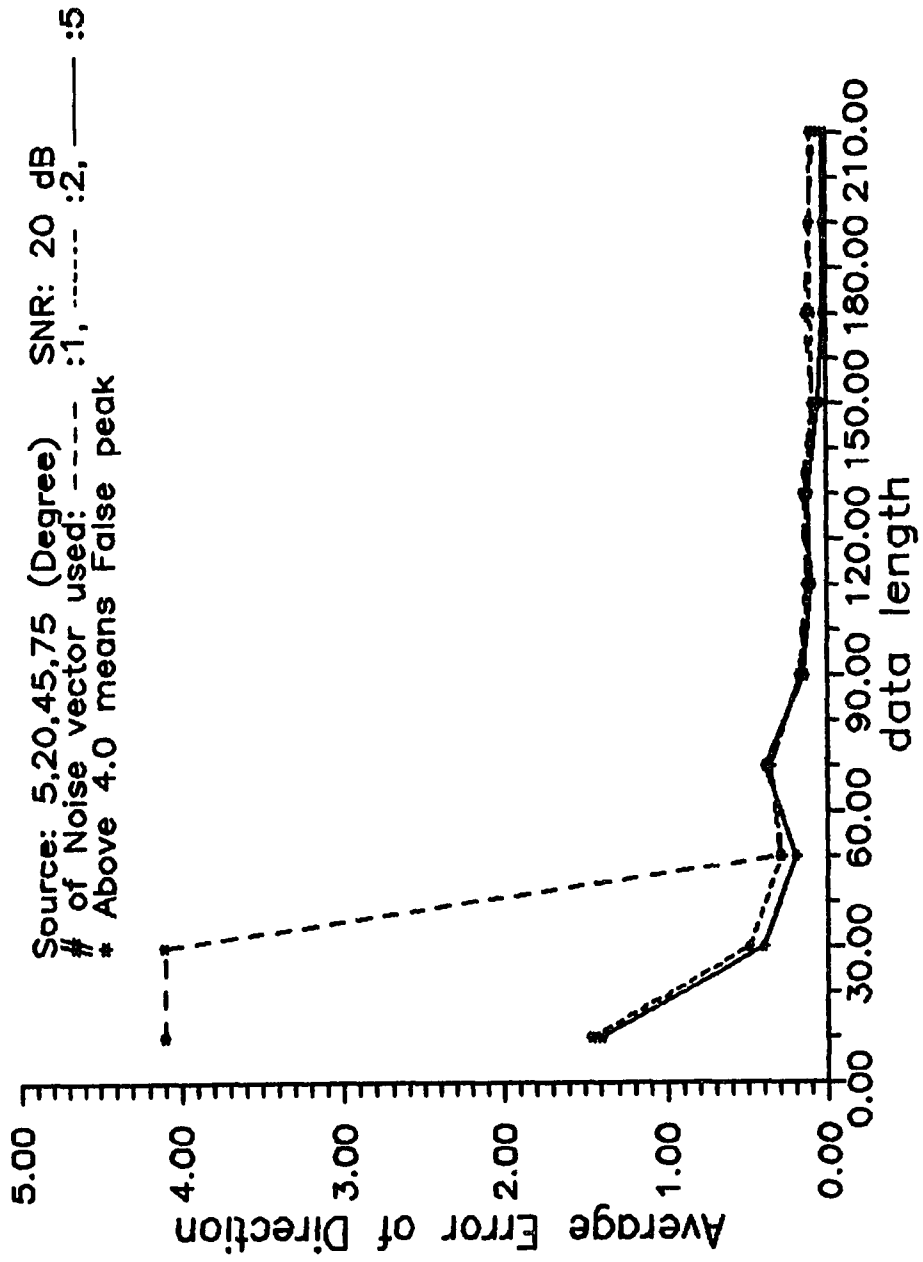


Fig 5-9

Direction: 5,20,45,75 SNR: 20 dB  
5 element MRA  
Data Length: 30  
# of Noise vector used:1

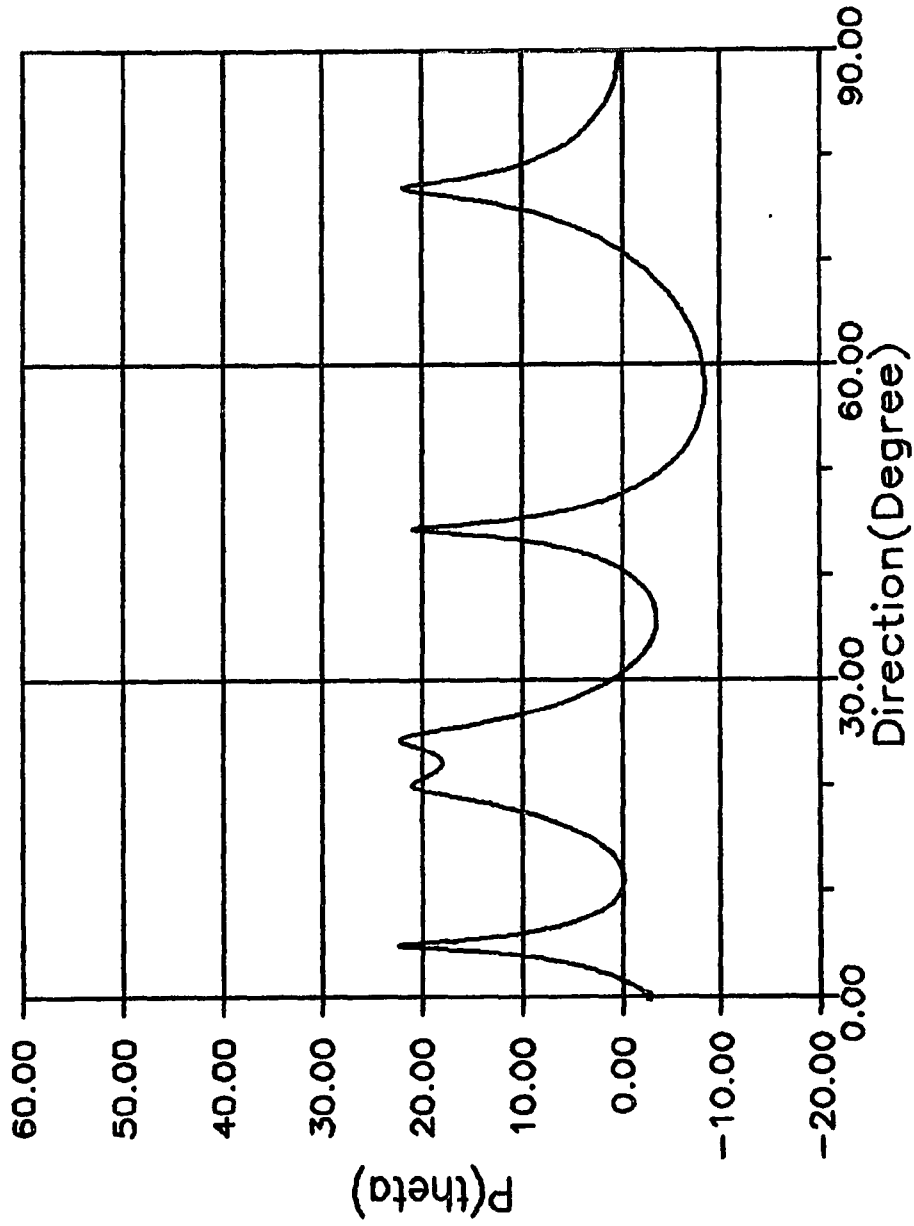


Fig 5-10

Direction: 5,20,45,75 SNR: 20 dB  
5 element MRA  
Data Length: 30  
# of Noise vector used:2

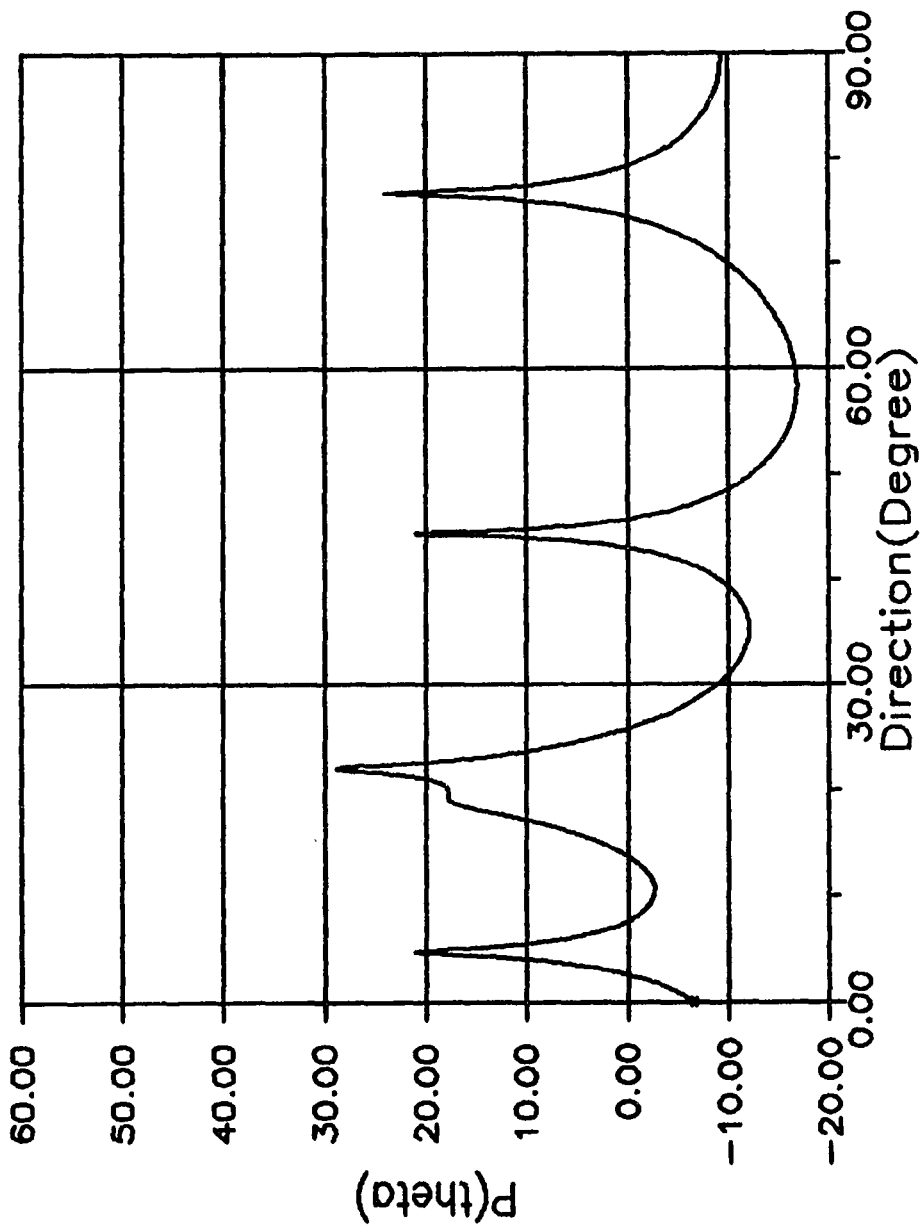
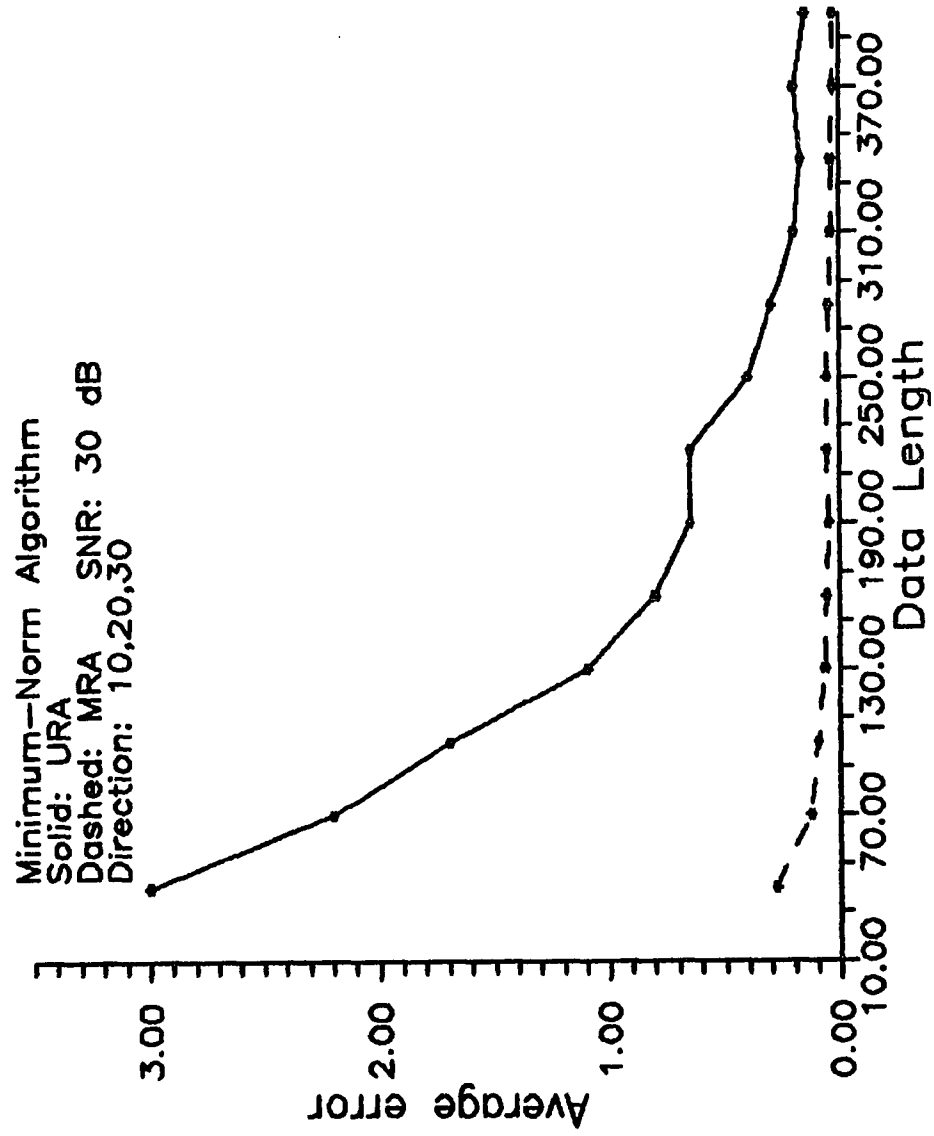


Fig 5-11



## 6. PERFORMANCE OF THE MUSIC BASED DIRECTION FINDING USING DIFFERENT COVARIANCE MATRIX ESTIMATES FOR THE UNIFORM REGULAR ARRAY(URA) AND THE MINIMUM REDUNDANCY ARRAY(MRA)

### 1. Introduction

In the direction finding problem when any of the superresolution methods, such as the MUSIC for example, is used, the knowledge of the covariance matrix of the signal at the array element is a must. In real applications there is no way to get the exact expected value  $E[X X^\dagger]$  (=R the covariance matrix), where X is the received wave form vector at the M array elements. If one assumes X is ergodic then R might be obtained from an infinite average sum of the samples of X ;

$$R = \lim_{N \rightarrow \infty} \frac{1}{N} \sum_{n=1}^N X_n X_n^\dagger$$

However to obtain such an average is impractical. Therefore  $R$  can be only estimated from the finite sum;

$$\hat{R} = R_1 = \frac{1}{N} \sum_{n=1}^N x_n x_n^\dagger \quad (1)$$

Obviously  $R_1$  is the random matrix as its elements are a finite sum of random variables. Other possible structures for estimating  $R$  have been suggested in [1],[2]. Different estimates of the covariance matrix will result in different accuracies when used in direction finding.

In this chapter we will present four different such estimates; namely, the random sample, the doubly symmetric, the averaged Toeplitz and the optimized Toeplitz, forms. Using these estimates of the covariance matrix in the MUSIC algorithm, we estimate the direction of signals impinging on a uniform regular array (URA) with  $M$  elements, and compare their estimation error. We will then conclude on the best method to use for direction finding with MUSIC algorithm.



With the minimum redundancy array(MRA) instead of the URA, we discuss the possibilities of getting covariance matrix estimates. Using these estimates we again use the MUSIC algorithm and obtain the resulting estimation error in the direction finding process.

## 2. Estimates of the Covariance Matrix

for the Uniform Regular Array.

Four different estimates are proposed;

### a) The Random Sampled Covariance matrix

Using N sample we define  $\hat{R}$  of 4 element array

$$\hat{R} = R_1 = \overline{X X^\dagger} = \begin{bmatrix} \overline{x_1 x_1^*} & \overline{x_1 x_2^*} & \overline{x_1 x_3^*} & \overline{x_1 x_4^*} \\ & \overline{x_2 x_2^*} & \overline{x_2 x_3^*} & \overline{x_2 x_4^*} \\ \text{conjugate} & & \overline{x_3 x_3^*} & \overline{x_3 x_4^*} \\ \text{symmetric} & & & \overline{x_4 x_4^*} \end{bmatrix} \quad (2)$$

where the overbar here is used for the  $N$  sample average rather than the expected value. That is

$$R_1 = \frac{1}{N} \sum_{n=1}^N X_n X_n^\dagger$$

and

$$\overline{x_i x_j^*} = \frac{1}{N} \sum_{n=1}^N x_{in} x_{jn}^* \quad (3)$$

where  $X_n$  is the  $n$ 'th sample of the vector  $X$  and  $x_{in}$  is the  $n$ 'th sample of the output of the  $i$ 'th element.

Since  $N$  is finite the elements of  $R_1$  are random variable, and hence  $\overline{x_1 x_2^*}$  is not necessarily equal to  $\overline{x_2 x_3^*}$  or to  $\overline{x_3 x_4^*}$ , contrary to the case when  $N$  goes to infinite. Therefore  $R_1$  is Hermitian but not necessarily Toeplitz.

#### b) Doubly Symmetric Covariance Matrix

Doubly symmetric matrix is both Hermitian about the principal diagonal and symmetric about the cross diagonal (the diagonal from bottom left to top right). We invoke the matrix theorem

concerning transpose about the cross diagonal, ie., flipping the matrix about the diagonal that runs upward to the right at 45 degree. If the transpose about the cross diagonal is denoted by prescript  $T(R)$ , then the doubly symmetric covariance matrix  $R_2$  can be obtained from  $R_1$  as follows;

$$R_2 = (R_1 + {}^T R_1) / 2$$

For the 4-element URA we have

$$R_2 = \begin{bmatrix} r_0 & r_1 & r_2 & r_3 \\ r_1^* & r_0' & r_1' & r_2 \\ r_2^* & r_1'^* & r_0' & r_1 \\ r_3^* & r_2^* & r_1^* & r_0 \end{bmatrix} \quad (4)$$

where,

$$r_0 = ( \overline{x_1 x_1^*} + \overline{x_4 x_4^*} ) / 2$$

$$r_0' = ( \overline{x_2 x_2^*} + \overline{x_3 x_3^*} ) / 2$$

$$r_1 = ( \overline{x_1 x_2^*} + \overline{x_3 x_4^*} ) / 2$$

$$r_1' = ( \overline{x_2 x_3^*} )$$

$$r_2 = ( \overline{x_1 x_3^*} + \overline{x_2 x_4^*} ) / 2$$

$$r_3 = ( \overline{x_1 x_4^*} )$$

c) The Average Toeplitz Covariance Matrix.

The average Toeplitz covariance matrix  $R_3$  is obtained from  $R_1$  by simple averaging along the different diagonals, That is

$$R_3 = \begin{bmatrix} r(0) & r(1) & r(2) & r(3) \\ r(1)^* & r(0) & r(1) & r(2) \\ r(2)^* & r(1)^* & r(0) & r(1) \\ r(3)^* & r(2)^* & r(1)^* & r(0) \end{bmatrix} \quad (5)$$

Where

$$r(0) = (\overline{x_1 x_1^*} + \overline{x_2 x_2^*} + \overline{x_3 x_3^*} + \overline{x_4 x_4^*}) / 4$$

$$r(1) = (\overline{x_1 x_2^*} + \overline{x_2 x_3^*} + \overline{x_3 x_4^*}) / 3$$

$$r(2) = (\overline{x_1 x_3^*} + \overline{x_2 x_4^*}) / 2$$

$$r(3) = (\overline{x_1 x_4^*})$$

d) Optimized Toeplitz Covariance Matrix using Maximum Likelihood Algorithm. (Burg's Algorithm)

The procedure of finding this estimate for the covariance matrix is given in [1]. For a matter of completeness we summarize the idea from that paper:

The task is " *One wish to select a covariance matrix of specified structure that corresponds in a reasonable way to a given set of vector samples.*" The author of [1] assumes that the vector random process at the array elements is zero-mean multivariate Gaussian, and that different samples of this vector are independent. The idea is then to choose the covariance matrix of this multivariate Gaussian so that to maximize the joint probability of occurrence of the vector samples.

In fact, the information in the vector sample is neatly contained in the sample covariance matrix  $R_1$ , so we end up with a performance index function  $p(R_1, R)$  in the two matrices  $R_1$ , and  $R$ .  $R$ , which is to be found, is constrained to be a Toeplitz covariance matrix, while  $R_1$  is a random sample covariance matrix that was shown to be Hermitian.

Let a vector  $X$  be  $M$ -dimensional Gaussian vector with zero mean and covariance matrix  $R$ . Then its probability density function is given by

$$p(X) = (2\pi)^{-M/2} |R|^{-1/2} \exp(-X^\dagger R^{-1} X / 2) \quad (6)$$

where  $|R|$  stands for the determinant of  $R$ .

Now instead of a single vector sample suppose that we have  $N$  independent vector samples,  $X_n$ ,  $n=1, \dots, N$ . then the probability density for this set of vectors will be :

$$p(X_1, X_2, \dots, X_N) = (2\pi)^{-NM/2} |R|^{-N/2} \exp(-\sum_{n=1}^N X_n^\dagger R^{-1} X_n / 2) \quad (7)$$

We consider the situation where  $R$  is unknown except that it is a member of a certain family  $\mathcal{R}$  of feasible covariances. For example, an important case is when  $\mathcal{R}$  is the collection of the positive definite Hermitian Toeplitz matrices. Notice that given the set of the vector samples  $X_n$ ,  $n=1, \dots, N$ , then  $R \in \mathcal{R}$  which maximizes (7) is the *Maximum-Likelihood Estimation* of the covariance matrix. Taking a Logarithm of (7) we get:

$$\log P(x_1, x_2, \dots, x_N) =$$

$$-(NM/2) \log(2\pi) - (N/2) \log |R| - (1/2) \sum_{n=1}^N x_n^\dagger R^{-1} x_n \quad (8)$$

Dropping the leading constant term and dividing through by  $N/2$ , we define objective function  $P(R_1, R)$  to be

$$P(R_1, R) = -\log |R| - (1/N) \sum_{n=1}^N x_n^\dagger R^{-1} x_n \quad (9)$$

Obviously maximizing  $P(R_1, R)$  is equivalent to maximizing (8).

Using matrix relation,

$$x^\dagger R^{-1} x = \text{tr} (R^{-1} x x^\dagger),$$

in (9) we get;

$$P(R_1, R) = -\log |R| - \text{tr}(R^{-1} (1/N) \sum_{n=1}^N x_n x_n^\dagger) \quad (10)$$

With the definition of the sample covariance matrix  $R_1$ ,

$$R_1 = 1/N \sum_{n=1}^N x_n x_n^\dagger$$

We arrive at the equation for  $P(R_1, R)$

$$P(R_1, R) = - \log |R| - \text{tr}(R^{-1} R_1) \quad (11)$$

Our objective is then to find the  $R$  which belongs to the class of positive definite Hermitian and Toeplitz matrices  $\mathcal{R}$ , and which would maximize  $P(R_1, R)$ , where  $R_1$  is a given sample covariance matrix obtained from the measurement.

This is a variational problem. That is, we must first derive the variation of the functional  $P$  in terms of the variation of  $R$ . The variation of  $R$  is defined as follows

$$\delta R = \begin{bmatrix} \delta R(1,1) & \delta R(1,2) & \dots & \delta R(1,M) \\ \delta R(2,1) & \delta R(2,2) & \dots & \delta R(2,M) \\ \vdots & \vdots & \ddots & \vdots \\ \delta R(M,1) & \delta R(M,2) & \dots & \delta R(M,M) \end{bmatrix}$$

where  $\delta R(i,j)$  is the variation of  $i,j$ 'th element of  $R$ . Now taking the variation of both sides of (11) we have



$$\delta [P(R_1, R)] = -\delta \log |R| - \delta \operatorname{tr}(R^{-1} R_1)$$

After some simple derivation detailed in the appendix, we get

$$\delta [P(R_1, R)] = \operatorname{tr} [(R^{-1} R_1 R^{-1} - R^{-1}) \delta R] \quad (12)$$

For an extremum of the functional  $P(R_1, R)$ , it is necessary that its variation equals zero for any variation  $\delta R$  that belongs to  $\mathcal{X}$ .

That is

$$\operatorname{tr} [(R^{-1} R_1 R^{-1} - R^{-1}) \delta R] = 0 \quad (13)$$

for every  $\delta R \in \mathcal{X}$ .

In particular it must be true for  $\delta R = R$ . In which case we have

$$\operatorname{tr} [(R^{-1} R_1 R^{-1} - R^{-1}) R] = 0$$

or 
$$\operatorname{tr} [R^{-1} R_1] = M \quad (14)$$

Substituting in (11) we get as a necessary condition for  $P(R_1, R)$  to be maximum, that is

$$P(R_1, R) = -\log |R| - M \quad (15)$$

From the form for  $P(R_1, R)$  in (14) and from (15) we can restate our variational problem as follows instead of maximizing  $P(R_1, R)$ ;

minimize the determinant of R under the constraints that

$$1) R \in \mathcal{R}$$

$$2) \text{tr} [R^{-1}R_1] = M \text{ where } M \text{ is the number of the array elements}$$

In fact this constrained minimization problem can be solved using Lagrange multiplier  $\lambda$ . That is

$$\delta [ -\log |R| - \lambda \text{tr}(R^{-1}R_1) ] = -\text{tr} [ (R^{-1} - \lambda R^{-1}R_1R^{-1})\delta R ] \quad (16)$$

where we again used equation (A-2) and (A-3) of the appendix.

Again using  $\delta R = R$  we get

$$\text{tr} [ I - \lambda R^{-1}R_1 ] = 0$$

or

$$\lambda \text{tr} [R^{-1}R_1] = M$$

That is  $\lambda=1$  and we are back to the problem of setting the variation of (11) to zero. This shows that the constrained minimization stated above is equivalent to maximizing the functional in (11)

- The Inverse Iteration Algorithm

Using the fact that the variational problem in (12) is linear in  $R_1$  the author in [1] proposes to use what he termed the Inverse Iteration Algorithm. That is ; at any stage, he begins with an approximation  $R_k$  and finds a new approximation  $R_{k+1}$  as follows:

1) Find  $D_k$  which belong to  $\mathcal{X}$  so that  $P(R_1 - D_k, R_k)$  satisfy

equation (13) such as

$$\text{tr} [ \{ R_k^{-1} (R_1 - D_k) R_k^{-1} \} \delta R_k ] = 0 \quad (17)$$

Where  $\delta R_k$  is the variation of  $R_k$ . This equation means inside of  $\{ \dots \}$  is orthogonal to the change  $\delta R_k$  in  $\mathcal{X}$  space.

2) Put  $R_{k+1} = R_k + D_k$

To find  $D_k \in \mathcal{X}$ , let us first assume that  $Q_m$   $m=1,2, \dots, M$ , form a basis for  $\mathcal{X}$  then we can write

$$D_k = \sum_{m=1}^M b_m Q_m$$

and (17) can be rewritten as

$$\text{tr} \left[ \left( R_k^{-1} \left( R_1 - \sum_{m=1}^M b_m Q_m \right) R_k^{-1} \right) Q_j \right] = 0 \quad (18)$$

for every  $Q_j$   $j=1, \dots, M$ . After rearrangement of (18) we get

$$\sum_{m=1}^M \text{tr} \left[ R_k^{-1} Q_m R_k^{-1} Q_j \right] b_m = \text{tr} \left[ R_k^{-1} R_1 R_k^{-1} Q_j \right] \quad (19)$$

$$j=1, \dots, M$$

This is a system of  $M$  equations in  $M$  unknowns;  $b_m$ ,  $m=1, \dots, M$ . The solution of these equations yields  $D_k$  and hence the next approximation  $R_{k+1}$ . In fact from (19) if we define

$$A_{ij} = \text{tr} \left[ R_k^{-1} Q_i R_k^{-1} Q_j \right]$$

and

$$c_j = \text{tr} \left[ R_k^{-1} R_1 R_k^{-1} Q_j \right]$$

then the aforementioned linear equation is given by the set of linear equations

$$A b = c \quad b = [b_1, b_2, \dots, b_M]^T$$

### 3. Covariance Matrix for Minimum Redundancy Array.

For a 4-element Minimum Redundancy Array, the location of the elements are  $(0, 2\lambda/2, 5\lambda/2, 6\lambda/2)$ . In a notation consistent to the notation of Uniform Regular Array we can write

$$\begin{aligned}
 \mathbf{x} &= [x_1, x_3, x_6, x_7]^T \\
 \mathbf{R} &= \overline{\mathbf{x} \mathbf{x}^\dagger} = \begin{bmatrix} \overline{x_1 x_1^*} & \overline{x_1 x_3^*} & \overline{x_1 x_6^*} & \overline{x_1 x_7^*} \\ & \overline{x_3 x_3^*} & \overline{x_3 x_6^*} & \overline{x_3 x_7^*} \\ \text{conjugate} & & \overline{x_6 x_6^*} & \overline{x_6 x_7^*} \\ \text{symmetric} & & & \overline{x_7 x_7^*} \end{bmatrix} \quad (20)
 \end{aligned}$$

Defining  $r(0)$  by,

$$r(0) = 1/4 [ \overline{x_1 x_1^*} + \overline{x_2 x_2^*} + \overline{x_5 x_5^*} + \overline{x_7 x_7^*} ]$$

$$r(j-i) = \overline{x_i x_j^*}$$

the matrix (20) can be written as,

$$R = \begin{bmatrix} r(0) & r(2) & r(5) & r(6) \\ & r(0) & r(3) & r(4) \\ \text{conjugate} & r(0) & r(1) & \\ \text{symmetric} & & & r(0) \end{bmatrix} \quad (21)$$

In the matrix of (21) we notice the existence of all delay lags  $r(0)$  to  $r(6)$ . The number of lags(=6) =  $M(M-1)/2$ . This is in fact the property of the Minimum Redundancy Array wherein the element locations are chosen so that many delay lags rather than only  $M$  lags (as in the case of URA) is generated. For other values of  $M$  it is possible to generate only  $N < M(M-1)/2$  different lags, nevertheless  $N \gg M$  (see [3])

The different entries in the Hermitian covariance matrix (21) can be augmented to the following Toeplitz, Hermitian matrix.

$$R_T = \begin{bmatrix} r(0) & r(1) & r(2) & r(3) & r(4) & r(5) & r(6) \\ r(1)^* & r(0) & r(1) & r(2) & r(3) & r(4) & r(5) \\ r(2)^* & r(1)^* & r(0) & r(1) & r(2) & r(3) & r(4) \\ r(3)^* & r(2)^* & r(1)^* & r(0) & r(1) & r(2) & r(3) \\ r(4)^* & r(3)^* & r(2)^* & r(1)^* & r(0) & r(1) & r(2) \\ r(5)^* & r(4)^* & r(3)^* & r(2)^* & r(1) & r(0) & r(1) \\ r(6)^* & r(5)^* & r(4)^* & r(3)^* & r(2)^* & r(1) & r(0) \end{bmatrix} \quad (22)$$

Notice that in Toeplitz matrix except for  $r(0)$  the other elements are forced to be the same rather than obtained from the average of the elements in a diagonal as in the Uniform Regular Array. Because of this fact we cannot choose an optimum covariance matrix by using burg's algorithm. Such an approach is possible only when there is redundancy in the covariance element.

Different augmentation might lead to:

$$R_H = \begin{bmatrix} r(0) & r(2) & r(3) & r(1) & r(5) & r(4) & r(6) \\ r(2)^* & r(0) & r(1) & r(1)^* & r(3) & r(2) & r(4) \\ r(3)^* & r(1)^* & r(0) & r(2)^* & r(2) & r(1) & r(3) \\ r(1)^* & r(1) & r(2) & r(0) & r(4) & r(3) & r(5) \\ r(5)^* & r(3)^* & r(2)^* & r(4)^* & r(0) & r(1)^* & r(1) \\ r(4)^* & r(2)^* & r(1)^* & r(3)^* & r(1) & r(0) & r(2) \\ r(6)^* & r(4)^* & r(3)^* & r(5)^* & r(1)^* & r(2)^* & r(0) \end{bmatrix} \quad (23)$$

This is a Hermitian but not Toeplitz.

The matrix  $R_H$  can be obtained from  $R_T$  by considering the linear transformation between the corresponding random vector  $X_H$  and  $X_T$  respectively. That is

$$X_H = C X_T$$

and in detail:



$$\begin{bmatrix} x_1 \\ x_3 \\ x_4 \\ x_2 \\ x_6 \\ x_5 \\ x_7 \end{bmatrix} = \begin{bmatrix} 1 & 0 & 0 & 0 & 0 & 0 & 0 \\ 0 & 0 & 1 & 0 & 0 & 0 & 0 \\ 0 & 0 & 0 & 1 & 0 & 0 & 0 \\ 0 & 1 & 0 & 0 & 0 & 0 & 0 \\ 0 & 0 & 0 & 0 & 0 & 1 & 0 \\ 0 & 0 & 0 & 0 & 1 & 0 & 0 \\ 0 & 0 & 0 & 0 & 0 & 0 & 1 \end{bmatrix} \begin{bmatrix} x_1 \\ x_2 \\ x_3 \\ x_4 \\ x_5 \\ x_6 \\ x_7 \end{bmatrix} \quad (24)$$

Notice that;

$$\begin{aligned}
 R_T &= \overline{X_T X_T^\dagger} \\
 R_H &= \overline{X_H X_H^\dagger} = \overline{C X_T (C X_T)^\dagger} \\
 &= \overline{C X_T X_T^\dagger C^T} = C R_T C^T
 \end{aligned}$$

The Eigenvector and Eigenvalue of  $R_T$ ,  $R_H$ , are defined as follows;

$$\begin{aligned}
 R_T v_T &= \lambda_T v_T \\
 \text{and ,} & \\
 R_H v_H &= C R_T C^T v_H \\
 &= \lambda_H v_H
 \end{aligned} \quad (25)$$

$$\rightarrow R_T C^T v_H = \lambda_H C^T v_H \quad (26)$$

where we used the fact that  $C C^T = I$ . (Identity Matrix)

From (25) and (26) we conclude that for every eigenvector  $v_T$  of  $R_T$  and its corresponding eigenvalue  $\lambda_T$  there exists another eigenvector  $C^T v_H$  and a corresponding eigenvalue  $\lambda_H$  for  $R_T$ , where  $v_H$  and  $\lambda_H$  are an eigenvector and a corresponding eigenvalue of  $R_H$ . Hence the set of eigenvectors  $\{v_{Ti}; i=D+1, \dots, M\}$  which corresponds eigenvectors  $\{C^T v_{Hi}; i= D+1, \dots, M\}$ , where  $v_{Hi}$   $i= D+1, \dots, M$ , are the eigenvector of  $R_H$ .

The direction finding formula of the MUSIC algorithm of Toeplitz covariance matrix is given by

$$P(\theta) = \frac{1}{a(\theta)^\dagger \left( \sum_{k=D+1}^M v_{Tk} v_{Tk}^\dagger \right) a(\theta)} \quad (27)$$

where  $D$  is the number of sources and  $M$  is the dimension of  $R$ .

When using the Hermitian matrix of (24), we must first transform each eigenvector by  $C^T$  to get  $C^T v_{Hi}$ . Then the corresponding MUSIC formula is given by

$$P(\theta) = \frac{1}{\mathbf{a}(\theta)^{\dagger} \left( \sum_{k=D+1}^M (Cv_{Tk})(Cv_{Tk})^{\dagger} \right) \mathbf{a}(\theta)} \quad (28)$$

#### 4. Simulation Results

The different methods of obtaining estimates for the covariance matrix were evaluated in a simulation of a MUSIC algorithm for finding the direction of 3 sources located at 10, 25, and 45 degrees from broadside. The angle of arrival estimation were compared to the actual direction, and the average estimated error was calculated. Figure 6-1 compares the average of estimated error when using the random sampled covariance matrix with that when using the doubly symmetric covariance matrix. Notice that the first case outperforms the second. Figure 6-2 compares the average of the estimated error when using the average Toeplitz covariance matrix with that when using the random sampled covariance matrix. Again the method of the two outperforms the second. Figure 6-3 depicts the same comparison between using the optimized Toeplitz covariance and using the average Toeplitz covariance. The second

method only slightly outperform the first. In figure 6-4 on the comparison is done between two different structure of arrays; the uniform regular array and the minimum redundancy array. For the first we used the optimized Toeplitz method which gave the best result for the uniform regular array. Notice that the MRA gave much better results. Figure 6-5 shows all the result in one graph.

## 5. Conclusion.

The effect of different estimates for the covariance matrix on the performance of multi-source direction finding was considered in this chapter. The estimates considered are random sample, the doubly symmetric, the averaged Toeplitz and the optimized Toeplitz when using MUSIC algorithm for direction finding. Simulation results shows that the optimized Toeplitz method give the best results. When the array is of the MRA type little redundancy exist and only the random sample method can be used as an estimate for the covariance matrix. Nevertheless simulation shows that this array outperforms the URA even when the best estimate for the covariance matrix is used.

## Appendix

Few matrix equation will be first generated and then be use to derive (110 of the text

1.

$$\delta|R| = |R| \operatorname{tr}[R^{-1} \delta R] \quad (\text{A-1})$$

can be obtained directly from the definition of a determinant of a matrix  $|R|$  and its inverse  $R^{-1}$  in terms of the cofactors of  $R$ .

We will demonstrate this through a 2x2 matrix example. Let

$$R = \begin{bmatrix} a & b \\ c & d \end{bmatrix}, \text{ then } \delta|R| = a\delta d + d\delta a - b\delta c - c\delta b$$

$$R^{-1}\delta R = \frac{1}{|R|} \begin{bmatrix} d & -b \\ -c & a \end{bmatrix} \begin{bmatrix} \delta a & \delta b \\ \delta c & \delta d \end{bmatrix}$$

$$\operatorname{tr}[R^{-1}\delta R] = \frac{1}{|R|} (d\delta a - b\delta c - c\delta b + a\delta d)$$

Hence

$$\delta|R| = \frac{1}{|R|} \operatorname{tr}[R^{-1} \delta R]$$

$$2. \quad \delta \log |R| = \frac{\delta |R|}{|R|} = \text{tr} [ R^{-1} \delta R ] \quad (\text{A-2})$$

$$3. \quad R R^{-1} = I \\ \delta R R^{-1} + R \delta R^{-1} = \delta I = 0$$

$$\text{Hence} \quad \delta R^{-1} = -R^{-1} \delta R R^{-1} \quad (\text{A-3})$$

Now From (10),

$$\delta [ P(R_1, R) ] = -\delta \log |R| - \delta \text{tr} [ R^{-1} R ]$$

But from (A-2)

$$\delta \log |R| = \text{tr} [ R^{-1} \delta R ]$$

and from (A-3)

$$\delta ( R^{-1} ) = -R^{-1} \delta R R^{-1}$$

$$\text{also} \quad \delta \text{tr} [ R^{-1} R_1 ] = \text{tr} [ \delta ( R^{-1} ) R_1 ]$$

$$\text{Then} \quad \delta [ P(R_1, R) ] = -\text{tr} [ R^{-1} \delta R ] + \text{tr} [ R^{-1} \delta R R^{-1} R_1 ]$$

$$\text{But} \quad \text{tr} [ R^{-1} \delta R R^{-1} R_1 ] = \text{tr} [ R^{-1} R_1 R^{-1} \delta R ]$$

$$\text{Therefore} \quad \delta P(R_1, R) = \text{tr} [ ( R^{-1} R R^{-1} - R^{-1} ) \delta R ] \quad (\text{A-4})$$

## References

- [1] J.P. Burg , D.G. Luenberger, D. L. Wenger," Estimation of Structured Covariance Matrices" IEEE Proc. Vol. 70, No 9, September 1982
- [2] S. L. Maple, Jr,"Digital Spectral Analysis with Applications" Prentice Hall
- [3]S.U. Pillai, Y. Bar-Ness, and F. Haber,"A new approach to array geometry for improved spatial spectrum estimation," Proc. IEEE,vol. 73 10,pp 1522-1524, Oct. 1985.

Fig 6-1

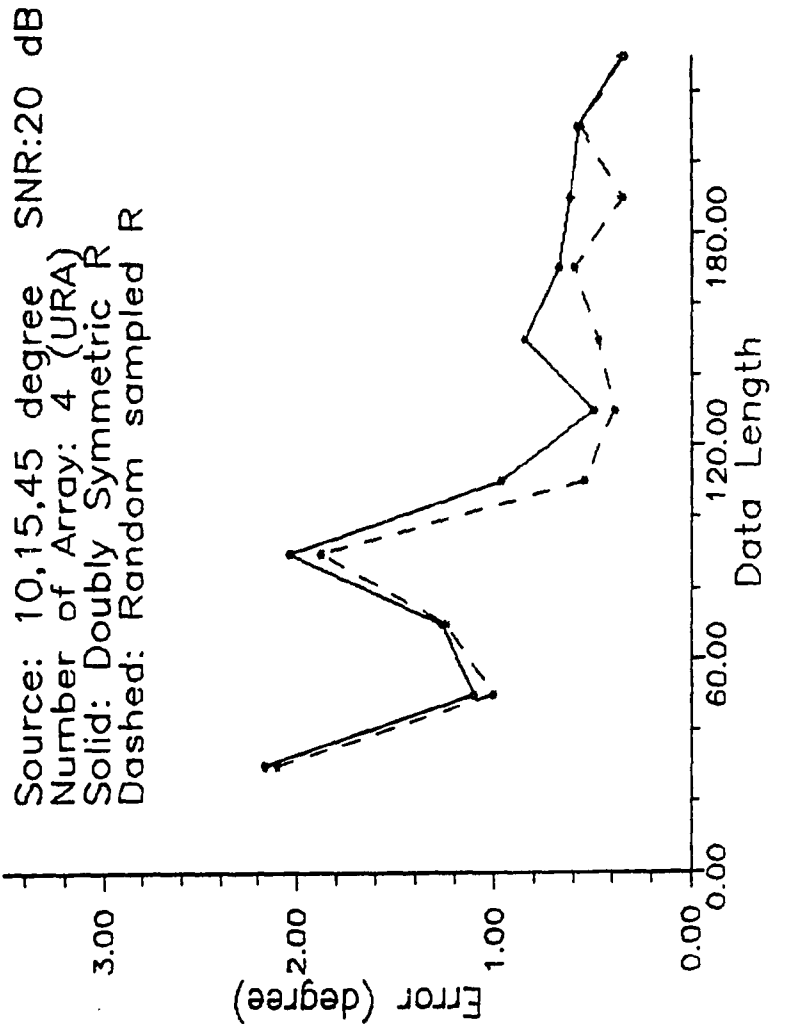




FIG 6-2

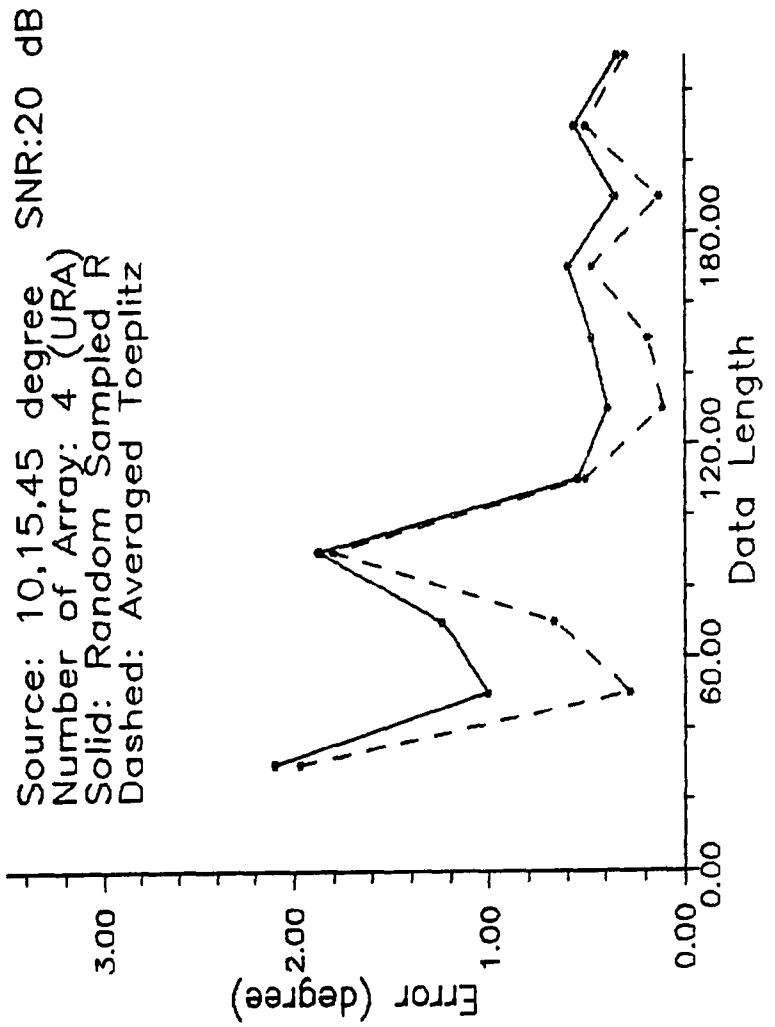


Fig 6-3

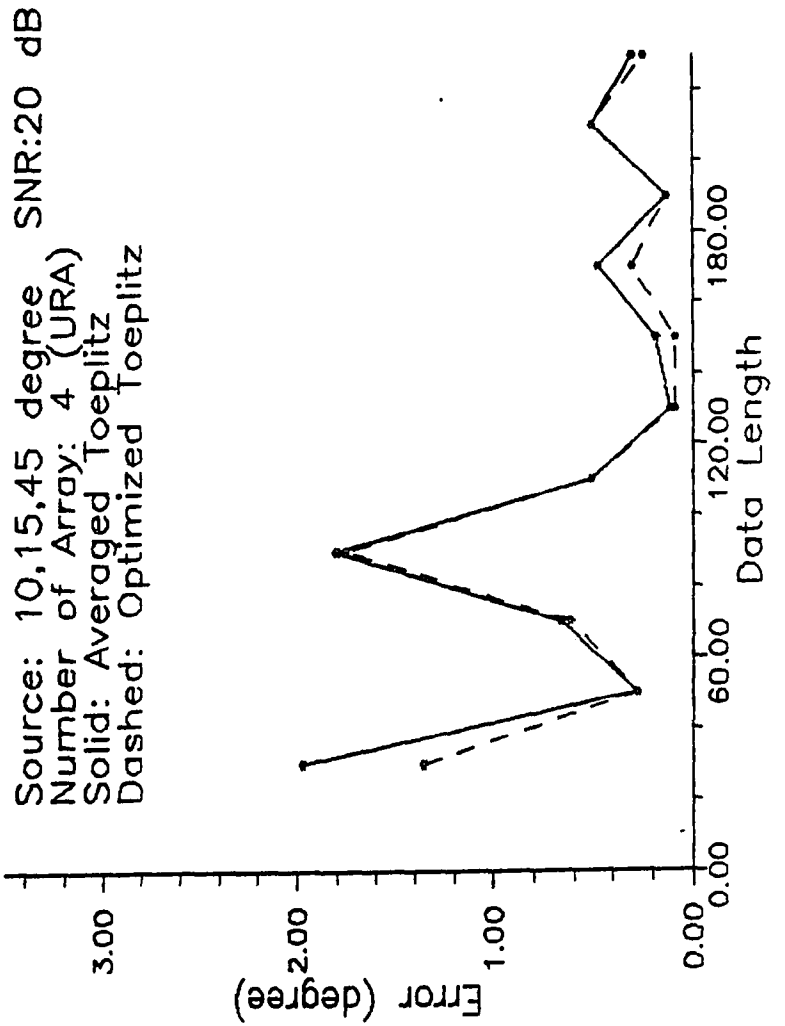
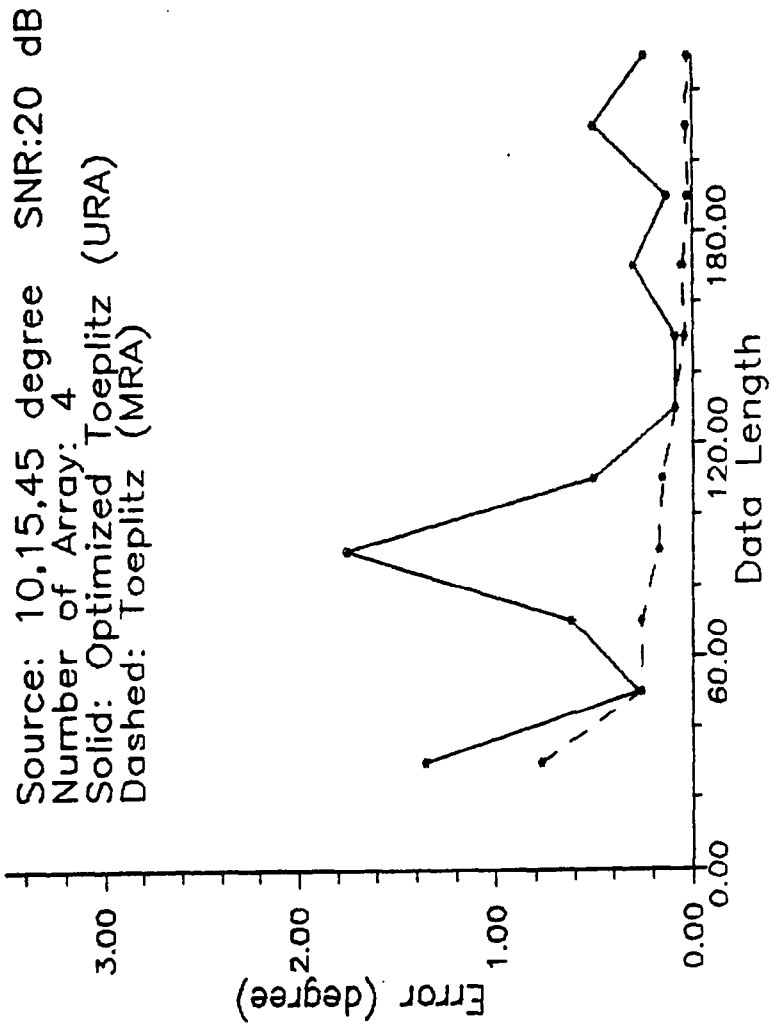


Fig 6-4



From the Top:  
Doubly Symmetric, Random Sampled,  
Averaged Toeplitz, Optimized Toeplitz,  
Toeplitz (MRA)

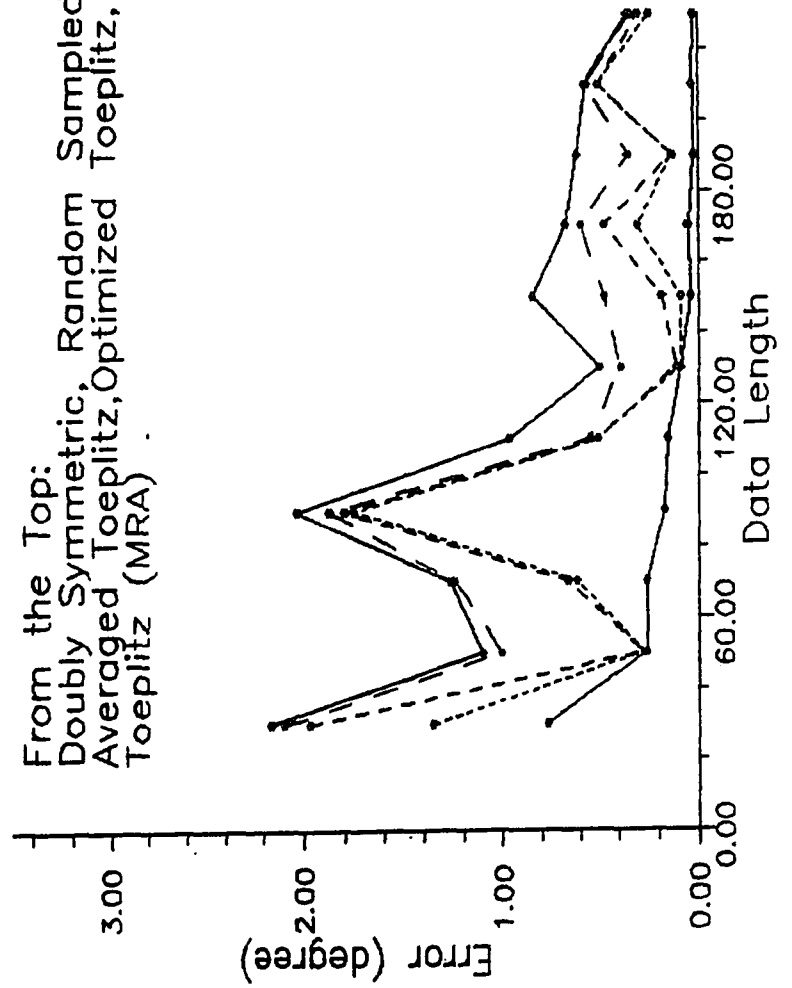


FIG 6-5

## 7. THE ERROR PROBABILITY OF ESTIMATING THE NUMBER OF TWO CLOSELY LOCATED SOURCES.

### 1. Introduction

The problem of estimating the number of signals impinging on an array is very important. Its value is a crucial parameter by itself, but also required in some approaches of finding the direction of these signals. The eigenspace method for direction finding relies heavily on the knowledge of the actual number of sources.

Every estimation problem has errors associated with it. The probability of these errors are of interest. Such probability of errors obviously depends on the method used as well as on the parameters of the process implemented. In the estimation of number of sources, of interest is, both underestimation (that is when our estimation is smaller than the actual number) or overestimation (that is when the estimated number is larger than the actual number). Particularly when the actual number of sources is only two and when these sources are very close to one another the question of underestimating is rather interesting.

In some old methods of estimating the number of signal subjective approaches were used [1]. That is, equal eigenvalues with certain tolerance, are taken to correspond to noise eigenvalues. The number of sources is then taken to be the dimension of the array minus the number of these equal eigenvalues. Errors will occur particularly when some of the eigenvalues, which correspond to signal sources are close, to the noise eigenvalues.

Recently researchers have been using information theoretical criteria instead of these subjective approaches. Akaike [2] used the so called Akaike Information Criterion (AIC), while Schwartz and Riessanen [3] used the so called Minimum Description Length (MDL) to determine the order of polynomial by which dynamic system might be approximated. Later Wax and Kailath [4] used both methods in estimating the number of sources impinging on an array. They show that MDL results in smaller estimation errors than AIC and that these errors diminish when the length of data used becomes infinitely large. They did not, however, explicitly present the values of these errors. Wang and Kaveh [5] gave an analytical form for the probability of error for both underestimating and overestimating the number of sources. Applying Taylor series approximation of a logarithmic function they could present the

probability of error as an *erf* (error function), and hence, could use existing numerical tables. As they admit their approximations are valid only when the number of sensors  $M$  is very large.

In this chapter we study the validity of Wang and Kaveh's approximation for the particular case of two sources close to each other. We show that such approximations are not only very sensitive to  $M$  but also to SNR. In fact they are valid only at very low SNR and very close sources, a situation which is unlikely to occur in practice. The probability of error in such situations turns out to be one. Using analytical expression without the aforementioned approximation leads to a more pessimistic result, that is, to a higher probability of error than what Wang and Kaveh predicted. Direct simulation gave very close results to those obtained when using the analytical expression with no approximation. Therefore one might question whether the whole method of estimating the number of sources using MDL is of any value.

Before going into the main topic we first briefly review the basic concept of direction finding of narrow band signals. The waveform received at the  $M$  element array is a linear combination of the  $D$  incident wave fronts and noise. Thus the waveform vector  $X$  can be expressed as follows:

$$\begin{bmatrix} X_1 \\ X_2 \\ \vdots \\ X_M \end{bmatrix} = \begin{bmatrix} a(\theta_1), a(\theta_2), \dots, a(\theta_D) \end{bmatrix} \begin{bmatrix} F_1 \\ F_2 \\ \vdots \\ F_D \end{bmatrix} + \begin{bmatrix} W_1 \\ W_2 \\ \vdots \\ W_M \end{bmatrix}$$

or,

$$X = A F + W \quad (1)$$

The incident signals are represented in amplitude and phase at some arbitrary reference point by the complex quantities  $F_1, F_2, \dots, F_D$ . The noise, whether sensed along with the signal or generated internally, is given by the complex vector  $W$ . The element  $a(i,j)$  of the matrix  $A$  is a function of the signals' arrival angles and the array element locations. That is,  $a(i,j)$  depends on the  $i$ 'th array element, its position relative to the origin, and its response to a signal incident from the direction of the  $j$ 'th signal. The covariance matrix  $R$  is given by

$$R = \overline{X X^\dagger} = A \overline{F F^\dagger} A^\dagger + \overline{W W^\dagger} \quad (2)$$

where the overbar is used for the expectation and  $\dagger$  is the



transpose conjugate. Under the basic assumption that the incident signal and noise are uncorrelated the matrix  $\overline{F F^\dagger}$  and  $\overline{W W^\dagger}$  are diagonal.

Let  $\lambda_i$  and  $e_i$ ,  $i= 1, 2, \dots M$ , be the eigenvalues and corresponding eigenvectors of R with  $\lambda_i$  in descending order, that is  $\lambda_1 > \lambda_2 > \dots > \lambda_M$ .

The MDL criterion which estimates the number of source by finding k that minimizes the function  $\Lambda(k,N)$ , where;

$$\Lambda(k,N) = N(M-k) \log\left(\frac{a(k)}{g(k)}\right) + 1/2 k(2M-k) \log N \quad (3)$$

N is the data length,

$$a(k) = \frac{1}{M-k} \sum_{i=k+1}^M \hat{\lambda}_i, \quad (4)$$

and

$$g(k) = \left( \prod_{i=k+1}^M \hat{\lambda}_i \right)^{1/(M-k)} \quad (5)$$

$\hat{\phantom{x}}$  : estimated value

## 2. Detection Performance

Let  $H_k$  denote the hypothesis that the number of actual sources is  $k$ . We can derive the probability of underestimating the number of sources given  $H_k$ , by

$$P_u(k) = P \{ (\hat{k} < k) \mid H_k \} \quad (6)$$

where  $\hat{\phantom{k}}$  means estimated value. The probability of overestimating the number of sources given  $H_k$  is

$$P_o(k) = P \{ (\hat{k} > k) \mid H_k \} \quad (7)$$

It is reasonable to assume that the probability of overestimation or underestimation as a function of difference between  $k$  and  $\hat{k}$  is decreasing fast. That is,

$$P \{ (\hat{k} = k-1) \mid H_k \} \gg P \{ (\hat{k} \leq k-2) \mid H_k \} \quad (8)$$

and

$$P \{ (\hat{k} = k+1) \mid H_2 \} \gg P \{ (\hat{k} \geq k+2) \mid H_2 \} \quad (9)$$

so that

$$\begin{aligned}
 P_u(k) &\simeq P\{ (\hat{k} = k-1) \mid H_k \} \\
 &= P\{ \Lambda(k-1, N) < \Lambda(k, N) \mid H_k \} \quad (10)
 \end{aligned}$$

and

$$\begin{aligned}
 P_o(k) &\simeq P\{ (\hat{k} = k+1) \mid H_k \} \\
 &= P\{ \Lambda(k+1, N) < \Lambda(k, N) \mid H_k \} \quad (11)
 \end{aligned}$$

Note that the probability of incorrectly estimating the number of sources given  $H_k$  is

$$\begin{aligned}
 P_E &= P\{ (\hat{k} \neq k) \mid H_k \} \\
 &\simeq P_u(k) + P_o(k) \quad (12)
 \end{aligned}$$

By definition of  $a(k)$  and  $g(k)$  we can easily get,

$$a(k-1) = \frac{1}{M - (k-1)} \hat{\lambda}_k + \frac{M - k}{M - (k-1)} a(k) \quad (13)$$

$$[g(k-1)]^{M-(k-1)} = \hat{\lambda}_k [g(k)]^{M-k} \quad (14)$$

Now,

$$(M-(k-1)) \log [ a(k-1)/g(k-1) ]$$

$$= \log \frac{[a(k-1)]^{M-(k-1)}}{[g(k-1)]^{M-(k-1)}}$$

and by using (13) and (14) we get,

$$= \log \frac{\left[ \frac{1}{M-(k-1)} \hat{\lambda}_k + \frac{M-k}{M-(k-1)} a(k) \right]^{M-(k-1)}}{\hat{\lambda}_k [g(k)]^{M-k}}$$

and after simple evaluation,

$$= \log \frac{[a(k)]^{M-k}}{[g(k)]^{M-k}} \frac{\left[ \frac{M-k}{M-(k-1)} + \frac{\hat{\lambda}_k}{(M-(k-1)) a(k)} \right]^{M-(k-1)}}{[\hat{\lambda}_k / a(k)]}$$

$$= (M-k) \log \frac{a(k)}{g(k)} + \log Q_u (\hat{\lambda}_k / a(k)) \quad (15)$$

where

$$Q_u(\hat{\lambda}_k / a(k)) = \frac{\left[ \frac{M-k}{M-(k-1)} + \frac{1}{M-(k-1)} (\hat{\lambda}_k / a(k)) \right]^{M-(k-1)}}{[\hat{\lambda}_k / a(k)]} \quad (16)$$

Notice also that (15) can be written in the form

$$\log \left[ \frac{a(k-1)}{g(k-1)} \right]^{M-(k-1)} = \log \left[ \frac{a(k)}{g(k)} \right]^{M-k} + \log Q_u(\hat{\lambda}_k / a(k)) \quad (16.a)$$

Similarly we have

$$(M-(k+1)) \log \frac{a(k+1)}{g(k+1)} = (M-k) \log \frac{a(k)}{g(k)} + \log Q_o(\hat{\lambda}_{k+1} / a(k)) \quad (17)$$

where

$$Q_o(\hat{\lambda}_{k+1} / a(k)) = \frac{\left[ \frac{M-k}{M-(k+1)} - \frac{1}{M-(k+1)} (\hat{\lambda}_{k+1} / a(k)) \right]^{M-(k+1)}}{[\hat{\lambda}_{k+1} / a(k)]} \quad (18)$$

Define the penalty function of MDL by:

$$p(k,N) = 1/2 k(2M-k) \log N \quad (19)$$

then we can rewrite  $P_u(k)$  and  $P_o(k)$  in terms of  $q_u$  ,  $q_o$ .

(see appendix A)

$$P_u(k) \simeq P \left[ \log q_u(\hat{\lambda}_k/a(k)) < \frac{p(k,N) - p(k-1,N)}{N} \mid H_k \right] \quad (20)$$

and

$$P_o(k) \simeq P \left[ - \log q_o(\hat{\lambda}_{k+1}/a(k)) > \frac{p(k+1,N) - p(k,N)}{N} \mid H_k \right] \quad (21)$$

### 3. Probability of error for the case of two close sources

Analytical development of eigenvalue and eigenvector of covariance matrix R that is constructed from a signal received two close sources is done in Ch. 2.7 of [6] pp 52-55. From [6] we

find that the eigenvalues for two uncorrelated sources are given by:

$$\lambda_{1, 2} = \frac{1}{2} M (P_1 + P_2) \left[ 1 \pm \sqrt{1 - \frac{4P_1 P_2 (1 - |\phi|^2)}{(P_1 + P_2)^2}} \right] + \sigma_n^2 \quad (22)$$

where  $P_i$  ( $i=1,2$ ) are the power of two sources and  $\phi$  is given by:

$$\phi = \frac{\sin ( 1/2 M k d \theta )}{M \sin( 1/2 k d \theta )} \quad (24)$$

where  $k = 2\pi/\lambda$ ,  $d = \lambda/2$  and  $\theta$  is the difference of source bearings.

For the condition  $P = P_1 = P_2$  equation (22) can be simplified to give:

$$\lambda_{1, 2} = P M ( 1 \pm |\phi| ) + \sigma_n^2 \quad (24)$$

Using the result of previous section we can get from (16) and (18)

$Q_u, Q_o$  for the two sources case

$$Q_u(\hat{\lambda}_2/a(2)) = \left[ \frac{M-2}{M-1} + \frac{1}{M-1} (\hat{\lambda}_2/a(2)) \right]^{M-1} / \left[ \hat{\lambda}_2 / a(2) \right] \quad (25)$$

$$Q_o(\hat{\lambda}_3/a(2)) = \left[ \frac{M-2}{M-3} - \frac{1}{M-3} (\hat{\lambda}_3/a(2)) \right]^{M-3} \left[ \hat{\lambda}_3/a(2) \right] \quad (26)$$

For the case of two source signals, (20) and (21) give the probability of underestimating and overestimating the actual number of sources (being=2) by one or three, respectively. That is

$$P_u(2) \cong P \left[ \log Q_u(\hat{\lambda}_2/a(2)) < \frac{p(2,N) - p(1,N)}{N} \mid H_2 \right] \quad (27)$$

$$P_o(2) \cong P \left[ -\log Q_o(\hat{\lambda}_3/a(2)) > \frac{p(3,N) - p(2,N)}{N} \mid H_2 \right] \quad (28)$$



with  $Q_u(\hat{\lambda}_2/a(2))$  and  $Q_o(\hat{\lambda}_3/a(2))$  are given by (25) and (26), respectively.

Again for the case of two close sources, it is reasonable to assume that we will have  $\hat{k}=3$  with very small probability,  $P_o(2) \simeq 0$ . Hence the error in the detection of the number of sources will be mainly due to  $\hat{k}=1$ ; the underestimated case, and hence the total error probability  $P_E \cong P_u(2)$ . For  $M$  relatively large,  $\log Q_u$  and  $\log Q_o$  can be approximated by the following expression [5] (See appendix B)

$$\log Q_u(x) \cong 1/2 (x-1)^2 \quad (29)$$

$$\log Q_o(x) \cong - 1/2 (x-1)^2 \quad (30)$$

Also notice from (4) that, for large  $M$  and a given  $k$ ,  $a(k)$  can be approximated by  $\sigma_n^2$ . In particular for  $k=2$ ,  $a(2) \cong \sigma_n^2$ . Therefore together with (29) and (30), (27) and (28) become,

$$P_u(2) \approx P \left[ \left( \frac{\hat{\lambda}_2}{\sigma_n^2} - 1 \right) < \sqrt{(2/N)[p(2,N)-p(1,N)]} \mid H_2 \right] \quad (31)$$

$$P_o(2) \approx P \left[ \left( \frac{\hat{\lambda}_3}{\sigma_n^2} - 1 \right) > \sqrt{2/N [p(3,N)- p(2,N)]} \mid H_2 \right] \quad (32)$$

According to Brillinger [7], the asymptotic distribution (that is with large data length) of  $\hat{\lambda}_i$  is normal with  $E\{\hat{\lambda}_i\} = \lambda_i$  and  $\text{var}\{\hat{\lambda}_i\} = \lambda_i^2/N$ , i.e.

$$\hat{\lambda}_i \sim N(\lambda_i, \lambda_i^2/N) \quad (33)$$

Hence  $P_u(2)$  and  $P_o(2)$  became (see appendix C)

$$P_u(2) \approx \text{erf} \left[ \frac{\frac{\sigma_n^2}{\lambda_2} \sqrt{2[p(2,N)-p(1,N)]} - \sqrt{N}(\lambda_2 - \sigma_n^2)}{\lambda_2} \right] \quad (34.a)$$

$$P_o(2) = 1 - \text{erf} \left( \sqrt{2[p(3,N)- p(2,N)]} \right) \quad (34.b)$$

#### 4. Adequacy of the approximation for $\log Q_u(x)$

For the case of two close sources, it is reasonable to assume that we will have  $\hat{k}=3$  with a very small probability;  $P_u(2) \cong 0$ . Hence the error in the detection of the number of sources will be due to having  $\hat{k}=1$ ; the underestimation case. Therefore the total error probability  $P_E \cong P_u(2)$ .  $P_u(2)$  can be obtained from the (34a) provided the approximation of  $\log Q_u(x)$  by (29) is satisfactory. To examine the adequacy of this approximation we define a normalized error by

$$\text{Error} = \frac{|\log Q_u(x) - \{1/2(x-1)^2\}|}{|\log Q_M(x)|} \quad (35)$$

where  $x$  is

$$x = \lambda_2 / \sigma_n^2 \quad (36)$$

The value of this error as a function of  $x = \lambda_2 / \sigma_n^2$  is given in

figure 7-1. From this figure we notice that in order to have a sufficiently small error ( $\cong 5\%$ ),  $x$  must be close to one. Increasing the number of array element from 15 to 30 reduces the error by only a small amount. Figure 7-2 and 7-3 show the meaning of the requirement (that is  $x$  should be close to one), in terms of signal to noise ratio. From these figures we conclude that, an SNR as low as -15 dB, and an angle separation between the two sources, less than 1.5 degrees, are required to obtain an adequate approximation.

From Brillinger [7] we know that  $\hat{\lambda}_2$  has normal distribution and so is  $x = \hat{\lambda}_2 / \sigma_n^2$ . Using this distribution we calculated and depict in figure 7-4, the expected value of  $\log Q_u(x)$  and  $(x-1)^2/2$  while in figure 7-5, we depict the variance of these random variables. For the abscissa of these figure we used the expected value of the normal random variable  $\bar{x} = \lambda_2 / \sigma_n^2$ , and for the variance of  $x$  we chose  $\sigma_x^2 = \bar{x}^2 / 25$ .

From these two figures we notice that

$$E [ \log Q_u(x) ] < E [ 1/2 (x-1)^2 ] \quad (37)$$

and

$$\text{Var} [ \log Q_u(x) ] < \text{Var} [ 1/2 (x-1)^2 ] \quad (38)$$

Using either  $\log Q_u(x)$  or  $1/2 (x-1)^2$ , we calculate the underestimating probability  $P_u(2)$  and  $P'_u(2)$

$$P_u(2) = P \left( \log Q_u(x) < \frac{P(2,N)-P(1,N)}{N} \mid H_2 \right) \quad (39)$$

$$P'_u(2) = P \left( 1/2 (x-1)^2 < \frac{P(2,N)-P(1,N)}{N} \mid H_2 \right) \quad (40)$$

The random variable in (39) has both average and variance smaller than the average and variance of the random variable in (40). The relation of the distribution of these random variable is sketched in figure 7-6, where  $y = \log Q_u(x)$  and  $y' = 1/2 (x-1)^2$ . From this figure it is easy to conclude that

$$P'_u(2) < P_u(2) \quad (41)$$

for every value of the constant in the right side of the inequality in (39) and (40). That is for every data length  $N$  and every array size  $M$  (see equation(19)). Equation (41) shows that the probability of error in estimating the number of sources when using the approximating function  $1/2 (x-1)^2$  is optimistic. In reality (i.e. by using the function  $\log Q_u(x)$ ) the probability of error is much higher. The error in the value of probability of error is larger when SNR is larger, since then both the expected values and the variance of  $\log Q_u(x)$  and  $1/2 (x-1)^2$  becoming further apart (see figure 7-4,7-5 and 7-3).

## 5. Results

Figure 7-7 and 7-8 present the error probability in estimating the number of sources (actual number=2 ) as a function of angle separation, when approximating and actual functions are used, respectively. From these figures it is clear that the  $P_E$  decreases when the angle of separation increases. Also  $P_E'(2) \ll P_E(2)$ . The error probability as a function of data length is shown in figure 7-9 when the approximation function is used and in

figure 7-10 when the actual function is used. Again it is very clear that  $P'_E(2) \ll P_E(2)$  for a large range of data length. The error probability as a function of SNR is depicted in figure 7-11 when using the approximation function and in figure 7-12 when using the actual function. These errors become smaller when SNR is higher, nevertheless, as before  $P'_E(2) < P_E(2)$  for every SNR. Figure 7-13 and 7-14 are the same as figure 7-11 and 7-12 except for the angle separation; here  $\theta_1 - \theta_2 = 1.0$  degree instead of 1.5 degree before. Notice that the error probabilities  $P'_u(2)$  and  $P_u(2)$  become closer when the angle separation is smaller and the accuracy of using the approximating function becomes better.

## 6. Conclusion

The use of MDL in estimating the number of sources impinging on an array was considered in this chapter. Logarithmic function of a normal random variable is involved in calculating the error probability of underestimating (that is when the estimated number is smaller than the actual number) or overestimating (that is when the estimated number is larger than the actual number) of the

number of sources. Approximation function to this logarithmic function is sometimes used to obtain analytical form for the error probability. We show in this chapter that such approximation is very poor and usually provides an optimistic results regarding the error probability. That is, it predicts a lower probability of error in estimating the number of sources than obtained when using the actual function. Only when SNR is very low and the angle of separation is very small the approximation might have some value. Such difference in error probability when using the approximation versus the actual function, which sometimes turns out to be very large, was discovered in many simulation runs with different SNR, different angle separation, different number of array element, different data length, etc. Although these simulations were performed with only two signal sources, it is believed that the same conclusion is in effect with a large number of sources. In conclusion, one might question whether the whole method of estimating the number of sources using MDL is of any value.



Appendix A

From (10) together with (3) we have

$$P_u(k) = P \left[ N(M - (k-1)) \log \frac{a(k-1)}{g(k-1)} + p(k-1, N) \right. \\ \left. \left( N(M-k) \log \frac{a(k)}{g(k)} + p(k, N) \mid H_k \right) \right] \quad (A-1)$$

where we also used (19). Equivalently

$$P_u(k) = P \left[ \log \left[ \frac{a(k-1)}{g(k-1)} \right]^{M-(k-1)} - \log \left[ \frac{a(k)}{g(k)} \right]^{M-k} \right. \\ \left. \left( \frac{p(k, N) - p(k-1, N)}{N} \mid H_k \right) \right]$$

Finally by using (16.a) we get

$$P_u(k) = P \left[ \log Q_u(\hat{\lambda}_k / a(k)) < \frac{|p(k,N) - p(k-1,N)|}{N} \mid H_k \right] \quad (A-2)$$

Similarly from (11) and (3) we have

$$P_o(k) = P \left[ N(M-(k+1)) \log \frac{a(k+1)}{g(k+1)} + p(k+1,N) \right. \\ \left. < N(M-k) \log \frac{a(k)}{g(k)} + p(k,N) \mid H_k \right]$$

where we also again used (19). Equivalently

$$P_o(k) = P \left[ \log \left[ \frac{a(k+1)}{g(k+1)} \right]^{M-(k+1)} - \log \left[ \frac{a(k)}{g(k)} \right]^{M-k} \right. \\ \left. < \frac{|p(k,N) - p(k+1,N)|}{N} \mid H_k \right]$$

Finally by using (17)

$$P_o(k) = P \left[ \log Q_o(\hat{\lambda}_{k+1} / a_k) < \frac{|p(k,N) - p(k+1,N)|}{N} \mid H_k \right]$$

or

$$P_0(k) = P \left[ -\log Q_0(\hat{\lambda}_{k+1} / a_k) > \frac{|p(k+1, N) - p(k, N)|}{N} \mid H_k \right] \quad (A-3)$$

## Appendix B

For the case of two sources, we write from (25),

$$\log Q_u(x) = \log \left[ \left( \frac{M-2}{M-1} + \frac{1}{M-1} x \right)^{M-1} / x \right] \quad (B-1)$$

Using Taylor expansion we get

$$\log x \cong (x-1) - 1/2 (x-1)^2, \quad 0 < x \leq 2 \quad (B-2)$$

$$\log(1+x) \cong x - x^2/2 \quad 0 < x \leq 2 \quad (B-3)$$

Now

$$\frac{M-2}{M-1} + \frac{1}{M-1} x = 1 + \frac{x-1}{M-1} \quad (B-4)$$

For large  $M$  the second term on the right of B-4 satisfies the condition of B-3, so that

$$\begin{aligned}
 \log \left( \frac{M-2}{M-1} + \frac{1}{M-1} x \right)^{M-1} &= (M-1) \log \left( 1 + \frac{x-1}{M-1} \right) \\
 &\cong (M-1) \left[ \frac{x-1}{M-1} - \frac{(x-1)^2}{2(M-1)^2} \right] \\
 &= x-1 - \frac{(x-1)^2}{2(M-1)} \\
 &\cong x-1
 \end{aligned} \tag{B-5}$$

for large  $M$ , from (B-1) together with B-5, we have

$$\begin{aligned}
 \log Q_u(x) &\cong x-1 - \log x \\
 &= (x-1) - [x-1 - 1/2(x-1)^2] \\
 &= 1/2(x-1)^2
 \end{aligned} \tag{B-6}$$

By similar step we show that

$$\log Q_o(x) \cong -1/2(x-1)^2 \tag{B-7}$$

## Appendix C

From the result of Appendix B

$$\log Q_u(\hat{\lambda}_2 / a(2)) \cong \frac{1}{2} \left( \frac{\hat{\lambda}_2}{\sigma_n^2} - 1 \right)^2$$

$$\log Q_o(\hat{\lambda}_3 / a(2)) \cong -\frac{1}{2} \left( \frac{\hat{\lambda}_3}{\sigma_n^2} - 1 \right)^2$$

$$\text{where } a(2) = \frac{1}{M-2} \sum_{i=3}^M \hat{\lambda}_i = \sigma_n^2$$

So

$$P_u(2) \cong P \left[ \left( \frac{\hat{\lambda}_2}{\sigma_n^2} - 1 \right) < \sqrt{(2/N) [ p(2,N) - p(1,N) ]} \mid H_2 \right] \quad (C-1)$$

$$P_o(2) \cong P \left[ \left( \frac{\hat{\lambda}_3}{\sigma_n^2} - 1 \right) > \sqrt{(2/N) [ p(3,N) - p(2,N) ]} \mid H_2 \right] \quad (C-2)$$

From the Brillinger the asymptotic distribution of  $\hat{\lambda}_i$  are normal with  $E[\hat{\lambda}_i] = \lambda_i$ , and  $\text{Var}[\hat{\lambda}_i] = \lambda_i^2 / N$  so

$$\begin{aligned}
P_u(2) &\cong P \left[ \hat{\lambda}_2 < \sigma_n^2 \sqrt{(2/N) [p(2,N) - p(1,N)] + \sigma_n^2} \right] \\
&= \text{erf} \left[ \frac{\sigma_n^2 \sqrt{2[p(2,N) - p(1,N)]} - \sqrt{N} (\lambda_2 - \sigma_n^2)}{\lambda_2} \right] \quad (C-3)
\end{aligned}$$

$$P_o(2) \cong P \left[ \hat{\lambda}_3 > \sigma_n^2 \sqrt{(2/N)[p(3,N) - p(2,N)] + \sigma_n^2} \right]$$

Since  $\lambda_3$  is same as  $\sigma_n^2$  and  $\text{Var}[\hat{\lambda}_3] = \sigma_n^2/N$ , so

$$P_o(2) = 1 - \text{erf} \left[ \sqrt{2 [p(3,N) - p(2,N)]} \right] \quad (C-4)$$

#### References:

- [1] M.S. Bartlett, "A note on the multiplying factors for various  $\chi^2$  approximation," J. Roy. Stat. Soc., ser. B, vol. 16, pp. 296-298 1954
- [2] Akaike, "A new look at the statistical model identification," IEEE Trans. Automat. Contr., vol. AC-19, pp. 716-732

- [3] J. Rissanen, "Modeling by shortest data description,"  
Automatica, vol. 14, pp. 465-471, 1978
- [4] M. Wax, T. Kailath, "Detection of signals by information  
theoretic Criterion," IEEE. Trans ASSP. vol ASSP-33, No2, April  
pp. 387-392 1985
- [5] Wang, M. Kaveh, "On the Performance of signal-subspace  
processing-Part1; Narrow-band systems," IEEE Trans ASSP, Vol.  
ASSP 14 OCT. pp. 1201-1209 1986
- [6] J.E. Hudson, "Adaptive Array Principle," Stevenage, U.K.  
perigrinus, 1981
- [7] D.R. Brillinger, "Time series: data analysis and Theory,  
expanded, San Francisco, CA: Holden-Day, 1981

Fig 7-1 Approximation error as a function of  $x$

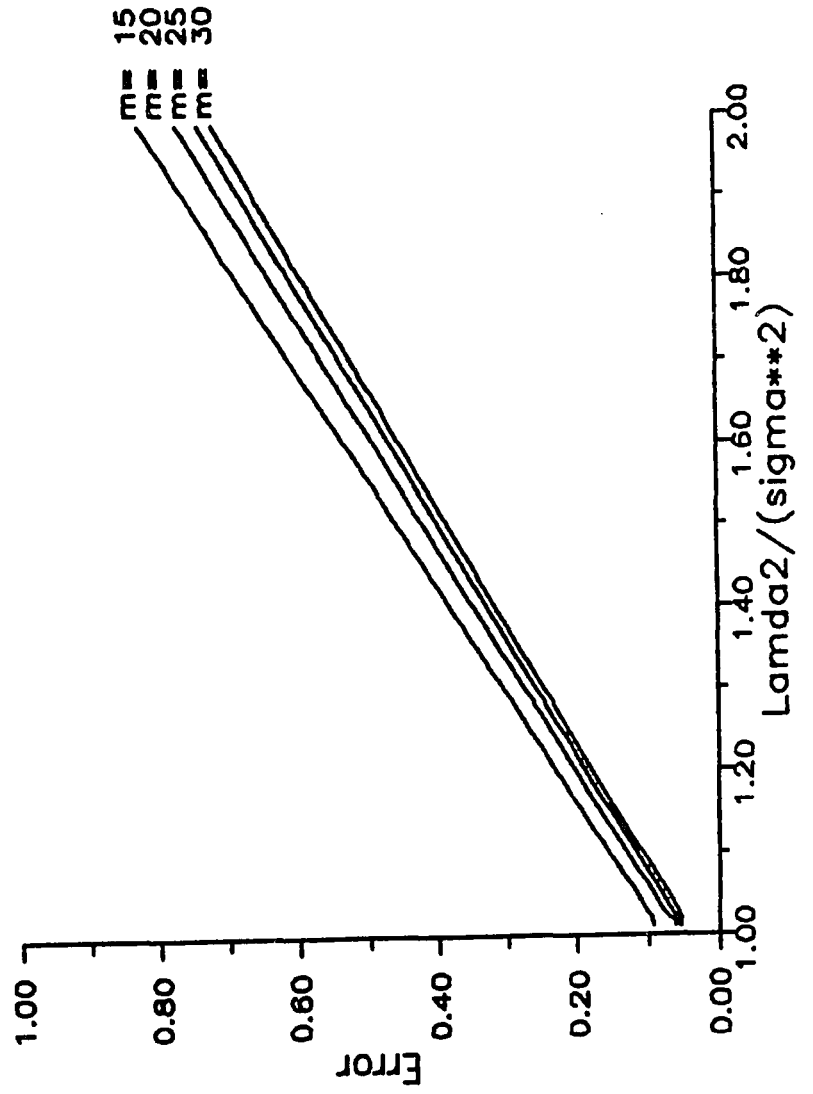




Fig 7-2 The SNR, needed to obtain Satisfactory Approximation

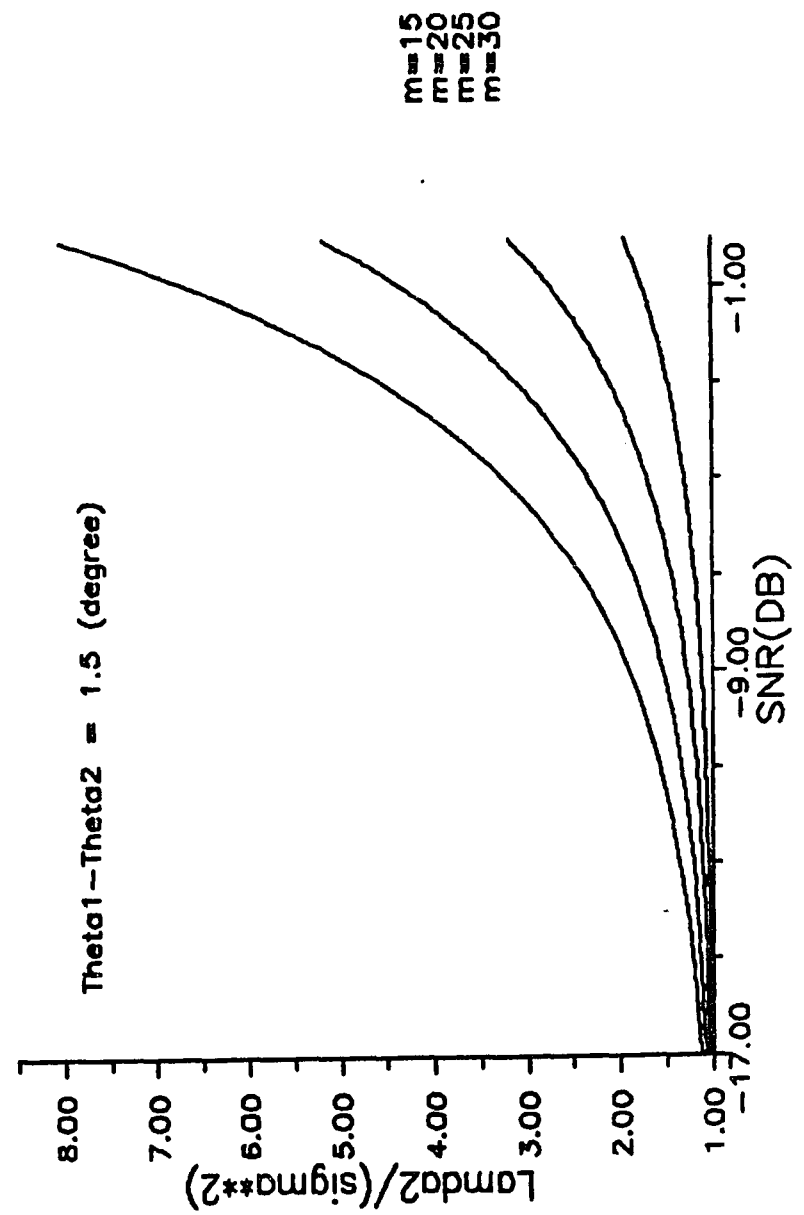


Fig 7-3 The SNR, Needed to Obtain Satisfactory Approximation

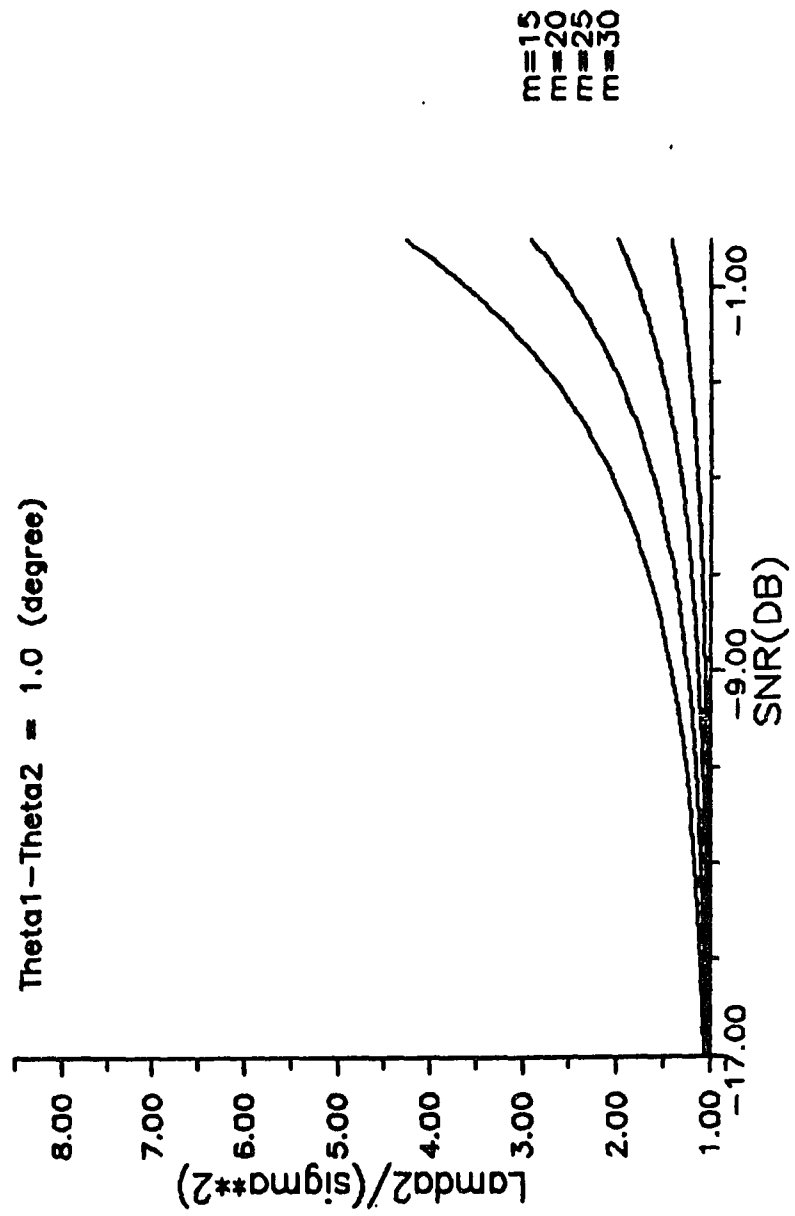


FIG 7-4 The Expected Value of Random Variable  $\log Qu(x)$  (Solid), and  $0.5(x-1)^{**2}$  (dashed) as a function of  $\bar{x} = \text{lamda}2/(\text{sigma}^{**2})$ ; the expected value of the normal random variable  $x$   $(\text{sigma } x)^{**2} = (\text{aver}(x)^{**2})/25$

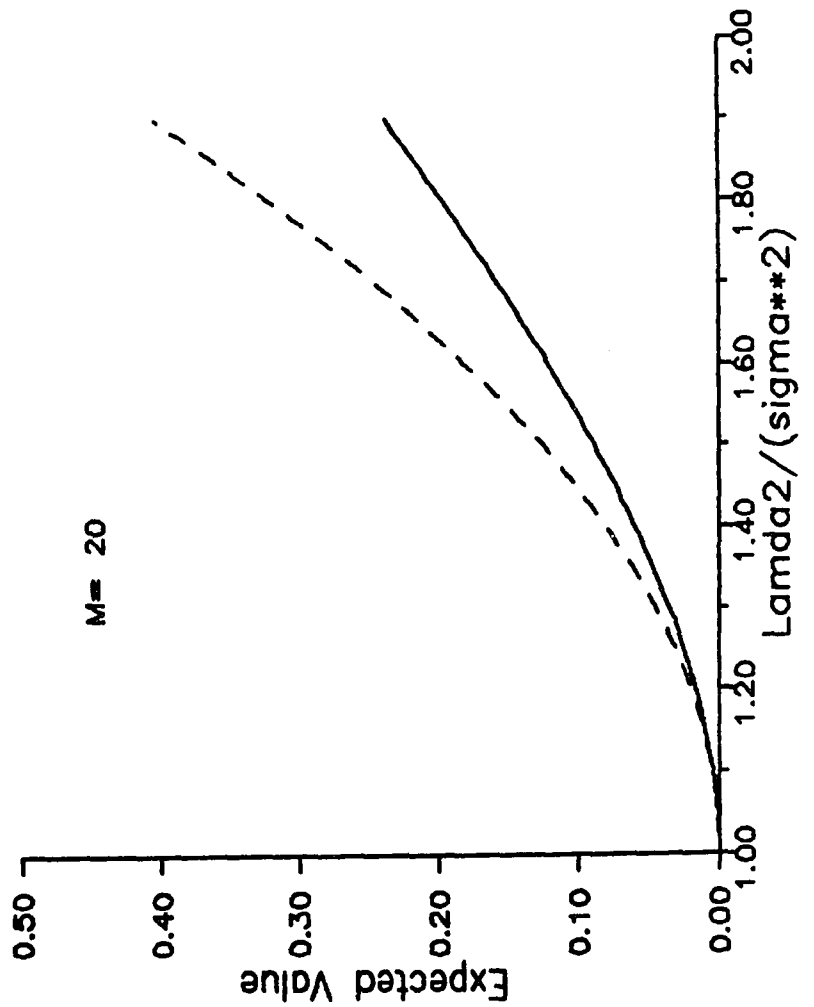


FIG 7-5 The variance of the Random Variable  $\log Q_u(x)$  (Solid), and  $0.5(x-1)^2$  (dashed) as a function of  $\bar{x} = \text{lamda}^2 / (\text{sigma}^2)$ ; the expected value of the normal random variable  $x$   $(\text{sigma } x)^2 = (\text{aver}(x)^2) / 25$

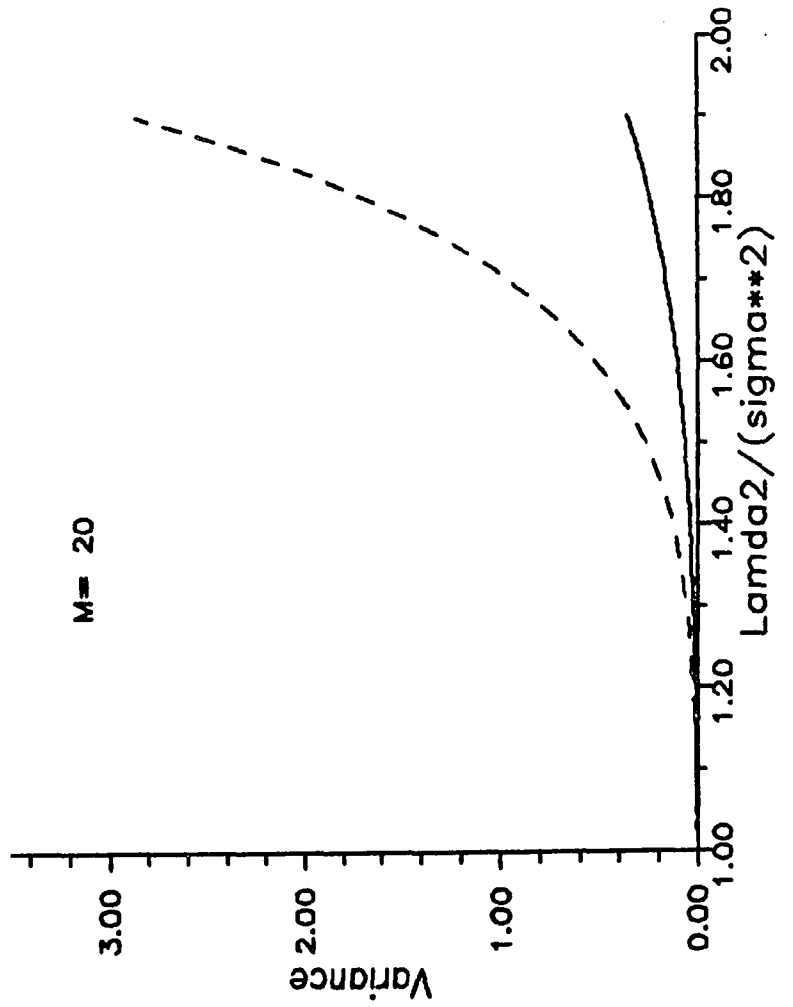


FIG 7-6

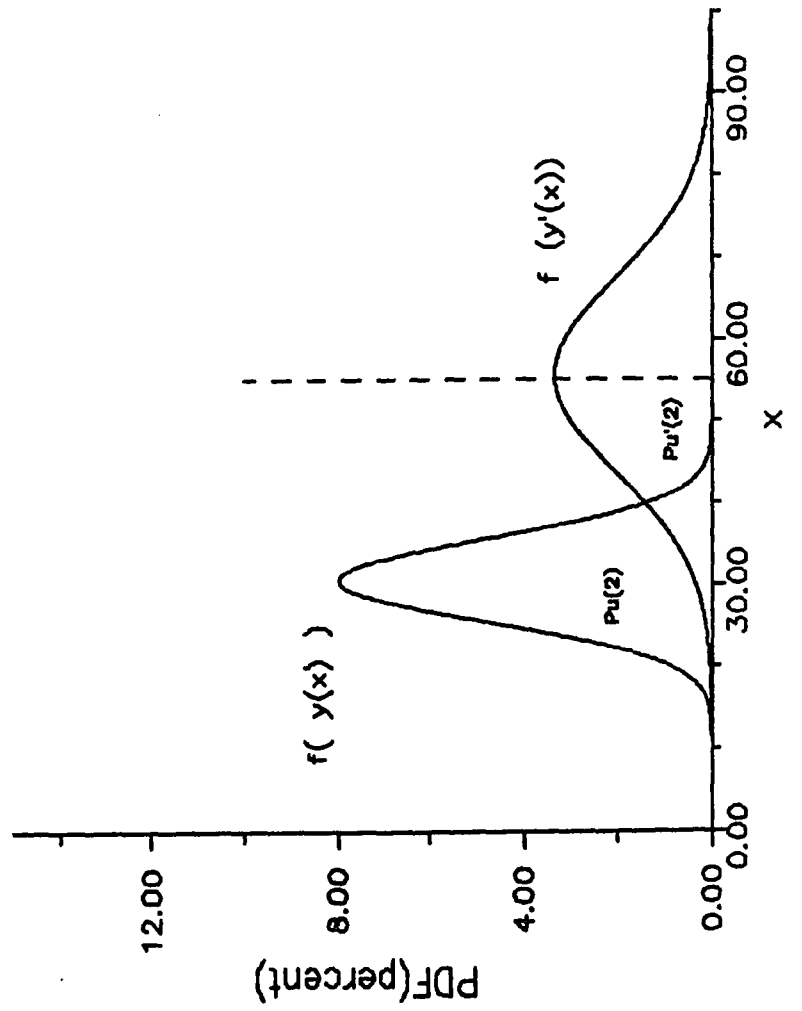


Fig 7-7 Error Probability of using  
the approximated Function  
 $P_u'(2)$ . SNR = -3.14 dB  
Data Length = 2000

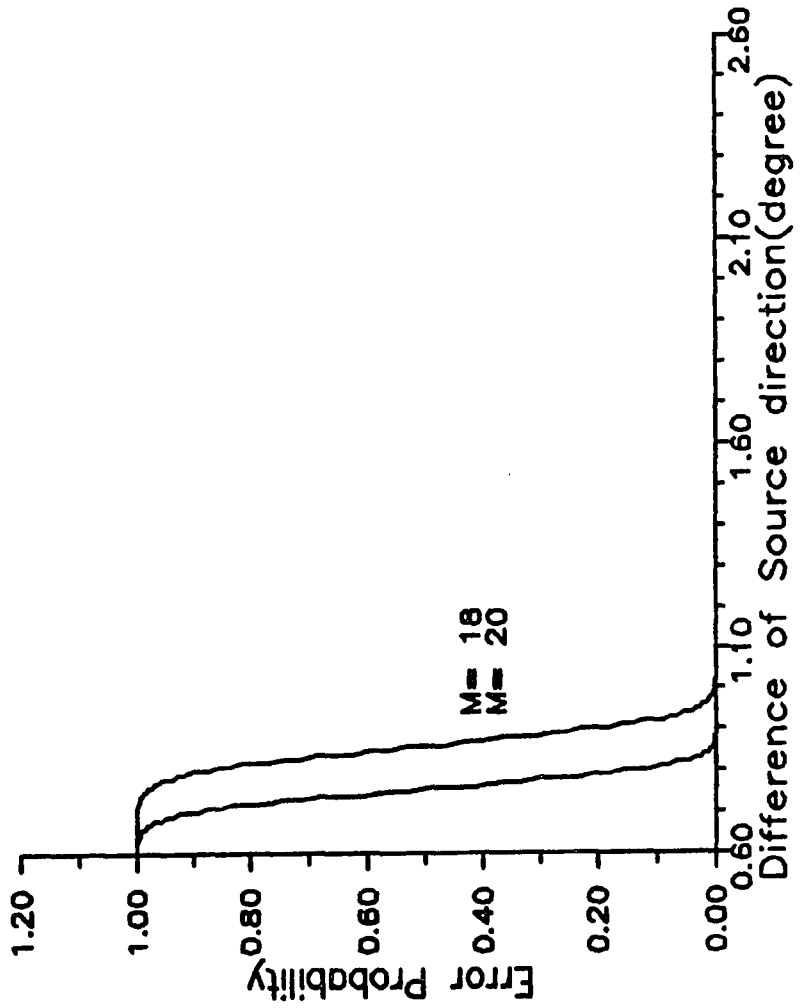


Fig 7-8 Error Probability using  
the Actual Function  $P_u(2)$   
SNR = -3.14 N = 2000

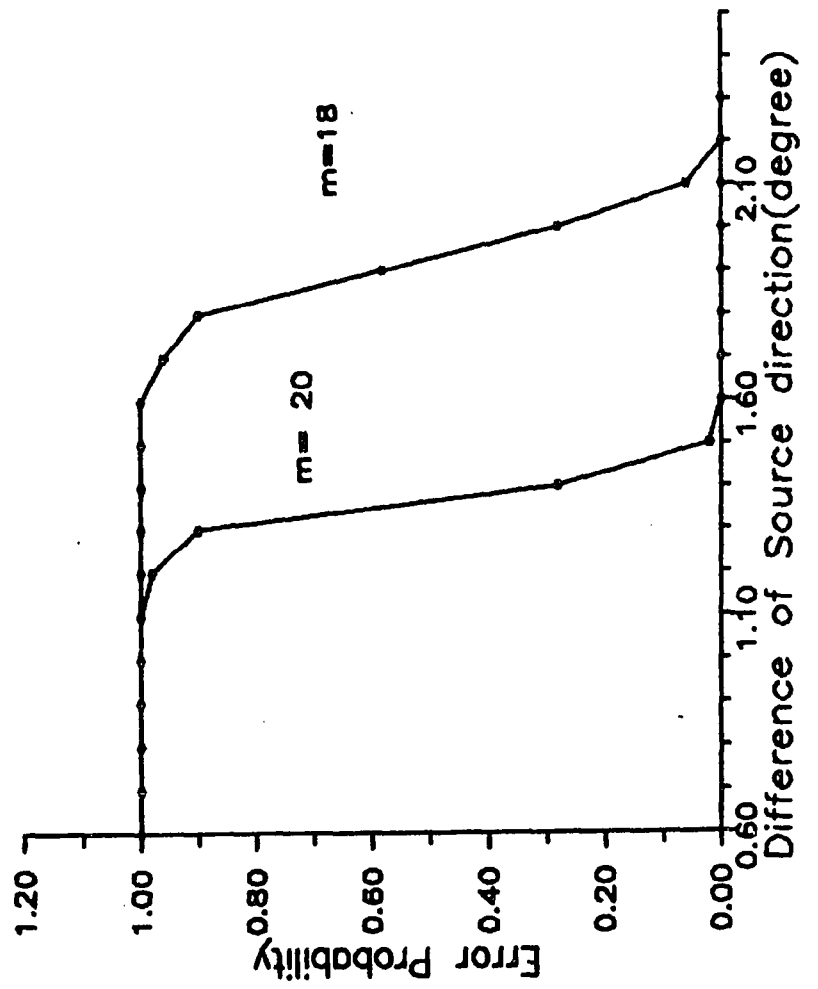


FIG 7-9 Error Probability as function  
 of data length N. approximation  
 Function  $P_u(2)$  is used. SNR = -1.2 dB  
 Theta1 = 1.5 (degree)

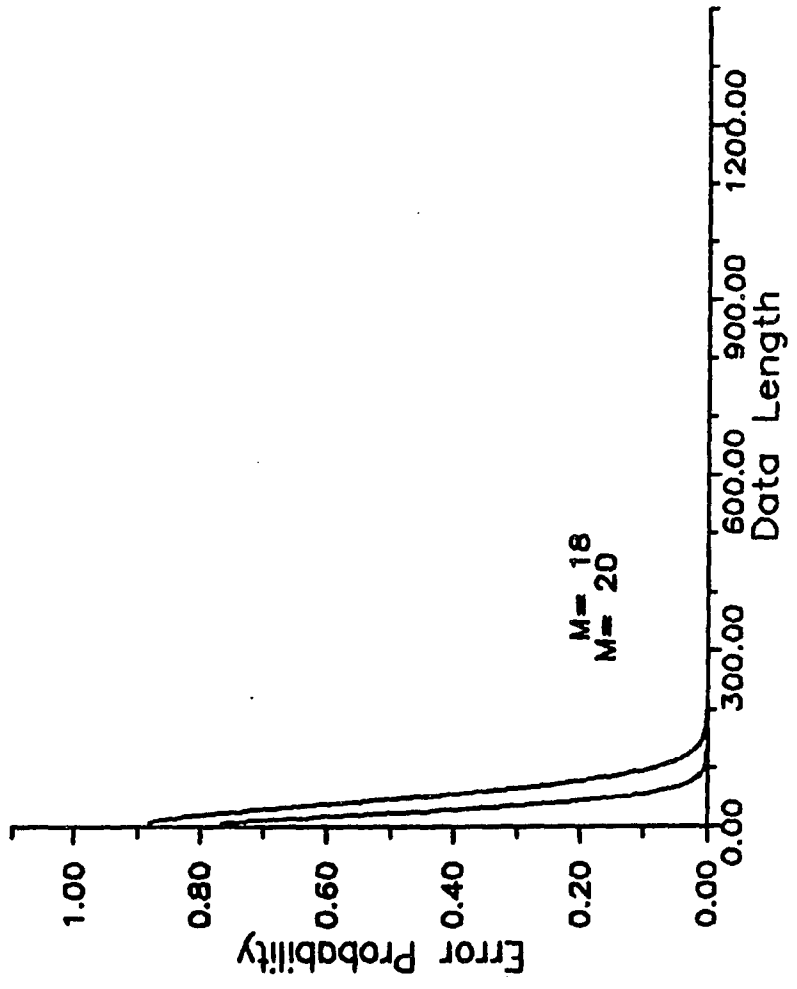




Fig 7-10 Error Probability as Function of data length N. Actual Function  $P_u(2)$  is used. SNR= -1.2 dB  
 $\Theta_1 - \Theta_2 = 1.5$  (degree)

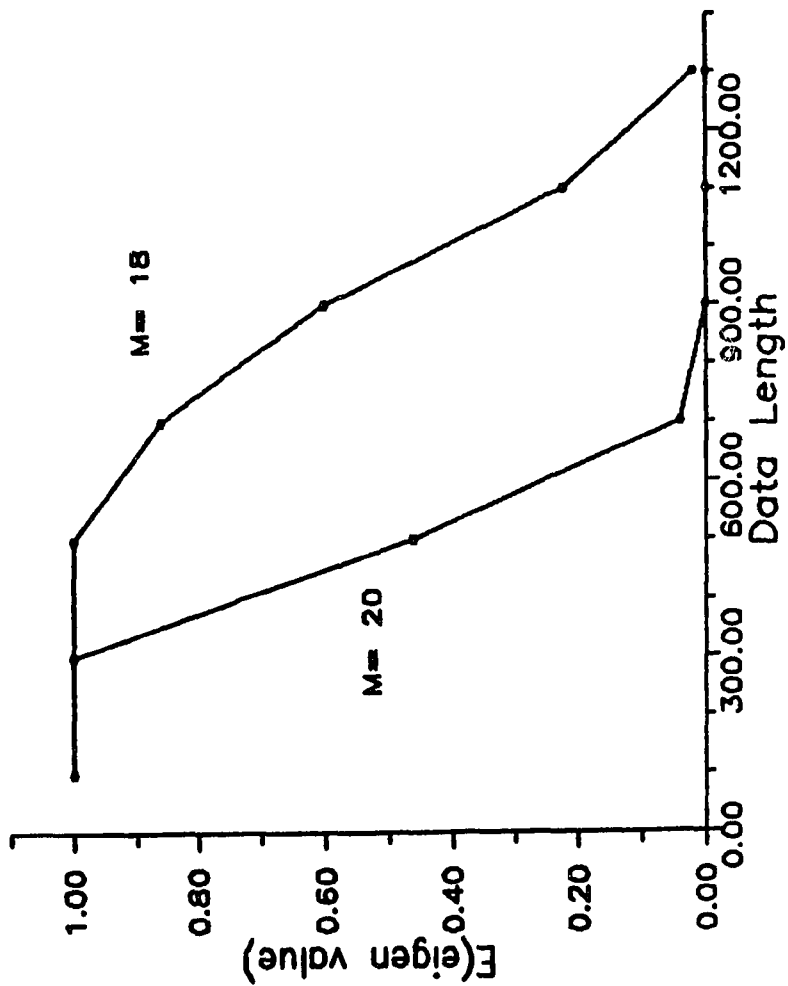


Fig 7-11 Error Probability as a Function of SNR,  $P_u(2)$  Approximation Function is used.  $M=20$   $\Theta_1 - \Theta_2 = 1.5$  (degree)

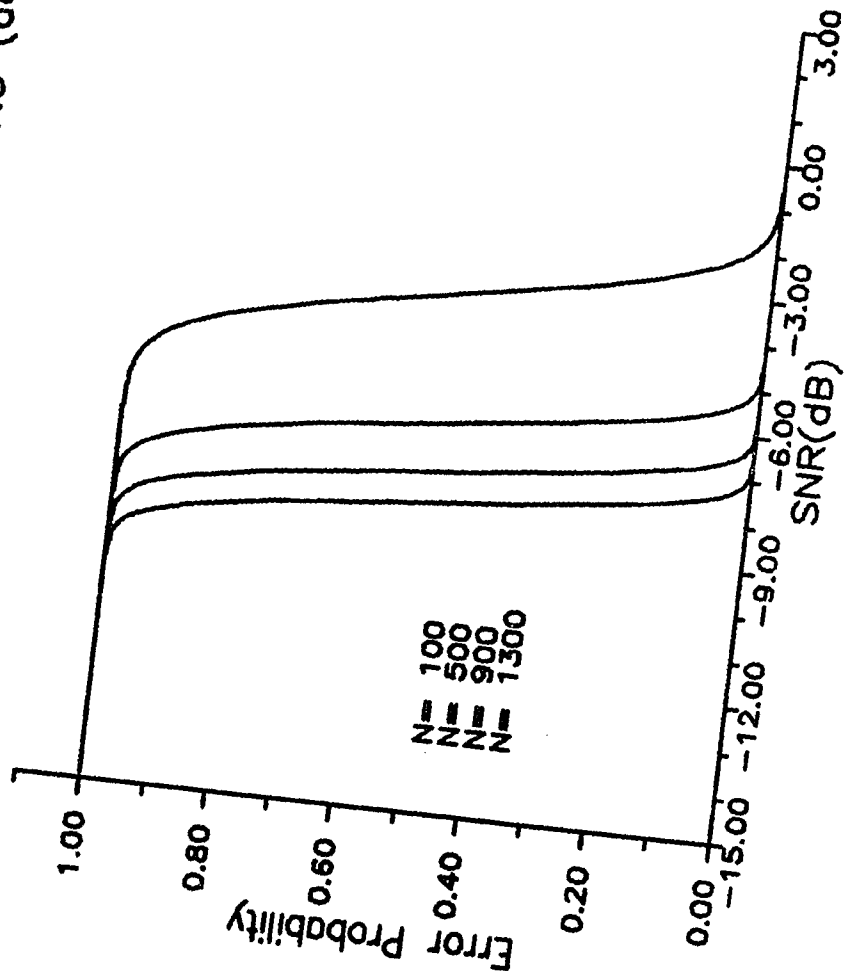


Fig 7-12 Error Probability as a Function  
as a function of SNR.  $P_u(2)$   
Actual Function is used.  $M=20$   
 $\Theta_1 - \Theta_2 = 1.5$  (degree)

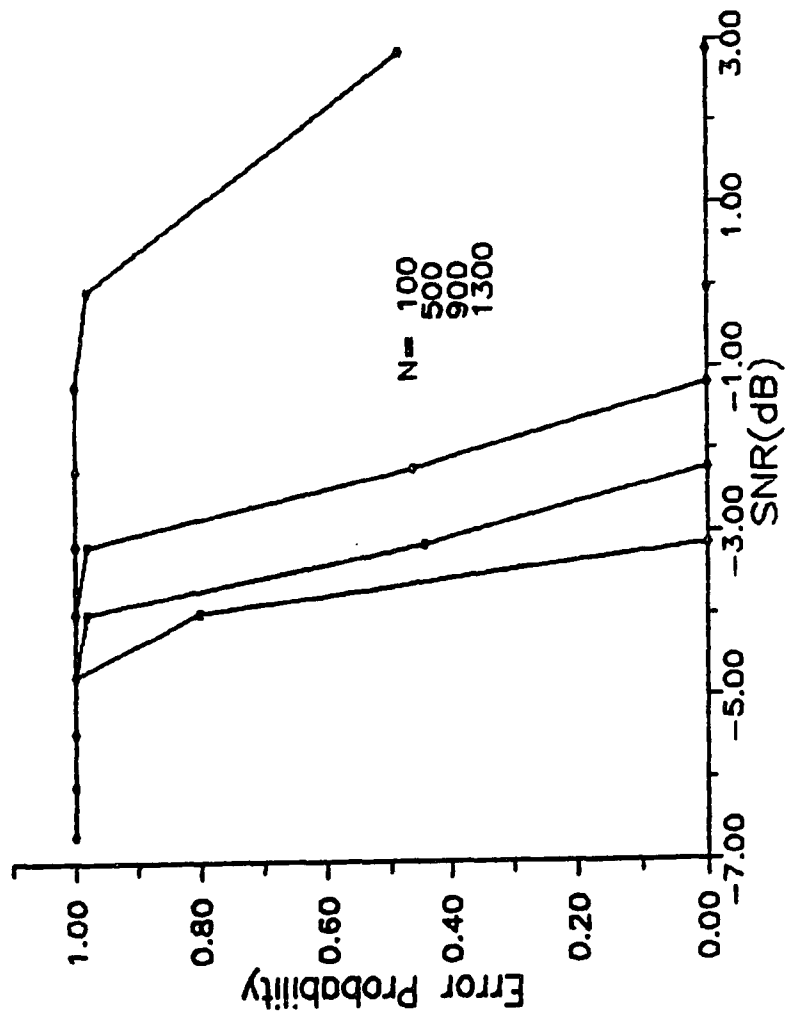


Fig 7-13 Error Probability as a Function of SNR,  $P_u(2)$  Approximation Function is used.  $M=20$  Theta1 = Theta2 = 1.0 (degree)

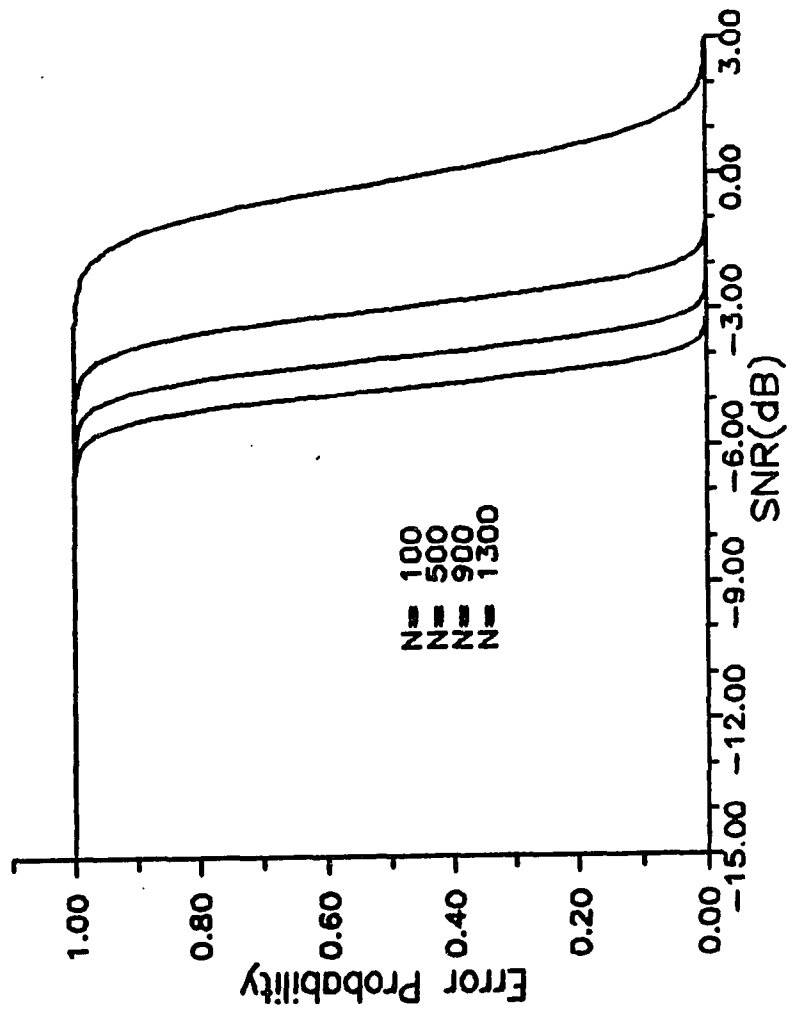


FIG 7-14 Error Probability as a Function  
as a function of SNR.  $P_u(2)$   
Actual Function is used.  $M=20$   
 $\Theta_1 = \Theta_2 = 1.0$  (degree)

